The Differences are in the Details: The Mechanism of Flavin Reduction in Class 1A and Class 2 Dihydroorotate Dehydrogenases

by

Rebecca L. Fagan

A dissertation submitted in partial fulfillment
of the requirements for the degree of
Doctor of Philosophy
(Biological Chemistry)
in The University of Michigan
2009

Doctoral Committee:

Assistant Professor Bruce A. Palfey, Chair
Professor Dave P. Ballou
Professor E. Neil G. Marsh
Assistant Professor Sylvie Garneau-Tsodikova
Assistant Professor Patrick J. O'Brien

Acknowledgements

First and foremost, I would like to express my deep appreciation and respect for my advisor, Bruce Palfey. He has taught me a great deal about science. I have to thank him for always pushing me to do more, for allowing useful distractions, and for never stopping teaching me. Bruce's guidance has greatly assisted in both my professional and personal development.

I would like to thank the entire Palfey lab for making it a great place to do science. I would especially like to acknowledge those individuals that had a part in the work presented in this thesis. Maria Nelson, a former technician in the lab, did the initial isotope effect studies on the *E. coli* enzyme and Paul Pagano, a former undergraduate, studied the reductive half-reaction of the human enzyme both presented in Chapter 2. This work laid the foundation for my thesis project and has greatly increased our knowledge of the mechanism of Class 2 DHODs. Bhramara Tirupati, a former postdoctoral fellow in the lab, characterized several active mutants of the Class 1A enzyme. This work allows comparisons to be made between Class 1A mutants and the

Class 2 mutants discussed in Chapter 4. Finally, Rebecca Kow, a former undergraduate, characterized the Thr178 mutant enzymes discussed in Chapter 5. Her work was the first indication that the proton-relay network found in Class 2 enzymes is important for catalysis.

I would also like the members of my thesis committee – Dave Ballou, Neil Marsh, Pat O'Brien, and Sylvie Garneau-Tsodikova. All have been helpful and supportive throughout my years here.

Thanks to the entire Biological Chemistry Department; it is a great place to do science. Thanks for providing a stimulating scientific environment. I have truly enjoyed my time here. I would like to personally thank Beth Goodwin for all her assistance.

Last but not least, I must thank my friends and family. Thanks to my parents, Dave and Gail, for always being supportive. You hard work and sacrifice have allowed me to become the person I am today. Thanks to my brothers and sisters, nieces and nephews. You all mean so much to me. A big thanks goes out to all my friends, those in Michigan and those far away. I must also thank Dustin. Your love and support mean the world to me. Thank you for always being there for me.

Preface

Several enzymes in pyrimidine metabolism catalyze very similar oxidation/ reduction reactions. The work presented here focuses on the detailed mechanism of one group of these enzymes, the dihydroorotate dehydrogenases (DHODs). This thesis consists of five chapters. The first chapter is a review article about flavoenzymes in pyrimidine metabolism that has recently been submitted for publication in *Frontiers of Biosciences*. It focuses on the structural and mechanistic differences and similarities between these flavoproteins, an overall theme of the entire thesis. Chapters 2 and 3 focus on the detailed order of bond-breaking in DHODs from different phylogenetic classes. Both chapters have been previously published [Fagan, R. L., Nelson, M. N., Pagano, P. M., and Palfey, B. A. (2006) Mechanism of Flavin Reduction in Class 2 Dihydroorotate Dehydrogenases. *Biochemistry*, **45**, 14926-14932; Fagan, R. L., Jensen, K. F., Björnberg, O., and Palfey, B. A. (2007) Mechanism of Flavin Reduction in the Class 1A Dihydroorotate Dehydrogenases from *Lactococcus lactis*. *Biochemistry,* **46**, 4028-4036] and have been reproduced here with only minor modifications. Chapters 4 and 5 focus on the specific role that conserved amino acids play in dihydroorotate oxidation by Class

2 DHODs. Chapter 4 focuses on pyrimidine-binding residues found in the active site of all phylogenetic classes DHODs, while Chapter 5 focuses on a putative proton-relay network found only in Class 2 DHODs. Both of these chapters will be submitted as manuscripts to *Biochemistry*.

Table of Contents

List of Figures

List of Tables

List of Appendices

List of Abbreviations

5FU, 5-fluorouracil

Bis-Tris, 2-[bis-(2-hydroxyethyl)-amino]-2-hydroxymethyl-propane-1,3-diol

CAPS, N-cyclohexyl-3-aminopropanesulfonic acid

CHES, N-cyclohexyl-2-aminoethanesulfonic acid

DHO, dihydroorotate

DHOD, dihydroorotate dehydrogenase

DPD, dihydropyrimidine dehydrogenase

DUS, dihydrouridine synthase

EDTA, ethylenediaminetetraacetic acid

FAD, flavin adenine dinucleotide

FMN, flavin mononucleotide

KCl, potassium chloride

K_d, dissociation constant

KIE, kinetic isotope effect

KP_i, potassium phosphate

k_{red}, reduction rate constant

MOPS, 3-(N-morpholino)propanesulfonic acid

OA, orotate

OMP, orotidine 5'-monophosphate

PP_i, pyrophosphate

PRPP, phosphoribityl pyrophosphate

TAPS, N-Tris(hydroxymethyl)methyl-3-aminopropanesulfonic acid

Tris, 2-amino-2-hydroxymethyl-propane-1,3-diol

Abstract

Several flavoproteins catalyze very similar oxidation/reduction reactions in pyrimidine metabolism. One such enzyme is dihydroorotate dehydrogenase (DHOD), which catalyzes the only redox step in *de novo* pyrimidine biosynthesis, the conversion of dihydroorotate (DHO) to orotate. Due to their important biological role, DHODs are interesting drug targets. A better understanding of the detailed chemical mechanism of DHODs from different phylogenetic classes could aid in class-specific inhibitor development.

During DHO oxidation, an active site base deprotonates C5 of DHO and a hydride is transferred from C6 to the isoalloxazine ring of the FMN prosthetic group. The active site bases differ between classes of DHODs – Class 1A enzymes have cysteine while Class 2 enzymes have serine – but the rest of the active site is nearly identical. The fundamental question of whether the scission of the two substrate C-H bonds is stepwise or concerted was addressed by determining deuterium kinetic isotope effects on flavin reduction under anaerobic conditions. Interestingly, different mechanisms were observed; Class 1A enzymes utilize a concerted mechanism while Class 2 enzymes use a

stepwise mechanism. When the active site base of the Class 1A enzyme from *L. lactis* was switched to that of Class 2 enzymes, the rate of flavin reduction was significantly decreased, but the mechanism of flavin reduction was not changed, indicating that the identity of the active site base is not responsible for determining the mechanism of DHO oxidation.

The active sites of all DHODs contain many strictly conserved residues that hydrogen-bond to pyrimidines. Site-directed mutagenesis was used to investigate their roles in DHO oxidation. Mutation of several analogous residues in the two classes caused different changes in the behavior of the enzymes. Some residues have been shown to be important for DHO binding, while others were critical for DHO oxidation.

Class 2 DHODs contain a small tunnel connecting the active site base to bulk solvent that is proposed to shuttle protons away from the active site during catalysis. A water molecule is found bound in this tunnel in all crystal structures, in contact with the ring of a phenylalanine and hydrogen-bonding to a threonine, implicating these conserved residues in the proton-relay network. Site-directed mutagenesis was employed to block and/or change the hydrophobicity of this tunnel and resulted in enzymes with decreased rate constants for flavin reduction and dramatically shifted pK_a values controlling reduction, indicating the importance of the proton-relay network in catalysis.

Chapter 1
Flavoenzymes in Pyrimidine Metabolism: Dihydroorotate Dehydrogenase, Dihydropyrimidine Dehydrogenase, and Dihydrouridine Synthase

Pyrimidine nucleotides play critical roles in cellular metabolism. Pyrimidines are used to make both DNA and RNA. In addition, pyrimidines are precursors of activated CDP-diacylglycerol phosphoglyceride for cell membranes and UDP-sugars for protein glycosylation and glycogen synthesis (1). Pyrimidines are either synthesized *de novo* or scavenged through salvage pathways. Pyrimidine biosynthesis is imperative for proliferating cells due to the increased demand for nucleic acid precursors. Accordingly, pyrimidine biosynthesis is up-regulated in tumors and neoplastic cells (2).

Three enzymes involved in various aspects of pyrimidine metabolism - *de novo* synthesis, pyrimidine catabolism, and tRNA modification - catalyze very similar redox reactions. Each reaction involves either the oxidation of a carbon-carbon single bond or the reduction of a carbon-carbon double bond in the pyrimidine ring (Figure 1-1). Each of these enzymes uses a redox-active flavin prosthetic group.

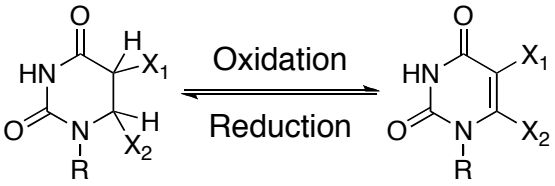

Figure 1-1: Oxidation/Reduction Reaction Catalyzed by Flavin-Dependent Pyrimidine Metabolizing Enzymes

For uracil/dihydrouracil, X_1=H, X_2=H, R=H; for uridine/dihydrouridine, X_1=H, X_2=H, R=sugar phosphate; for thymine/dihydrothymine, X_1=CH_3, X_2=H, R=H; for orotate dihydroorotate, X_1=H, X_2=CO_2^-, R=H

Flavins are derivatives of riboflavin (vitamin b_2), and consist of a tricyclic isoalloxazine ring system derivatized with a ribityl chain at N10. The ribityl chain is further derivatized to give flavin mononucleotide (FMN) or flavin adenine dinucleotide (FAD), the two common biological forms of the flavin prosthetic group (Figure 1-2). The ribityl chain and its modification can be thought of as a handle, held by the enzyme to keep the flavin in place. Flavoproteins generally make extensive contacts with these regions of the flavin, so that usually a noncovalent, but nondissociable, complex is formed.

Chemistry occurs on the isoalloxazine ring system, which is redox-active. Flavins are capable of a wide variety of chemistries. They can accept or donate hydrides as well as single electrons. They can also undergo either electrophilic or nucleophilic attack. In addition, when reduced they can react with molecular oxygen. Therefore, flavins are involved in almost all aspects of biology, not just pyrimidine metabolism. For an

extensive look at the reactions catalyzed by flavoproteins please refer to a recent review (3).

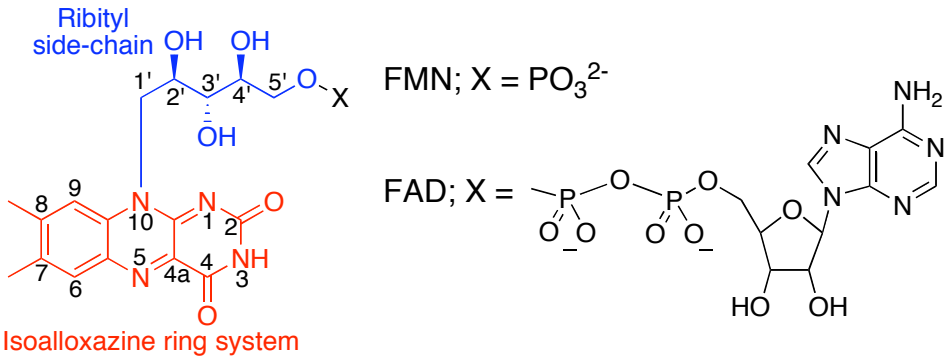

Figure 1-2: Flavin Structures

Flavins consist of a tricyclic isoalloxazine ring system attached to a ribityl chain at N10. In FMN, the ribityl chain is derivatized by a phosphate. In FAD, the ribityl chain is derivatized with an adenosine diphosphate.

The catalytic cycle of most flavoproteins can be divided into half-reactions (Figure 1-3). In the reductive half-reaction, the flavin prosthetic group is reduced while the first substrate is oxidized. Conversely, in the oxidative half-reaction, the flavin prosthetic group is oxidized while the second substrate is reduced. Studying the half-reactions that make-up the catalytic cycle can give detailed mechanistic information – a fact that has been exploited in the study of many flavoproteins.

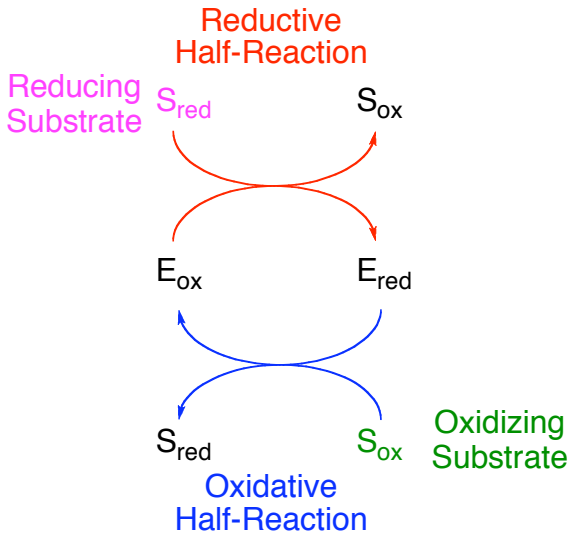

Figure 1-3: General Catalytic Cycle of Flavoproteins

The catalytic cycle can be broken into two half-reactions. In the reductive half-reaction, the reducing substrate is oxidized while the enzyme-bound flavin is reduced. In the oxidative half-reaction, the oxidizing substrate is reduced while the enzyme-bound flavin is oxidized.

Dihydroorotate Dehydrogenases

Biological Significance

Pyrimidines are synthesized *de novo* from other metabolites using six different enzymes (1). Initially, carbamoyl phosphate synthetase catalyzes the formation of carbamoyl phosphate from glutamine and bicarbonate at the expense of two molecules of ATP (Figure 1-4). Carbamoyl aspartate is then synthesized from carbamoyl phosphate and aspartate via aspartate transcarbamylase. Dihydroorotase catalyzes the intramolecular condensation of carbamoyl aspartate to form dihydroorotate (DHO). DHO is oxidized to orotate (OA) by the flavin-containing enzyme dihydroorotate

dehydrogenase (DHOD) in the only redox step in the pathway. Orotate phosphoribosyltransferase catalyzes the reaction of PRPP with OA to transfer the phosphoribose and form orotate monophosphate (OMP). OMP is then decarboxylated at the C6 position to form UMP by orotidine-5'-monophosphate decarboxylase, one of the most catalytically proficient enzymes known (4).

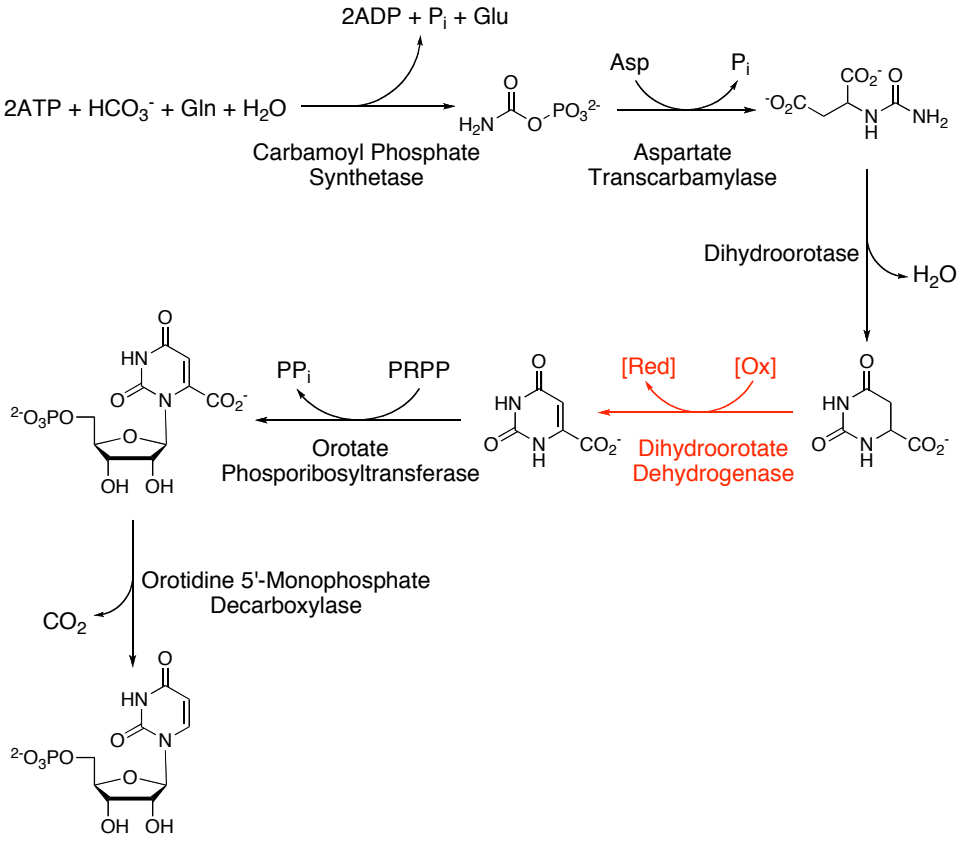

Figure 1-4: *De novo* Pyrimidine Biosynthetic Pathway

The fourth step in the pathway is catalyzed by the flavin-dependent enzyme, dihydroorotate dehydrogenase (DHOD), which and oxidizes dihydroorotate (DHO) to orotate (OA).

In most prokaryotes, each enzyme is encoded by a different structural gene, so that six monofunctional enzymes synthesize pyrimidines. In simple eukaryotes such as yeast, the six enzymes are encoded by five structural genes. One gene encodes a multifunctional enzyme that has both carbamoyl phosphate synthetase and aspartate transcarbamylase activities (5). In mammals, the six enzymatic activities are encoded by only three structural genes. A single polypeptide chain catalyzes the first three steps of pyrimidine biosynthesis. A second multifunctional enzyme catalyzes the final two steps (1). The other gene encodes DHOD.

DHOD was first isolated from the anaerobic bacterium *Zymobacterium oroticum* (6). This enzyme was found to use both reduced or oxidized pyridine nucleotide and OA or DHO as substrates. Early work on this enzyme showed that the hydrogen from the pyridine nucleotide was not directly transferred to the pyrimidine (7). In addition, the enzyme was found to contain more than one flavin (8). By the late 1960's, the enzyme was known to contain FAD, FMN, and a nonheme iron center (9). It was also known that radical intermediates were present during the reaction (10, 11). In the early 1960's, other DHODs were found associated with membranes (12). These enzymes differed from those isolated earlier. They were smaller and would not react with pyridine nucleotides, giving the first impression that DHODs from various organisms were quite different.

Due to the difficulty of working with membrane-bound enzymes, early work on the membrane-bound DHODs suggested that the enzymes did not contain flavin and were, rather, metal-containing enzymes (13, 14). However, we currently know that all DHODs contain flavin, even those known to associate with the membrane.

The application of the methods of molecular biology has clarified the extent of diversity of DHODs. DHODs have been divided into two broad classes based on amino acid sequence (15) (Figure 1-5). Several properties of the enzymes, including oxidizing substrate and subcellular location, segregate nicely into these classes allowing us to better understand the differences in the enzymes identified over 50 years ago. All DHODs contain a noncovalently bound FMN prosthetic group that oxidizes DHO to OA, but the second substrate used to regenerate the oxidized flavin varies based on enzyme class. Class 2 enzymes are membrane-bound monomers that are oxidized by ubiquinone (5). Class 1 enzymes, on the other hand, are cytosolic. Class 1 enzymes have been further divided into two subclasses. Class 1A enzymes are homodimers that are oxidized by fumarate (16). Class 1B enzymes, the first DHODs to be discovered, are $\alpha_2\beta_2$ heterotetramers that contain one subunit that resembles a Class 1A enzyme as well as a second subunit that contains an iron-sulfur cluster and an FAD, allowing these enzymes to be oxidized by NAD (17). Class 1 DHODs are found mostly in Gram-positive bacteria

while Class 2 DHODs are found in the majority of Gram-negative bacteria and eukaryotes.

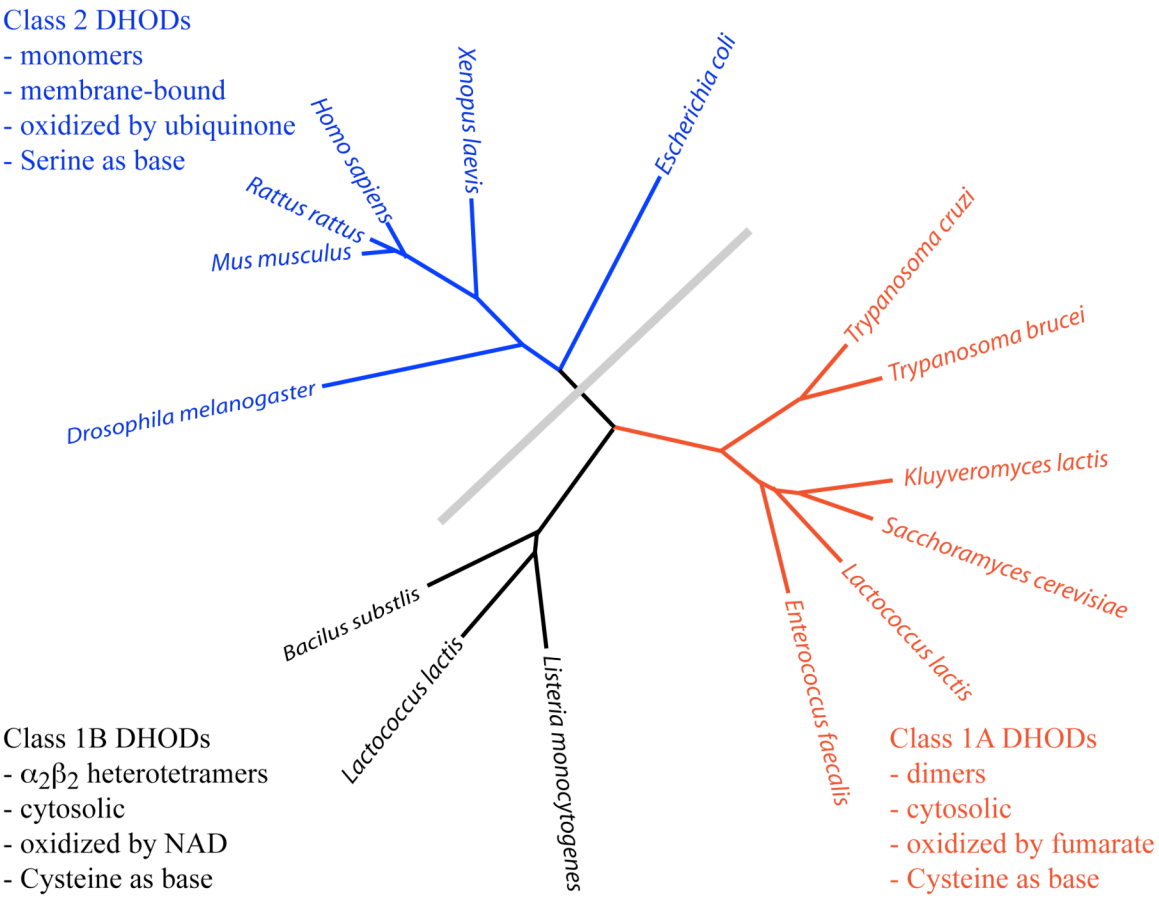

Figure 1-5: Phylogenetic Tree of DHODs

DHODs are separated into two classes. Class 2 enzymes are above the grey line. Class 1A enzymes have been divided into two subclasses and are below the grey line. Several properties of the enzymes segregate into these classes.

Mammals contain a Class 2 DHOD that is found in mitochondria. The enzyme is a membrane protein localized to the inner mitochondrial membrane (5, 18). The

electrons obtained from DHO are transferred to ubiquinone, directly linking pyrimidine biosynthesis with the respiratory chain (5). A mitochondrial targeting sequence and a membrane stop-transfer sequence on the amino end of the polypeptide chain are used to target the enzyme to mitochondria (19). It is unclear why DHODs are targeted to the mitochondria; the other enzymes involved in pyrimidine biosynthesis are cytosolic. The initial multifunctional enzyme that catalyzes the first three steps of pyrimidine biosynthesis (CAD) is associated with the cytoskeleton (1). Mitochondria are also known to be associated with the cytoskeletal network. It has been postulated that CAD binds to and translocates along the cytoskeleton to the mitochondria where DHOD is located (1).

The malaria parasite *Plasmodium falciparum* also contains a Class 2 DHOD that is highly homologous to the human enzyme. Once in a human host, the plasmodium parasite must replicate in the erythrocyte. Normal human erythrocytes cannot synthesize pyrimidines. The malarial parasite synthesizes enzymes for *de novo* pyrimidine biosynthesis, among other things, allowing the parasite to replicate. One of these essential enzymes is DHOD (20). In fact, the malarial parasite seems to maintain an active mitochondrial electron transport chain only to regenerate ubiquinone to be used by DHOD for pyrimidine biosynthesis (21).

Class 1 DHODs are found mainly in bacteria. However, two trypanosomes, *Trypanosoma cruzi* (22) and *Trypanosoma brucei* (23) contain only Class 1A DHODs. In *T. cruzi*, all six enzymes in the pyrimidine biosynthetic pathway are found in a polycistronic transcription unit. The enzymes are found on five genes; a multifunctional enzyme catalyzes the final two steps of the pathway.

Some organisms contain more than one DHOD. *Lactococcus lactis* and *Enterococcus faecalis* contain both a Class 1A and 1B enzyme (24-26). It is unclear why these organisms contain two DHODs. Knockout studies have shown that either enzyme can compensate for the loss of the other, and that only when both genes are removed is the organism dependent on pyrimidines from the environment (24). The yeast *Saccharomyces kluyveri* also contains two structurally different DHODs. One is closely related to the *Schizosaccharomyces pombe* mitochondrial Class 2 enzyme. The other resembles the *Saccharomyces cerevisiae* cytosolic Class 1A fumarate-utilizing DHOD (27).

Medical Implications

Due to the importance of pyrimidines, the enzymes of the *de novo* pyrimidine biosynthetic pathway have become drug targets. DHODs from both classes have been

investigated as drug targets for a variety of diseases. The Class 2 enzyme from humans has been an active drug target for years. Rapidly proliferating cells, such as cancer cells (28) or activated T-lymphocytes (29), require *de novo* biosynthesis to supply the pyrimidines needed for growth. Because of this, human DHOD has been targeted for the treatment of cancer and rheumatoid arthritis. Brequinar, an antitumor and immunosuppressive agent, and leflunomide, a pro-drug whose active metabolite, A77 1726, is an immunosuppressive agent, are two DHOD inhibitors that have gone through clinical trials (30-35). Both these medications have side effects, some being severe (30, 36-41). Nonetheless, leflunomide has been used clinically for the treatment of rheumatoid arthritis. Work continues on developing inhibitors directed at the human DHOD (42).

Other Class 2 enzymes have also been investigated as potential drug targets. DHODs from *Candida albicans* (a pathogenic yeast species) (43), *Helicobacter pylori* (the cause of most gastric ulcers) (44), and *Plasmodium falciparum* (the malarial parasite) (45-48) are all currently being investigated. Most Class 2 DHOD inhibitors bind at or near the ubiquinone-binding site. Sequence variability in this region has allowed the development of species-specific inhibitors. Consequently, this region is referred to as the

"species-selective inhibitor site" (48). Species-specific inhibitors have been discovered for both *P. falciparum* and *H. pylori*.

Class 1A DHODs are also intriguing drug targets, though they have received less attention. As mentioned earlier, two trypanosomes contain only Class 1A DHODs. Genetic studies have shown that DHOD is essential for the survival of *Trypanosoma cruzi* (49), validating DHOD as a drug target. This pyrimidine-binding site is structurally very similar to the pyrimidine-binding site of Class 2 enzymes, suggesting that it would not be a good target for specific inhibition. Nonetheless, small molecules that bind specifically to Class 1A DHODs have been discovered (50, 51). The underlying reason for the specificity of these compounds is not understood, especially since the pyrimidine binding sites in both classes of enzymes appear to be nearly identical. However, these compounds demonstrate the possibility of creating inhibitors specific for Class 1A enzymes.

Structures

Several structures of DHODs have been solved. There is at least one structure from each class/subclass, allowing us to compare and contrast the features of all DHODs. Structures of Class 2 enzymes from human (42, 52, 53), rat (54), *Plasmodium falciparum*

(47), and *Escherichia coli* (55) can be found in the PDB. Structures of Class 1A DHODs from *Lactococcus lactis* (51, 56-58), *Trypanosoma cruzi* (59, 60), *Trypanosoma brucei* (23), and *Enterococcus faecalis* (Rider, L. R. and Palfey, B. A., unpublished results) have been solved. Structures of only one Class 1B DHOD have been solved, the enzyme from *Lactococcus lactis* (61). DHODs have been solved in complex with inhibitors, products, and substrates.

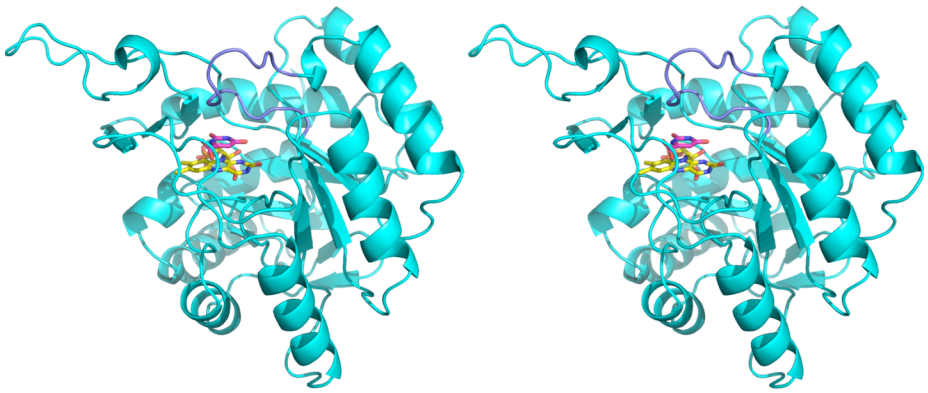

Figure 1-6: Stereo View of the TIM Barrel of DHODs

A monomer of the Class 1A enzyme from *L. lactis* is shown in cyan, with the FMN in yellow. The TIM barrel of all DHODs is very similar. The product OA is shown in pink. The active site loop is shown in purple. Coordinates taken from 2dor.

All DHODs have an $(\alpha/\beta)_8$ motif with a parallel eight-stranded β-barrel surrounded by eight α-helixes (Figure 1-6). The FMN prosthetic group is found at the C-terminal end of the barrel. DHO, OA, and inhibitors such as dihydrooxonate and

dihydroxybenzoates bind a cavity on the *si* face of the flavin that is occupied by water molecules in ligand-free structures. In all structures, a loop covers the active site and is proposed to be responsible for allowing substrate access. Neither the binding of ligands nor changes to the redox state of the flavin cause any large conformational changes in the crystallized protein, although some mutations open the active site loop.

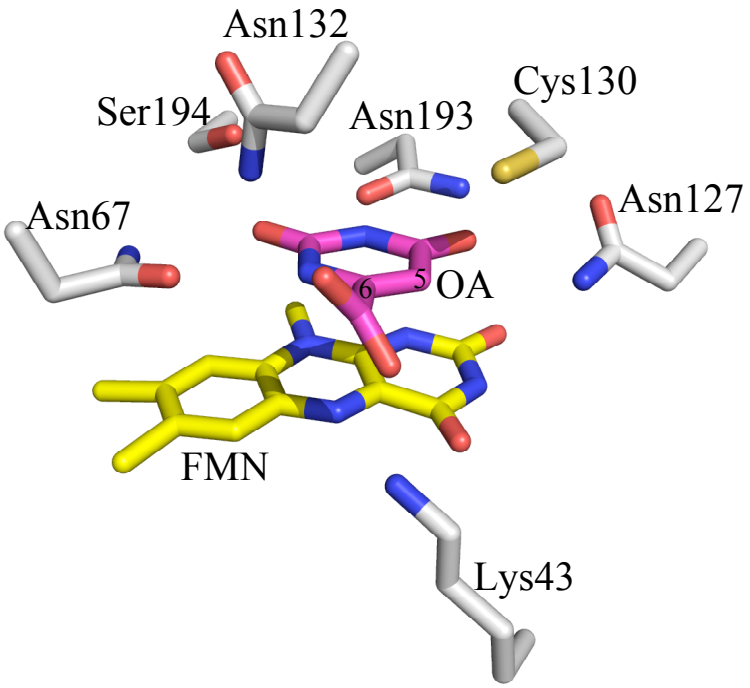

Figure 1-7: Pyrimidine-Binding Site of DHODs

The pyrimidine-binding site of the Class 1A DHOD from *L. lactis* is shown, but the pyrimidine-binding site of all DHODs is very similar. A ring of highly conserved residues make hydrogen bonds with OA (pink). OA stacks above the flavin (yellow) with C6 of OA in van der Waals contact with N5 of FMN. The active site base (Cys130) is positioned above C5 of OA. Coordinates taken from 2dor.

The pyrimidine-binding site is nearly identical in all classes of enzymes (Figure 1-7). Several strictly conserved residues make hydrogen bonds to the pyrimidine. Asparagine residues make hydrogen bonds to N3, N1, the C4 carbonyl, and the carboxylate of DHO/OA in all structures solved to date. In addition, the carboxylate of DHO/OA is hydrogen-bonded to two backbone amines and a conserved lysine residue. In all complexes, DHO/OA (or other pyrimidine-like molecules) is stacked parallel to the isoalloxazine ring of the flavin. C6 of DHO/OA is in van der Waals contact with N5 of the flavin and the active site base is positioned above C5 for deprotonation. The protein interactions with FMN are very similar in all DHODs.

Despite each being a TIM barrel, class-specific structural features exist. Class 2 enzymes are monomeric membrane-bound proteins (5). They contain a highly variable N-terminal extension that is responsible for membrane association (62). The extreme N-terminal hydrophobic helix is often removed to facilitate overexpression and crystallization. Nonetheless, the N-terminal extension folds into a separate domain that contains two α-helices. This domain is found on top of the catalytic $(\alpha/\beta)_8$ domain close to the FMN binding site (Figure 1-8). This domain contributes to the formation of a tunnel-like pocket that leads to the 7,8-dimethyl edge of the flavin. Many inhibitors of Class 2 DHODs, including brequinar and the active metabolite of leflunomide, bind in

this pocket. This pocket is also proposed to be the quinone-binding site, although no structure has yet been reported with bound quinone. Thus, Class 2 DHODs have two substrate binding-sites. The sequence variability in this region has led to the design of species-specific Class 2 inhibitors. Class 2 enzymes have a conserved tyrosine in this quinone-binding tunnel that is in contact with the flavin near the 7,8-dimethyl edge. This residue is responsible for quenching the fluorescence of Class 2 enzymes (63). Class 1 DHODs do not contain this tyrosine and therefore are fluorescent.

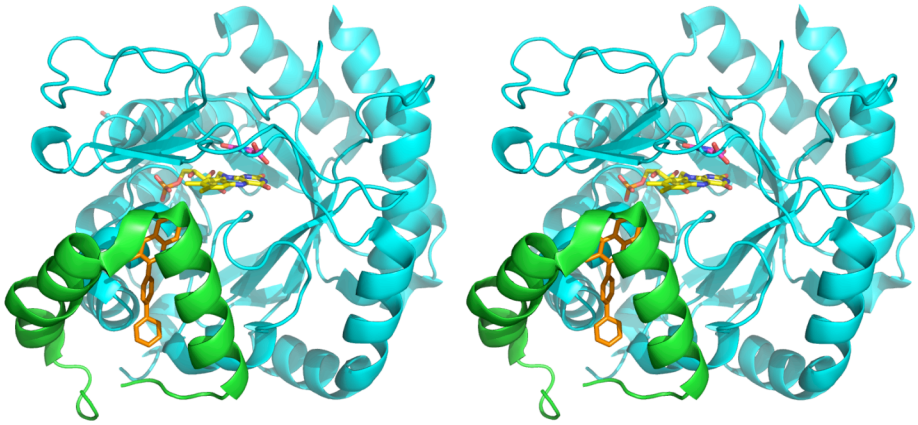

Figure 1-8: Stereo View of Class 2 DHODs

The Class 2 DHOD from *H. sapiens* is shown. The TIM barrel is shown in cyan. The N-terminal domain (green) help create a tunnel-like binding pocket leading to the edge of the flavin (yellow). Inhibitors bind in this pocket (Brequinar – orange). OA (pink) is bound in the pyrimidine-binding pocket on the *si* face of the flavin. Coordinates taken from 1d3g.

Small differences exist in the pyrimidine-binding site as well. In addition to the strictly conserved asparagine residues, Class 2 enzymes contain a threonine in the active site that hydrogen-bonds to the C2 carbonyl of DHO. The active site bases differ between the classes. Class 2 enzymes contain a serine. This residue is positioned above C5 of DHO in the proper orientation for deprotonation. The active site serine is hydrogen-bonded to a crystallographic water molecule that sits on a phenylalanine and hydrogen-bonds to a threonine residue, conserved in Class 2 enzymes. These residues are proposed to form a hydrogen-bonding network that helps activate serine as a base and shuttles protons from the active site to bulk solvent (64).

Class 1A enzymes are homodimers of TIM barrels. A conserved salt bridge is observed at the dimer interface of Class 1A enzymes. A strictly conserved lysine residue of one monomer interacts with either a glutamate or aspartate of the other monomer at the dimer interface. Dimer formation is necessary for activity in Class 1A DHODs (65).

The pyrimidine binding-site of Class 1A DHODs is again similar to all other DHODs. In addition to the conserved asparagine residues that interact with DHO/OA, Class 1A enzymes have a serine residue that hydrogen-bonds to the C2 carbonyl of DHO/OA; in Class 2 enzymes, this residue is a threonine. The active site base responsible for deprotonating C5 during DHO oxidation is a cysteine residue. This

residue is found in the same position as the active site serine in Class 2 enzymes, above C5 of DHO/OA in the proper orientation for proton transfer reactions with bound pyrimidines. The putative proton-relay network observed in Class 2 DHODs that connects the active site serine with bulk solvent is not present in Class 1A enzymes. In fact, the active site in these enzymes is much more solvent-exposed in general than the Class 2 enzymes.

The oxidizing substrate used by Class 1A enzymes is fumarate. Complexes of both fumarate (substrate) and succinate (product) have been solved (59; Rider, L. W. and Palfey, B. A., unpublished data). Both ligands bind to the same active site as DHO/OA. Fumarate and succinate bind almost parallel to the isoalloxazine ring of the flavin (Figure 1-9). C2, the site of protonation, sits under the active site cysteine, which acts as an acid in the oxidative half-reaction. C3 is in van der Waals contact with N5 of the isoalloxazine ring of the flavin, properly positioned for hydride transfer. The conserved active site asparagines are involved in either direct or water-mediated hydrogen-bonds to both fumarate and succinate. Thus, Class 1A DHODs contain a single active site for both half-reactions, unlike Class 2 enzymes.

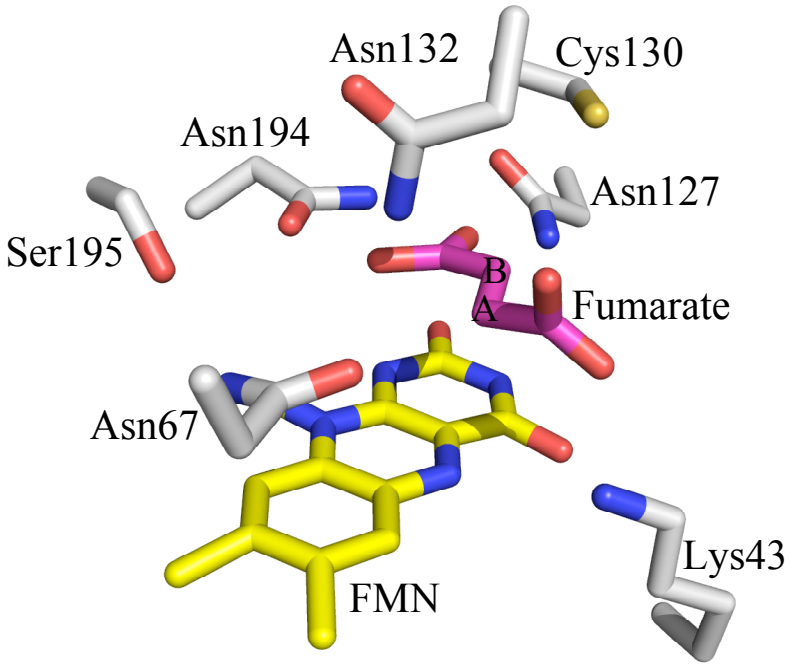

Figure 1-9: Fumarate Complex in Class 1A DHODs

Fumarate (pink) complexed with the Class 1A DHOD from *T. cruzi*. The same active site residues interact with fumarate and dihydroorotate. Fumarate is nearly parallel with the flavin (yellow) with CA in van der Waals contact with N5 of FMN. Cys130 is positioned above CB of fumarate and poised for acid catalysis. Coordinates taken from 2e6d.

The Class 1B enzymes are quite different from either class discussed thus far. Class 1B DHODs are $\alpha_2\beta_2$ heterotetramers. The overall structure is composed of two PyrDb-PyrK heterodimers with a small hydrophobic cavity located in the center. PyrDb is structurally homologous to Class 1A DHODs and contains the site of DHO oxidation (Figure 1-10). As seen in the 1A enzymes, OA is stacked on the *si* face of the flavin and the strictly conserved asparagine residues make hydrogen-bonds to the pyrimidine. In addition, a threonine residue hydrogen-bonds to the C2 carbonyl, as seen in Class 2

enzymes. The active site cysteine is positioned above C5 of OA in the proper orientation for deprotonation, and C6 is in van der Waals contact with N5 of the isoalloxazine of FMN.

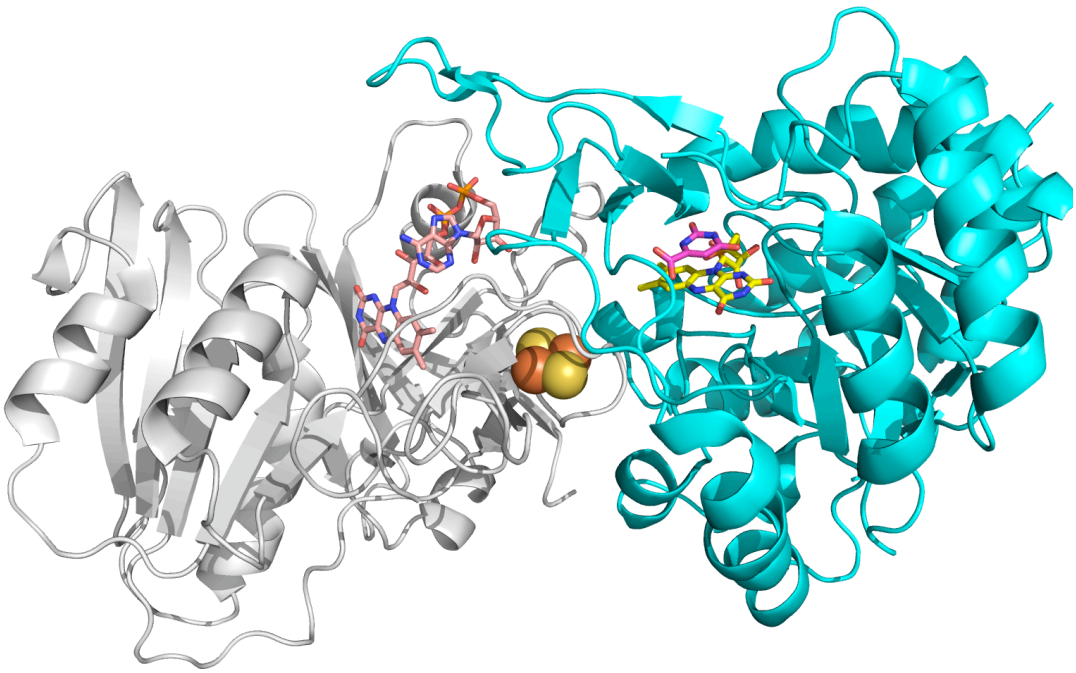

Figure 1-10: Class 1B DHOD Heterodimer

Heterodimer of the PyrDb (cyan) and PyrK (white) proteins from *L. lactis*. PyrDb is a TIM barrel containing the pyrimidine-binding site. OA (pink) is shown stacked above the FMN (yellow). The PyrK subunit contains an FAD (salmon) and an iron-sulfur cluster (space-filling). Coordinates taken from 1ep3.

The PyrK subunit is a member of the NADPH-ferredoxin reductase superfamily (61). Enzymes in this superfamily transfer electrons between pyridine nucleotides and proteins or protein domains. PyrK is made up of three domains. The N-terminal domain

forms a flattened β cylinder composed of six antiparallel β-strands capped by two short helices. This domain binds FAD and is similar to the flavin-binding domain of other members of the superfamily. Interestingly, FAD binds in a conformation in which the adenine and ribityl moieties are stacked (Figure 1-10). This unusual conformation is stabilized in part by a conserved salt bridge between the PyrDb and PyrK subunits found at the bottom of the FAD binding pocket. The interactions between the PyrDb subunit and the PyrK subunit are important for both FAD and iron-sulfur cluster binding. Neither prosthetic group binds tightly to the PryK subunit alone. In addition, FAD binding is required for maintenance of a stable tetrameric structure (61).

The second domain is thought to be an NAD-binding domain. The domain consists of a 5-strand parallel β-sheet sandwiched between two layers of α-helices. It is structurally similar to NAD-binding domains observed in the NADPH-ferredoxin reductase superfamily. The [2Fe-2S] cluster binds to the final domain. This domain is found between the FAD- and NAD-binding domains, with the iron-sulfur cluster close to the FAD-binding site. The iron-sulfur is found between the FAD-binding site of the PyrK subunit and the FMN-binding site of the PyrDb subunit (Figure 1-10), implying a role in electron transfer between the two subunits of the heterodimer (61). Thus,

electrons are likely to flow from DHO to FMN to the iron-sulfur cluster to FAD and finally to NAD or in the reverse direction.

Mechanisms

DHO is converted to OA with concomitant reduction of the enzyme-bound FMN during the reductive half-reaction of all DHODs. The oxidative half-reaction differs between classes of enzymes. Class 2 enzymes react with ubiquinone to regenerate the oxidized form of the flavin (5). Class 1A enzymes, on the other hand, use fumarate as the oxidizing substrate (16), while Class 1B use NAD (17). Thus, the overall catalytic cycle for each class of DHOD is different.

Studying turnover in DHODs is complicated. Flavoenzymes are often able to react with various electron acceptors. Most DHODs react with molecular oxygen, even though it is not thought to be the physiological oxidant. Therefore, DHODs have been assayed as DHO oxidases in the past. Even when using more physiologically relevant substrates, experiments are rarely done in the absence of oxygen, complicating turnover (15, 56). In these instances, the enzyme has two electron acceptors, oxygen and whatever electron acceptor was added. In addition, the physiological oxidizing substrate of Class 2 DHODs, ubiquinone, is not water-soluble, making its use very difficult *in vitro*.

The reduction potential of the enzyme-bound flavin has been studied to give insight into the chemistry. The midpoint potential of the OA/DHO couple is −258 mV (66). The reduction potential for the Class 2 enzyme from *E. coli* is reported as -310 mV (67). In this case, DHO is not a strong enough reducing agent to produce free reduced enzyme. It was instead proposed that the reaction is driven by a substantial increase in the affinity of OA for the reduced enzyme (K_d = 64 nM). This would mean that the reduced-enzyme orotate complex would need to be oxidized for product release to occur. A similar situation has been reported for the flavin-containing enzyme acyl CoA-dehydrogenase (68). The reduction potential of the Class 1A enzyme from *L. lactis* was found to be -245 mV (56). More recently, the reduction potential of *E. coli* DHOD was determined to be -231 mV (Fagan, R. L., unpublished results), near the value determined for the 1A enzyme. If this value is correct, DHO is a strong enough reductant to produce free reduced enzyme. Class 1B enzymes are more complicated. Instead of containing a single prosthetic group, they contain three, making the determination of reduction potentials more difficult. Nonetheless, potentials have been determined for each (69). The midpoint potential of the iron-sulfur cluster was found to be -213 mV (Figure 1-11). The two single-electron potentials of the FMN of the PyrDb subunit were also determined. The oxidized/semiquinone couple was -301 mV and the semiquinone/fully

reduced couple was -252 mV. The potentials of the FAD of the PyrK subunit were -312 mV for the oxidized/semiquinone couple and -297 mV for the semiquinone/fully reduced couple. These potentials allow reduction of the enzyme by both DHO and NADH.

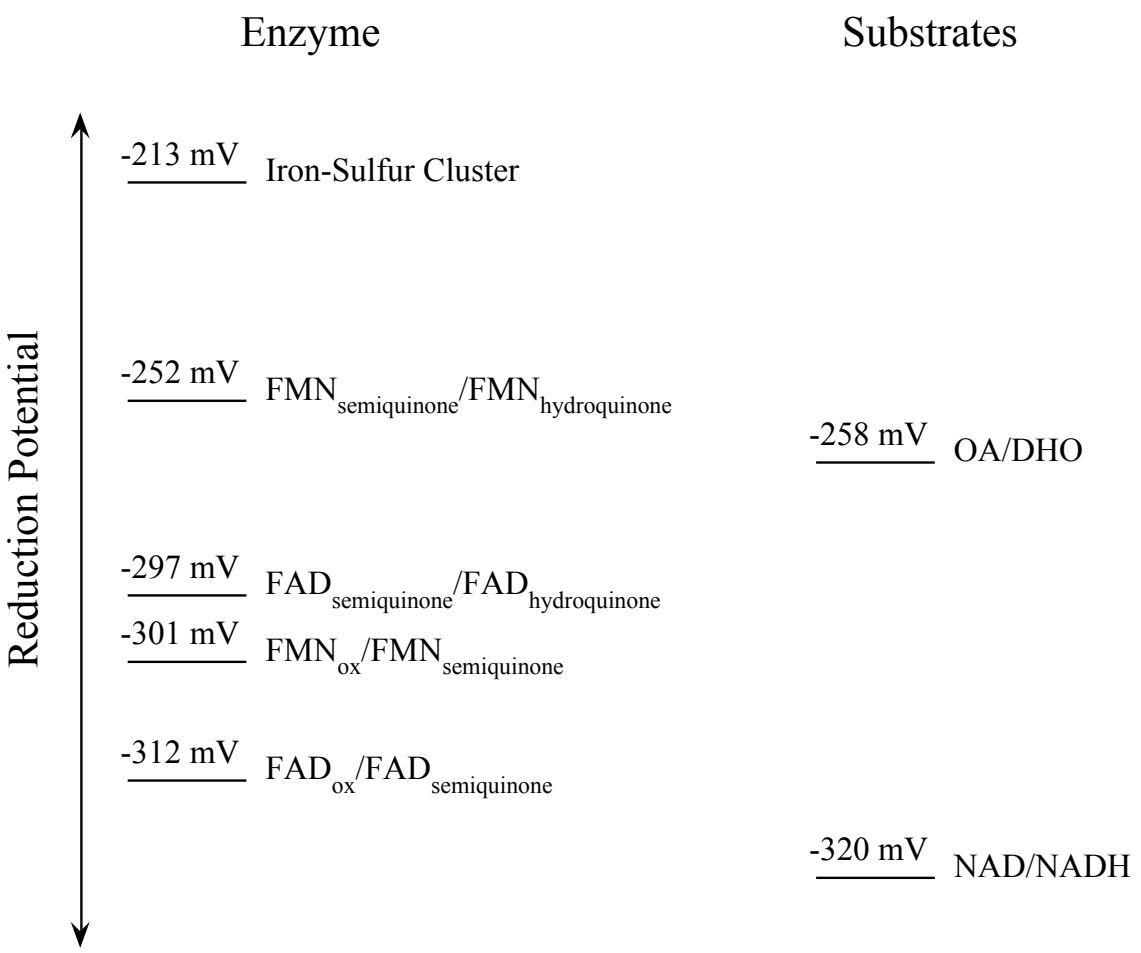

Figure 1-11: Reduction Potentials of Class 1B DHODs

The mechanism of oxidation of DHO by DHODs has been extensively studied due to its biological importance. Using a series of pyrimidine analogs with the Class 2

enzyme from rat, it was shown that the carboxylate on C6 of DHO is required for binding (70). In addition, the nitrogens at positions 1 and 3 were shown to be important for binding. No substituent larger than a methyl group could be tolerated at the C5 position. These results can be explained from the structure of DHODs. As mentioned earlier, the pyrimidine-binding site of all DHODs is nearly identical. The pyrimidine-binding site is small, with no extra room for large substituents on the pyrimidine. In addition, conserved active site residues make hydrogen bonds to N1, N3, and the carboxylate of DHO.

During the reaction of DHO, two carbon-hydrogen bonds are broken. An active site base (serine in Class 2 enzymes and cysteine in Class 1 enzymes) deprotonates the C5 position and a hydride is transferred from C6 of DHO to N5 of the isoalloxazine of FMN. These bonds could break at the same time in a concerted mechanism or sequentially in a stepwise mechanism (Figure 1-12). If a stepwise mechanism was used, one of two intermediates would form. If deprotonation occurs first, an enolate intermediate would form. Conversely, if hydride transfer occurs first, an iminium intermediate would form. The detailed mechanism of this reaction has been studied for years. Using quantum mechanical calculations, it was suggested that the reaction is stepwise with the formation of an enolate intermediate (71). Kinetic isotope effects have been used to experimentally probe the mechanism of various DHODs. DHO deuterated

at the 5-, 6-, or both the 5- and 6-positions were used as substrates, and isotope effects were determined. These experiments have been conducted both in steady-state assays and in reductive half-reaction experiments. Isotope effects determined in the steady-state for the Class 2 DHOD from bovine liver (72) and the Class 1B enzyme from *Clostridium oroticum* (73) were consistent with a concerted mechanism. Conversely, isotope effects determined in the steady-state using O_2 as an electron acceptor for the Class 1A enzyme from *Crithidia fasciculata* (74) were consistent with a stepwise mechanism.

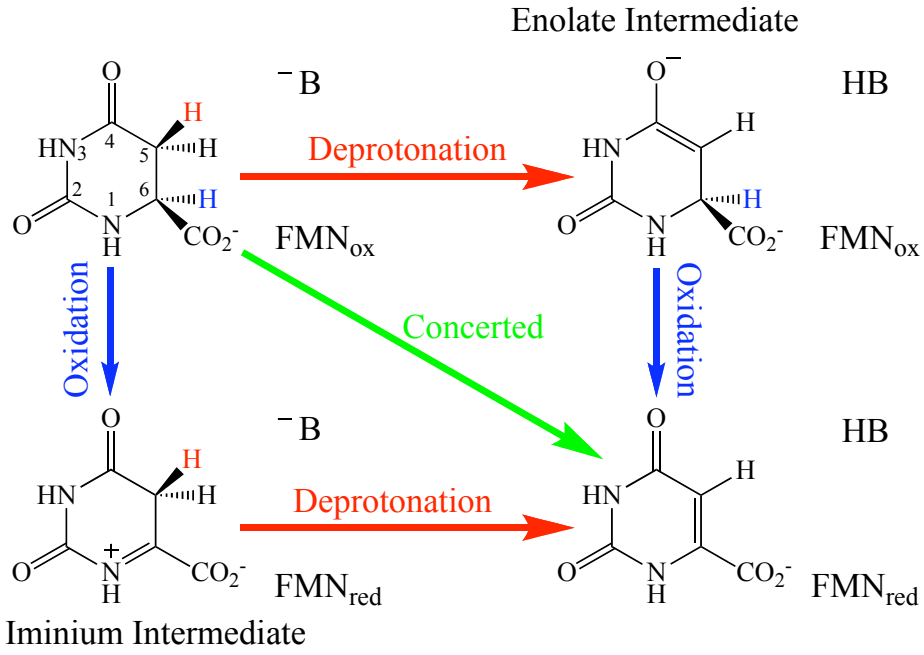

Figure 1-12: Possible Mechanisms of DHO Oxidation

The two carbon-hydrogen bonds of DHO could break simultaneously in a concerted mechanism or sequentially in a stepwise mechanism. If deprotonation occurs first, an enolate intermediate will form. If hydride transfer occurs first, an iminium intermediate will form.

These deuterium isotope effect experiments can instead be conducted by directly observing flavin reduction in the absence of an oxidizing substrate in stopped-flow experiments. In this case, the rate constant of flavin reduction is determined and used to calculate the isotope effects. Using this method, the Class 1A enzyme from *Lactococcus lactis* was found to use a concerted mechanism for DHO oxidation (75; Chapter 2), while the Class 2 enzymes from human and *Escherichia coli* used a stepwise mechanism (76; Chapter 1). When the strictly conserved active site asparagine residues were mutated to alanine, large effects were observed on the rate of flavin reduction in Class 2 DHODs (Chapter 4), while much smaller effects were observed for the Class 1A enzyme (Tirupati, B., unpublished results), suggesting that these residues are important for charge stabilization in the Class 2 DHODs, which use a stepwise mechanism, but are not as important for the Class 1A enzymes, which use a concerted mechanism. The conclusions from the reductive half-reaction experiments contradict those from steady-state kinetics, possibly due to the complexities of interpreting steady-state measurements. Alternatively, the mechanism of DHO oxidation could be species-specific, rather than class-specific.

The effect of pH on DHODs has been studied both by steady-state and transient methods. A pK_a of ~8.3 was observed in the Class 1A enzyme from *L. lactis* when

directly observing flavin reduction in anaerobic stopped-flow experiments (75; Chapter 2). This observed pK_a was attributed to the ionization of the active site cysteine, which acts as a base to deprotonate C5 of DHO during the reductive half-reaction. The pK_a observed in anaerobic stopped-flow experiments conducted with the Class 2 enzymes from human and *E. coli* was ~9 (67, 76; Chapter 1). Crystal structures of Class 2 DHODs show nothing in the active site that would lower the pK_a so dramatically (~4 pH units) from that of an unperturbed serine (77). Kinetic studies suggest that this is a consequence of the stepwise mechanism of DHO oxidation, rather than being a true thermodynamic pK_a. The deuterium isotope effect caused by label at the 5-position of DHO is lost when experiments are performed at pH values above the observed pK_a (76; Chapter 2). Above pH ~9, deprotonation becomes too fast to contribute to the rate of reduction, and the rate is determined only by hydride transfer.

The effects of pH have also been studied under steady-state conditions. In the Class 1B enzyme from *C. oroticum*, the pH dependence on the turnover number was bell-shaped, indicating two pK_a values of ~6.5 and ~9 (73). The pH dependence of the turnover number of the Class 1A enzyme from yeast showed only one pK_a of ~6.5 (78). In the Class 1A enzyme from *T. brucei*, a bell-shaped pH dependence on the turnover number of was observed with pK_a values of ~6.3 and ~9 (23). In all cases, the lower pK_a

was thought to represent the active site cysteine. The pH dependence of the turnover number of the Class 2 enzyme from bovine liver also showed two pK_a values, ~7.3 and ~8.3 (79). In this instance, the higher of the two (~8.3) was proposed to represent ionization of the active site base. In all instances, the pK_a values observed in the steady-state are much lower than those observed when directly watching flavin chemistry in stopped-flow experiments. The kinetic complexity of steady-state measurements could account for the observed differences in pH dependencies.

The oxidative half-reaction of DHODs is much less well-studied. Experiments using the physiological oxidizing substrate for each class have not been reported. Some experiments looking at the rate of oxidation of the enzyme-bound flavin have been conducted on Class 2 DHODs (48, 67). In these experiments, enzyme was reduced with nearly stoichiometric amounts of DHO or dithionite in the absence of oxygen. The reduced enzyme was then mixed with varying electron acceptors including oxygen, ferricyanide, and the ubiquinone analogs menadione and CoQ_1. The physiological substrate, ubiquinone, is not very soluble in water and therefore has not been studied extensively. With the quinone analogs, oxidation was rapid, with full flavin oxidation observed within 1 s (48, 67). It should be noted that the quinone-binding pocket leads to the 7,8-dimethyl edge of FMN (55). In addition, OA release from the *E. coli* enzyme was

shown to be very slow, so that during turnover, the quinone must react with the reduced enzyme-orotate complex (67). Thus, a quinone substrate does not have access to N5 of FMN, and flavin oxidation must occur by two single-electron transfers rather than a direct hydride transfer.

Dihydropyrimidine Dehydrogenases

Biological Importance

Pyrimidine degradation is catalyzed by three enzymes. This pathway converts uracil to β-alanine and thymine to β-aminoisobutyrate. The initial step in the pathway is catalyzed by the complex flavoprotein dihydropyrimidine dehydrogenase (DPD). This is the rate-limiting step in pyrimidine degradation. DPD catalyzes the NADPH-dependent conversion of uracil or thymine to the corresponding 5,6-dihydropyrimidine (Figure 1-13). The dihydropyrimidine is subsequently hydrolyzed between N3 and C4 by dihydropyrimidinase, a binuclear zinc enzyme. In the final step, the β-ureidopropionate or β-ureidoisobutyrate is hydrolyzed to ammonia, carbon dioxide, and β-alanine or β-aminoisobutyrate by β-alanine synthase (80). β-alanine is a putative neurotransmitter. In mammals, the pyrimidine degradation pathway is the leading supplier of β-alanine (81).

In fact, defects in DPD activity in humans are known to cause disorders with mental retardation, epileptic attacks, and convulsions as the predominant symptoms (82, 83).

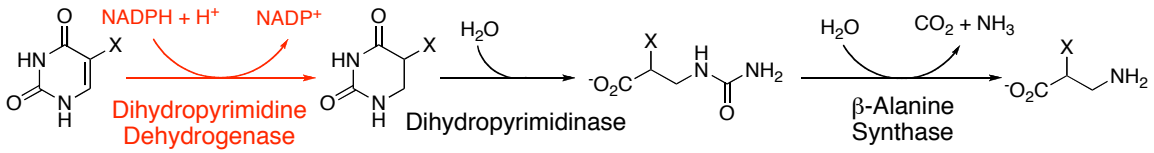

Figure 1-13: Pyrimidine Degradation

The first step of the pyrimidine degradation pathway, a reduction, is catalyzed by the flavin-containing enzyme dihydropyrimidine dehydrogenase (DPD). For uracil, X=H; for thymine, X=CH_3

DPD is a cytosolic enzyme. Activity has been found in many mammalian tissues, with the highest activity found in liver cells (84). DPD has been purified from the liver tissue of many organisms including rat (85, 86), pig (87, 88), cow (89), and human (90). The advancement of molecular biology techniques has allowed the cloning and overexpression in *E. coli* of pig liver DPD (88).

Medical Implications

5-Fluorouracil (5FU) is a commonly prescribed chemotherapeutic agent for the treatment of colorectal, breast, and head/neck cancer. 5FU, after its conversion to the deoxynucleoside monophosphate, blocks DNA synthesis by inhibiting thymidylate

synthase, the enzyme that converts dUMP to dTMP (91). 5FU is also a substrate for DPD. In fact, it is estimated that more than 80% of the administered dose of 5FU is rapidly degraded by DPD (92). Due to this rapid degradation, the efficiency of 5FU is severely lowered and extremely high doses are required. In addition, the degradation of 5FU leads to fluorinated products, such as F-β-alanine, that cause severe side effects (93, 94). Therefore, DPD activity is an important consideration in 5FU treatment.

DPD activity has been shown to vary widely in patients (95, 96), complicating the use of 5FU. Several polymorphisms and mutations within the human DPD gene have been associated with reduced DPD activity (97-99). Three to five percent of Caucasian cancer patients have been reported to have low DPD activity (100). Patients with low DPD levels are vulnerable to toxic affects caused by doses of 5FU calibrated to a level that anticipates high clearance. However, DPD activity is hard to accurately measure and current peripheral mononuclear blood cell assays do not provide reliable results (101, 102). Because of this, it has been suggested that patients undergo genotyping before 5FU treatment is administered. However, only small-scale studies have been completed. In one such study, genetic causes could only be found in 8 of 14 patients exhibiting 5FU toxicity (103). Currently, the predictive value of genotyping the DPD gene is called into question since the genotype-phenotype correlation is incomplete (100).

An alternative approach would be to inhibit the pyrimidine degradation pathway to increase the efficiency of 5FU (104). Compounds aimed at inhibiting DPD are being developed. These compounds would be administered in conjunction with 5FU. Mechanistic and structural information about DPD could aid in effective inhibitor design.

Structures

The only DPD to be crystallized to date is the enzyme from pig liver. Structures of ligand-free enzyme and various complexes have been solved (105, 106). The enzyme is a homodimer, with each monomer containing one FMN, one FAD, and four [4Fe-4S] clusters (87, 107-109).

Each monomer contains five domains (Figure 1-14). Domain I contains two iron-sulfur clusters. The first iron-sulfur cluster is coordinated by four cysteine thiols. However, the second is coordinated by three cysteine thiols and the side-chain of a glutamine residue (105, 106). The glutamine side-chain-iron distance is significantly shorter than the cysteine thiol-iron distances found in DPD. Domain I is exclusively α-helical in secondary structure and resembles the second domain of fumarate reductase from *E. coli*, also an iron-sulfur containing flavoprotein (99).

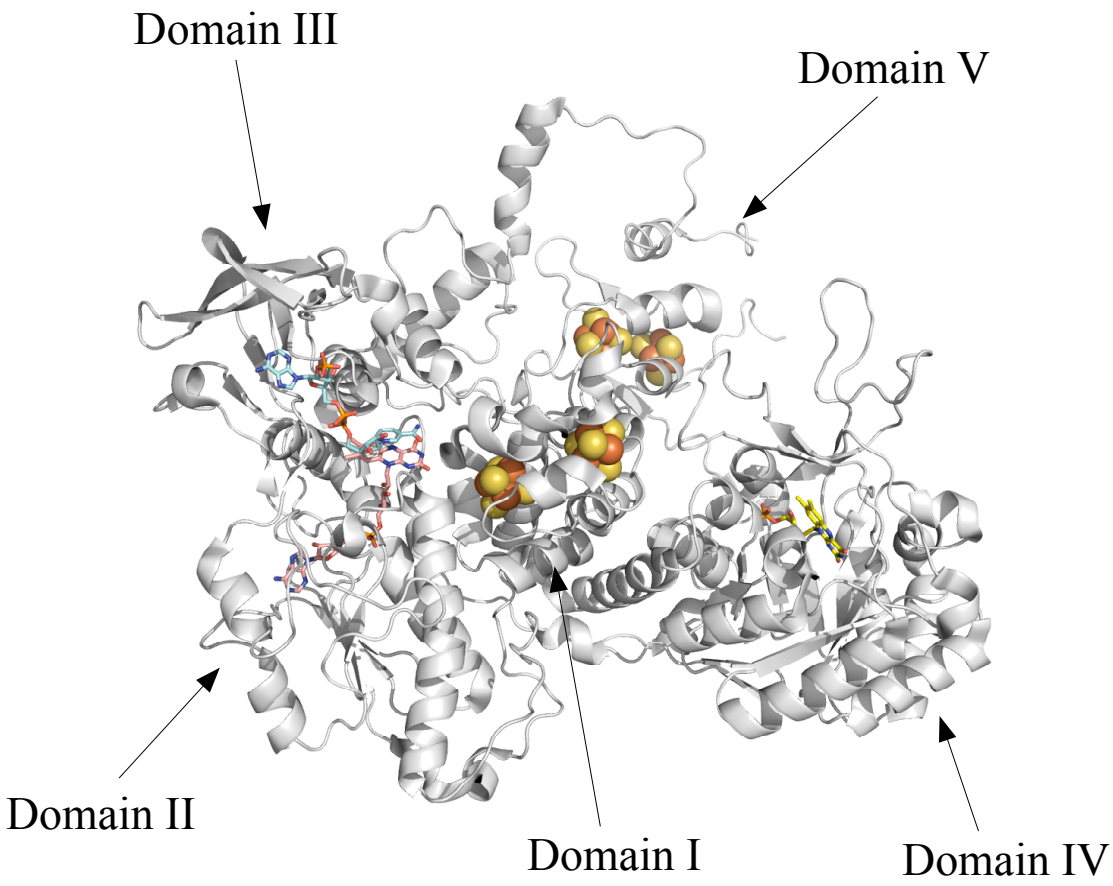

Figure 1-14: Monomer of Dihydropyrimidine Dehydrogenase

The [4Fe-4S] clusters of domains I and V are shown in space-filling. FAD in domain II is shown as salmon. NADPH in domain III is shown in cyan. Domain IV is a TIM barrel containing an FMN (yellow). Coordinates taken from 1gth.

Domains II and III contain the FAD-binding site and the NADPH-binding site, respectively (105, 106). The topologies of these domains are similar to one another and it is possible that they originated from gene duplication. These domains are structurally homologous to bovine adrenodoxin reductase (99). FAD is bound in an extended

conformation, as seen in adrenodoxin reductase, with its adenosine moiety buried in domain II. The isoalloxazine ring of FAD is pointed towards the NADPH-binding site.

Domain IV of DPD is structurally homologous to Class 1A DHODs. In fact, domain IV and the Class 1A DHOD from *L. lactis* share 22% sequence identity and 61% sequence homology (99). Domain IV, like DHODs, is a TIM barrel with FMN bound at the C-terminal end of the barrel. The residue side-chains interacting with FMN in both enzymes are well conserved. This domain also contains the pyrimidine-binding site, which will be described in detail later.

The final domain, domain V, contains two iron-sulfur clusters. In both clusters, the irons are coordinated only by cysteine thiols. This domain resembles bacterial eight-iron ferredoxins (110) with two α-helices on one side of the clusters and four antiparallel β-strands on the other side. The two [4Fe-4S] clusters of domain V are distant from any other redox centers in the monomer.

The monomers of the DPD dimer are related by a non-crystallographic 2-fold axis. In the dimer, domain V interacts more with domains I and IV of the other subunit than with any domains in its subunit. This means that two electron transfer chains exist in each DPD dimer and these chains cross the dimer interface twice. Thus, the two flavins are located on opposite ends of the protein and connected via the C-terminal Fe-S

domain from the same monomer and the N-terminal Fe-S domain from the other monomer (Figure 1-15). This would mean that DPD is only active as a dimer (99).

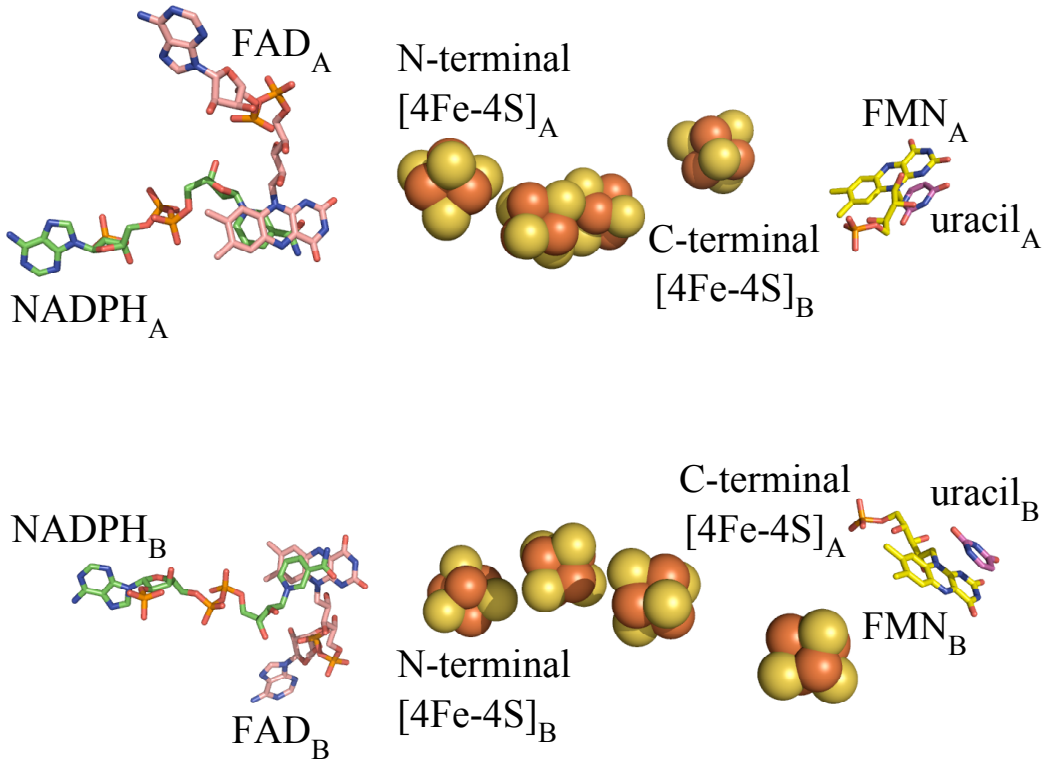

Figure 1-15: Redox Centers in Dihydropyrimidine Dehydrogenase

The DPD dimer contains two redox chains each made up of prosthetic groups from both subunits. The protein has been removed for clarity. Uracil, purple; FMN, yellow; [4Fe-4S] clusters, space-filling; FAD, salmon; NADPH, green. The subscripts indicate which subunit each prosthetic group belongs to. Coordinates taken from 1gth.

As mentioned earlier, domain IV contains both FMN and the pyrimidine-binding site. As with DHODs, the pyrimidine-binding site is found on the *si* face of the flavin. In DPD, pyrimidine substrates and inhibitors bind almost parallel to the isoalloxazine of the

flavin (Figure 1-16), replacing several ordered water molecules found in the ligand-free structure (105). In all complexes, conserved active site asparagines and a threonine make hydrogen bonds to the pyrimidine. As in DHODs, a flexible loop covers the active site. In ligand-free structures and structures determined at pH 4.7, this loop is in an open conformation and the active site is exposed to solvent (106). However, in the complexes

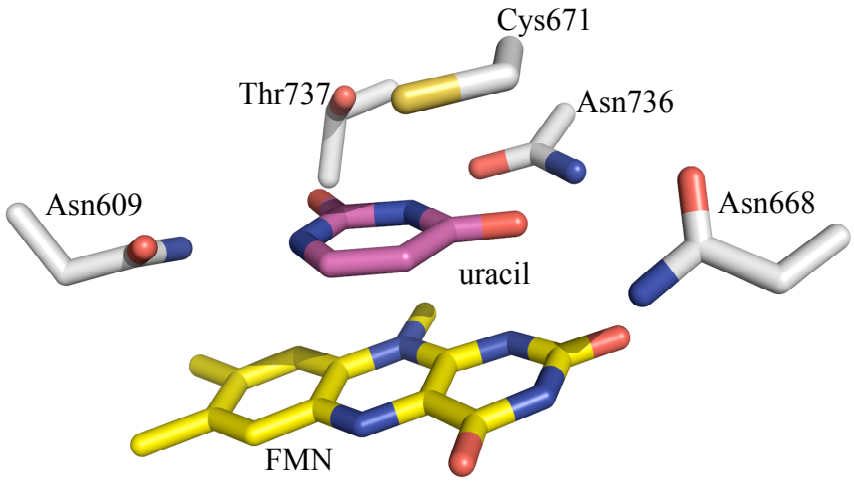

Figure 1-16: Pyrimidine-Binding Site of Dihydropyrimidine Dehydrogenase

Uracil (purple) stacks above the flavin (yellow). Conserved hydrogen-bonding residues are found in the active site, similar to dihydroorotate dehydrogenase. The active site acid (Cys671) is position above C5 of uracil for protonation. Coordinates taken from 1gth.

solved at pH 7.5, the loop is closed over the active site (105). With the active site loop in the closed position, Cys 671 is positioned above C5 of the pyrimidine. This residue is the active site acid required to protonate the C5 position of the pyrimidine, and is in a similar

position to the active site base found in DHODs (which catalyze the reverse reaction). In addition, when the active site loop is closed, a small hydrophobic pocket is formed adjacent to the pyrimidine binding-site. These residues create a hydrophobic environment for the methyl group found at C5 of thymine. The residues are located far enough away from the pyrimidine-binding site to allow larger substituents at C5 as well.

Mechanism

DPD catalyzes the NADPH-dependent reduction of uracil or thymine to the corresponding 5,6-dihydropyrimidine. In the reductive half-reaction, the enzyme-bound FAD on one end of the protein is reduced by NADPH (Figure 1-17). The C4 *pro-S* hydrogen of NADPH is transferred to N5 of the isoalloxazine of FAD (111). The electrons are then passed to the FMN on the opposite end of the protein, presumably via the iron-sulfur clusters. The reduced FMN then reacts with the pyrimidine in the oxidative half-reaction to generate oxidized flavin and the dihydropyrimidine.

Steady-state analysis of DPD in the presence of 2,6-dihydroxypyridine, a competitive inhibitor of uracil, resulted in a set of parallel lines when NADPH was the varied substrate, indicating a ping-pong mechanism (112). In addition, product inhibition and dead-end inhibition by both ADP-ribose and 2,6-dihydroxypyridine suggested a two-

site ping-pong kinetic mechanism (99). Structures of DPD clearly show that the enzyme contains two separate binding sites on opposite ends of the enzyme in accordance with the kinetic analysis.

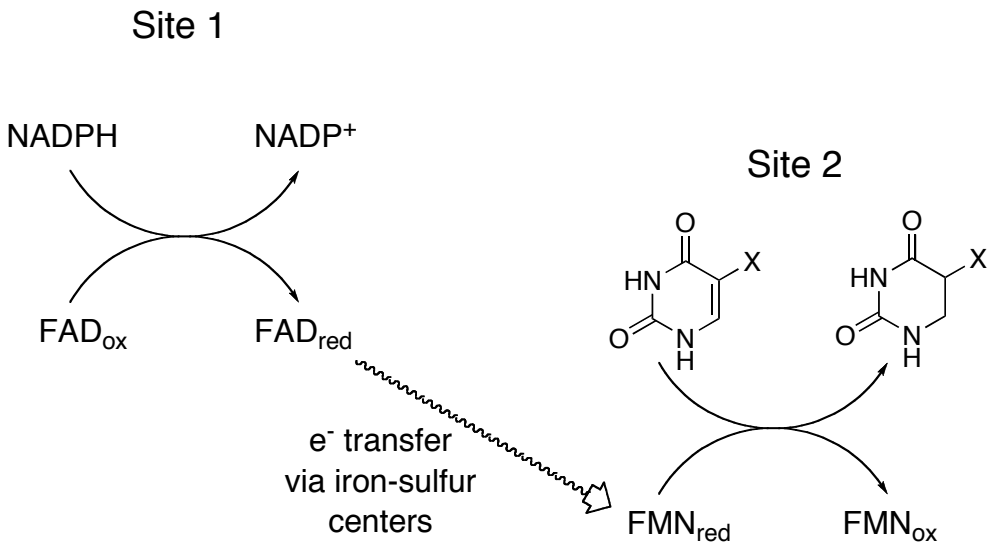

Figure 1-17: Mechanism of Dihydropyrimidine Dehydrogenase

NADPH reduces the FAD at one end of the enzyme. Electrons are then passed from FAD to FMN found at the other end of the enzyme via the iron-sulfur clusters. A hydride is then transferred from N5 of FMN to C6 of the pyrimidine and an active site acid protonates C5 of the pyrimidine.

The mechanism of DPD has been studied using both primary and solvent isotope effects (113). When using NADPD, an isotope effect of 1.1 on V/K_{NADPH} was observed, suggesting that hydride transfer is not rate limiting. However, large solvent isotope effects were observed (~2 on V/K_{NADPH} and ~3 on V). This was taken as evidence that

the reductive half-reaction is limiting during turnover and that one or more proton transfers accompany the rate-limiting step. It is thought that the structural rearrangement that accompanies NADPH binding is reflected in the solvent isotope effects. The crystal structures show that many hydrogen-bonds must be broken and reformed to convert between the nonproductive and productive NADPH-bound states.

The pH dependence of DPD activity has been also studied (113). Looking at effects on V/K_{NADPH} and V/K_{uracil} gives information about the two protein active sites. Two pK_a values are observed in the V/K_{NADPH} profile, 5.8 and 8.2. In addition, the inhibition constant observed for ADP-ribose, an inhibitor competitive with NADPH, was pH independent, suggesting that the observed pK_a values represent protein groups and not ionizable groups on the ligand. The structures show that there are no protein residues with titrable groups that are in the proper position to be important for catalysis. It has been suggested that both pK_a values reflect the pH-dependent conformational changes of the protein (99). The pH profile of V/K_{uracil} is also bell-shaped, giving pK_a values of 5.6 and 9.1 (113). The inhibition constant of 2,6-dihydoxypyridine also has a bell-shaped pH dependence. However, uracil does not contain ionizable groups in this range, again suggesting that both observed pK_as represent enzyme groups important for binding and catalysis. The lower pK_a was assigned to the active site cysteine needed to protonate the

pyrimidine. The higher pK_a was assigned to an active site lysine residue postulated to stabilize the reduced flavin at N1 (99).

The oxidative half-reaction of DPD is analogous to the reverse of the reductive half-reaction of DHODs discussed earlier. The reaction catalyzed by DPD involves hydride transfer from N5 of FMN to C6 of the pyrimidine and protonation at C5 via an active site acid. The structures show that a cysteine residue is positioned to act as the acid. Class 1A DHODs, which share high sequence homology with DPDs also contain an active site cysteine. Mutating the active site cysteine to alanine resulted in a large decrease in DPD activity, with the mutant enzyme retaining only 1% of wild-type activity (108). Mechanism-based inactivators that alkylate the active site cysteine have also been described. 5-Iodouracil is both a substrate and an inactivator of DPD (89). DPD catalyzes the NADPH-dependent reduction of 5-iodouracil to generate 5-iodo-5,6-dihydrouracil. This compound can act as an alkylating agent similar to iodoacetamide. 5-Iodo-5,6-dihydrouracil alkylates the active site cysteine required for catalysis, hence rendering the enzyme inactive. 5-Ethynyluracil was also shown to inactivate DPD in a similar manner (114).

Secondary-tritium isotope effects were used to probe the protonation reaction at C5 of uracil. The observed isotope effect was inverse in H_2O and became more inverse

in D_2O, nearing the equilibrium isotope effect expected for an sp^2 to sp^3 change (115). These data were taken as evidence of a stepwise mechanism with a late transition state for proton transfer. Deuterium isotope effects determined in anaerobic stopped-flow experiments show that Class 1A DHODs use a concerted mechanism (75). Even with the high degree of similarity between the two enzymes, it seems like they use different mechanisms to catalyze similar reactions.

The electron transfer reactions between the flavins have been difficult to study. Anaerobic titrations of the enzyme with NADPH or dihydrouracil resulted in the reduction of one flavin per subunit of enzyme (108). Thus, it is possible to reduce FAD or FMN, but not the iron-sulfur clusters of the enzyme. In addition, no EPR-active species was present in the ligand-free enzyme and only small amounts of flavin semiquinone were observed when enzyme was titrated anaerobically with NADPH or dihydrouracil (107). When enzyme was reduced with dithionite in the absence of oxygen at pH 9.5, two [4Fe-4S] clusters were identified. Both clusters had a reduction potential of ~ -0.4 V. The other two clusters could not be identified under any circumstances tried (107). The extremely low potentials of the iron-sulfur clusters called into question their participation in the chemical reaction. However, the crystal structures clearly show the flavins on opposite ends of the protein connected via the iron-sulfur clusters.

Dihydrouridine Synthase

Biological Importance

tRNAs contain a variety of modifications. Dihydrouridine is the result of one of the most common modifications and is present in eubacteria, eukaryotes, and some archea (116). Dihydrouridine is found mainly in the D-loop of tRNAs. This modification is formed by reduction of the double-bond of uridine (Figure 1-17) via the recently discovered flavin-containing enzyme dihydrouridine synthase (DUS) (117, 118). The four DUS enzymes in *Saccharomyces cerevisiae* each show distinct site-specificity on tRNA, with each enzyme oxidizing either one or two specific uridines in tRNA (119).

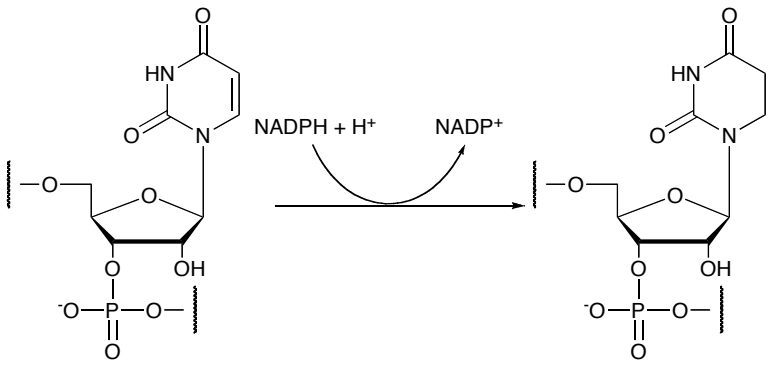

Figure 1-18: Reaction Catalyzed by Dihydrouridine Synthase

The biological role of dihydrouridine is not understood. NMR studies have shown that dihydrouridine increases conformational flexibility in tRNAs because its non-

planar structure disrupts base stacking interactions (120). In addition, it is known that dihydrouridine content varies among species, such that cold-weather species contain the highest amount of dihydrouridine while thermophilic species contain the lowest amount and sometimes none at all (121). This is consistent with the conformational flexibility hypothesis. It has also been suggested that RNA is more chemically stable in the absence of dihydrouridine (122). This could also explain the lack of dihydrouridine observed in some thermophilic species – it avoids the hydrolytic ring opening reaction at high temperatures. Recently, it has been shown that tRNAs lacking modification, including dihydrouridine, are degraded very rapidly in vivo, at rates nearing those of mRNA (123). Therefore, the biological role of tRNA modifications could be to protect the RNA from degradation.

Medical Implication

Increased amounts of dihydrouridine are found in cancers (124). Recently, human DUS2 has been shown to be responsible for the increased level of dihydrouridine found in pulmonary carcinomas (125). This makes human DUS a possible drug target. If dihydrouridine protects tRNAs from degradation, then blocking dihydrouridine formation would render the tRNAs susceptible, and presumably slow protein synthesis.

Structure

The structure of DUS from *Thermatoga maritima* has been solved (126). The enzyme is a TIM barrel similar to DHODs, and has a bundle of four α-helices at its C-terminus. Although no structure of a tRNA-enzyme complex exists, the active site can be identified based on the similarity of the enzyme to DHODs and DPDs. The active site of DUS is much more open than those of DHODs or DPDs. This is not surprising; the substrate used by DUS is much larger than the small pyrimidines used by the other enzymes. An active site cysteine residue can be identified, positioned similarly to the active site acid or base found in other pyrimidine metabolizing enzymes. The cysteine in DUS is proposed to act as an active site acid to protonate C5 of uridine during the reaction (127).

Mechanism

Little mechanistic work has been done on DUSs. An *in vivo* DUS-complementation assay has been developed to screen for residues important in catalysis (127). This screen utilizes an *Escherichia coli* strain that has all the DUS genes deleted. The strain is complemented with a plasmid-born DUS and the dihydrouridine content of the tRNA is then determined. This approach was used to identity a cysteine residue that

is essential for DUS activity (127). Using a homology model based on the *T. maritima* structure, this essential cysteine was shown to be the active site acid postulated to protonate C5 of uridine.

The catalytic cycle of DUS presumably can be broken down into two half-reactions. NADPH would bind and reduce the enzyme in the reductive half-reaction. The enzyme would then bind tRNA and catalyze the reduction of the double-bond of uridine in the oxidative half-reaction. This reaction would involve hydride transfer from N5 of the flavin to C6 of uridine and proton transfer from the active site cysteine to C5 of uridine.

Recently, the mechanism of DUS2 from *S. cerevisiae* was investigated (128). The *pro-R* hydrogen of NADPH was transferred to N5 of the isoalloxazine ring of the flavin rapidly in the reductive half-reaction. However, the oxidative half-reaction (reduction of the tRNA uracil) was shown to be extremely slow when using *in vitro* transcribed tRNA as a substrate - much too slow to be physiologically relevant. Using tRNA isolated from a DUS2 knockout strain of yeast, the rate constant increased 600-fold, indicating that other tRNA modifications are needed for DUS activity (128). The importance of the active cysteine was also demonstrated by studying the oxidative half-reaction. When mutated to alanine, the rate constant observed for reducing *in vitro*

transcribed tRNA was similar to that of wild-type. However, when using tRNA isolated from the DUS2 knockout strain of yeast, the mutant enzyme was several orders of magnitude slower than wild-type (128). Thus, the cysteine appears to be an effective acid catalyst only when an appropriately modified tRNA substrate is used. Presumably, the modification positions the substrate in a reactive conformation.

Epilog

The three enzymes described in this chapter each catalyze very similar half-reactions – the oxidation of a carbon-carbon single bond or the reduction of a carbon-carbon double bond in pyrimidine substrates. The other half-reactions vary widely. The similarities in the flavoprotein domain performing pyrimidine redox chemistry and the similarity of the catalytic apparatus strongly suggest that DHODs, DPDs, and DUSs evolved from a common precursor. The other half-reaction, often performed by an accessory domain or even another subunit, would represent an adaptation for disparate biological niches.

Each enzyme has similar TIM-barrel cores with an FMN prosthetic group and a pyrimidine-binding site (Figure 1-19). Extra domains help individual enzymes accomplish their particular jobs. Class 2 DHODs, for example, contain an N-terminal

helix bundle that provides the quinone-binding site – the substrate for the non-pyrimidine half-reaction. In contrast, DUS contains an accessory domain – a helical bundle - suspected to be important for tRNA binding, a part of the pyrimidine half-reaction. The other half-reaction with pyridine nucleotide apparently needs no accessory domain.

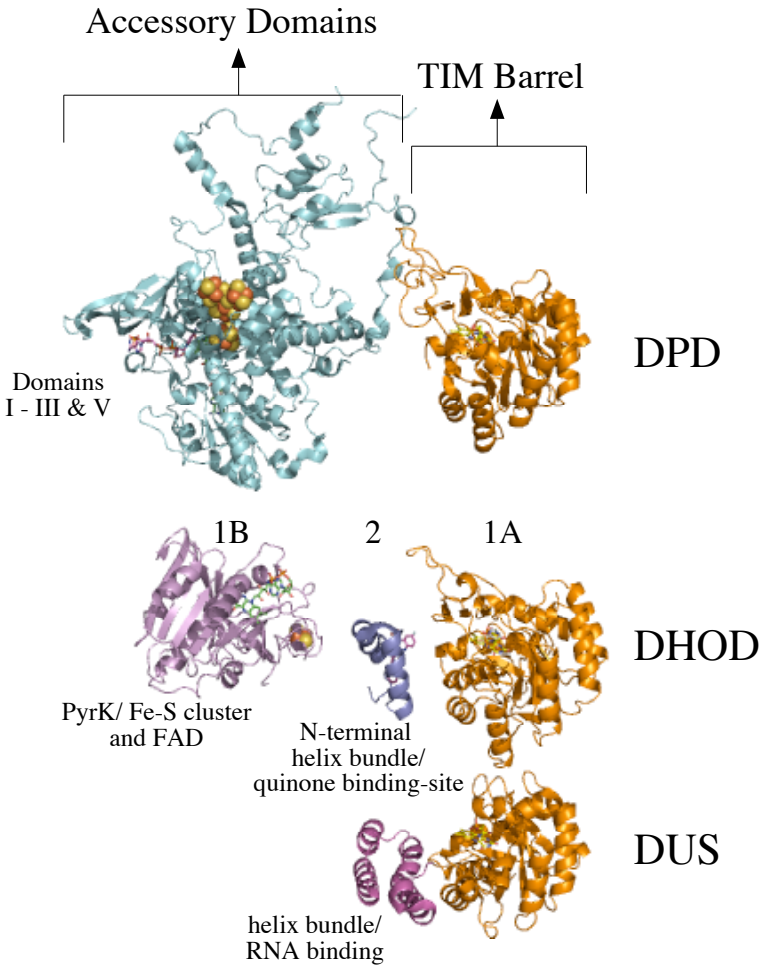

Figure 1-19: Structural Comparison of DHOD, DPD, and DUS

The TIM barrel of each enzyme is shown in orange. The extra domains are shown to the left. FMN, yellow; FAD, green; Fe-S clusters, space-filling; OA (white); Brequinar, purple; NADPH, pink. Coordinates taken from the following pdb files: 1gth, 1ep3, 1d3g, 2dor, and 1vhn.

The mechanisms of pyrimidine oxidation or reduction are accomplished by the same active site residues in these enzymes. In each case, a hydride is transferred between N5 of the isoalloxazine of the flavin and C6 of the pyrimidine, while proton transfer occurs between C5 of the pyrimidine and an active site cysteine or (for Class 2 DHODs) serine. Even with similar active site architectures and pyrimidine reactions, kinetic experiments suggest that the detailed mechanism of pyrimidine oxidation or reduction varies (72-76; 115). While the detailed order of bond-breaking in some of these enzymes remains a question, it is intriguing that enzymes that share so much structural and sequence homology might use alternative mechanisms to accomplish the same chemistry, and that there is enough plasticity to allow diverse non-pyrimidine half-reactions to be accomplished without disrupting that basic features of the pyrimidine half-reaction.

Segue

My thesis work has focused on the detailed mechanisms of DHO oxidation in Class 1A and Class 2 DHODs. While these different phylogenetic classes of enzymes use different substrates in their oxidative half-reactions, in their reductive half-reactions they catalyze the same chemical reaction – the conversion of DHO to OA. The pyrimidine binding site is nearly identical in these two enzyme classes with each class

having an FMN prosthetic group, and active site base (either cysteine in Class 1A enzymes or serine in Class 2 enzymes), and a ring of hydrogen-bonding residues around the pyrimidine. Nonetheless, the work presented here clearly shows these two enzymes classes use different mechanisms to accomplish the same chemistry. Kinetic isotope effects on flavin reduction show that the order of bond breaking is different in the two classes. Site-directed mutagenesis of analogous conserved hydrogen-bonding residues in the active site cause different effects on the kinetics of the reductive half-reaction in each class of enzyme. The active site bases are also different between the classes. The Class 2 enzymes contain a proton-relay system to shuttle protons from the active site to bulk solvent that is not found in the Class 1A enzymes. Even with very similar pyrimidine-binding sites, mechanistic difference have been found and characterized in these two phylogenetic classes of DHODs.

References

1. Evans, D. R. and Guy, H. I. (2004) *J. Biol. Chem.*, **279,** 33035-33038.

2. Weber, G. (2001) *Biochemistry (Moscow)*, **66,** 1164-1173.

3. Fagan, R. L. and Palfey, B. A. (2009) Flavin-dependent enzymes in *Comprehensive Natural Products Chemistry II, Vol 7: Cofactor Biosynthesis and Enzymology* (Begley, T. P.), Elsevier, In Press.

4. Radzicka, A. and Wolfenden, R. (1995) *Science*, **267,** 90-93.

5. Jones, M. E. (1980) *Annu. Rev. Biochem.*, **49,** 253-279.

6. Lieberman, I. and Kornberg, A. (1953) *Biochim. Biophys. Acta.*, **12,** 223-234.

7. Graves, J. L. and Vennesland, B. (1957) *J. Biol. Chem.*, **226,** 307-316.

8. Friedmann, H. C. and Vennesland, B. (1958) *J. Biol. Chem.*, **233,** 1398-1406.

9. Aleman, V. and Handler, P. (1967) *J. Biol. Chem.*, **242,** 4087-4096.

10. Aleman, V., Handler, P., Palmer, G. and Beinert, H. (1968) *J. Biol. Chem.*, **243,** 2569-2578.

11. Aleman, V., Handler, P., Palmer, G. and Beinert, H. (1968) *J. Biol. Chem.*, **243,** 2560-2568.

12. Taylor, W. H. and Taylor, M. L. (1964) *J. Bacteriol.*, **88,** 105-110.

13. Andrews, S., Cox, G. B. and Gibson, F. (1977) *Biochim. Biophys. Acta.*, **462,** 153-160.

14. Forman, H. J. and Kennedy, J. (1978) *Arch. Biochem. Biophys.*, **191,** 23-31.

15. Björnberg, O., Rowland, P., Larsen, S. and Jensen, K. F. (1997) *Biochemistry*, **36,** 16197-16205.

16. Nagy, M., Lacroute, F. and Thomas, D. (1992) *Proc. Natl. Acad. Sci. U. S. A.*, **89,** 8966-8970.

17. Nielsen, F. S., Andersen, P. S. and Jensen, K. F. (1996) *J. Biol. Chem.*, **271,** 29359-29365.

18. Carrey, E. A., Dietz, C., Glubb, D. M., Loffler, M., Lucocq, J. M. and Watson, P. F. (2002) *Reproduction*, **123,** 757-768.

19. Rawls, J., Knecht, W., Diekert, K., Lill, R. and Loffler, M. (2000) *Eur. J. Biochem.*, **267,** 2079-2087.

20. Gero, A. M. and O'Sullivan, W. J. (1990) *Blood Cells*, **16,** 467-484.

21. Painter, H. J., Morrisey, J. M., Mather, M. W. and Vaidya, A. B. (2007) *Nature*, **446,** 88-91.

22. Gao, G., Nara, T., Nakajima-Shimada, J. and Aoki, T. (1999) *J Mol Biol*, **285,** 149-161.

23. Arakaki, T. L., Buckner, F. S., Gillespie, J. R., Malmquist, N. A., Phillips, M. A., Kalyuzhniy, O., Luft, J. R., Detitta, G. T., Verlinde, C. L., Van Voorhis, W. C., Hol, W. G. and Merritt, E. A. (2008) *Mol. Microbiol.*, **68,** 37-50.

24. Andersen, P. S., Jansen, P. J. and Hammer, K. (1994) *J. Bacteriol.*, **176,** 3975-3982.

25. Marcinkeviciene, J., Jiang, W., Locke, G., Kopcho, L. M., Rogers, M. J. and Copeland, R. A. (2000) *Arch. Biochem. Biophys.*, **377,** 178-186.

26. Marcinkeviciene, J., Tinney, L. M., Wang, K. H., Rogers, M. J. and Copeland, R. A. (1999) *Biochemistry*, **38,** 13129-13137.

27. Zameitat, E., Knecht, W., Piskur, J. and Loffler, M. (2004) *FEBS Lett.*, **568,** 129-134.

28. Shawver, L. K., Schwartz, D. P., Mann, E., Chen, H., Tsai, J., Chu, L., Taylorson, L., Longhi, M., Meredith, S., Germain, L., Jacobs, J. S., Tang, C., Ullrich, A., Berens, M. E., Hersh, E., McMahon, G., Hirth, K. P. and Powell, T. J. (1997) *Clin. Cancer Res.*, **3,** 1167-1177.

29. Cutolo, M., Sulli, A., Ghiorzo, P., Pizzorni, C., Craviotto, C. and Villaggio, B. (2003) *Ann. Rheum. Dis.*, **62,** 297-302.

30. Burris, H. A., 3rd, Raymond, E., Awada, A., Kuhn, J. G., O'Rourke, T. J., Brentzel, J., Lynch, W., King, S. Y., Brown, T. D. and Von Hoff, D. D. (1998) *Invest. New Drugs*, **16,** 19-27.

31. Chen, S. F., Papp, L. M., Ardecky, R. J., Rao, G. V., Hesson, D. P., Forbes, M. and Dexter, D. L. (1990) *Biochem. Pharmacol.*, **40,** 709-714.

32. Cherwinski, H. M., McCarley, D., Schatzman, R., Devens, B. and Ransom, J. T. (1995) *J. Pharmacol. Exp. Ther.*, **272,** 460-468.

33. Cramer, D. V. (1995) *Transplant Proc.*, **27,** 80-82.

34. Herrmann, M. L., Schleyerbach, R. and Kirschbaum, B. J. (2000) *Immunopharmacology*, **47,** 273-289.

35. Makowka, L., Chapman, F. and Cramer, D. V. (1993) *Transplant Proc.*, **25,** 2-7.

36. Alldred, A. and Emery, P. (2001) *Expert Opin. Pharmacother.*, **2,** 125-137.

37. Cohen, S., Cannon, G. W., Schiff, M., Weaver, A., Fox, R., Olsen, N., Furst, D., Sharp, J., Moreland, L., Caldwell, J., Kaine, J. and Strand, V. (2001) *Arthritis Rheum.*, **44,** 1984-1992.

38. Emery, P., Breedveld, F. C., Lemmel, E. M., Kaltwasser, J. P., Dawes, P. T., Gomor, B., Van Den Bosch, F., Nordstrom, D., Bjorneboe, O., Dahl, R., Horslev-Petersen, K., Rodriguez De La Serna, A., Molloy, M., Tikly, M., Oed, C., Rosenburg, R. and Loew-Friedrich, I. (2000) *Rheumatology (Oxford)*, **39,** 655-665.

39. Li, E. K., Tam, L. S. and Tomlinson, B. (2004) *Clin. Ther.*, **26,** 447-459.

40. Makowka, L., Tixier, D., Chaux, A., Hill, D., O'Neill, P., Eiras-Hreha, G., Wu, G. D., Cunneen, S., Cajulis, E., Zajac, I. and et al. (1993) *Transplant Proc.*, **25,** 48-53.

41. Pally, C., Smith, D., Jaffee, B., Magolda, R., Zehender, H., Dorobek, B., Donatsch, P., Papageorgiou, C. and Schuurman, H. J. (1998) *Toxicology*, **127,** 207-222.

42. Walse, B., Dufe, V. T., Svensson, B., Fritzson, I., Dahlberg, L., Khairoullina, A., Wellmar, U. and Al-Karadaghi, S. (2008) *Biochemistry*, **47,** 8929-8936.

43. Zameitat, E., Gojkovic, Z., Knecht, W., Piskur, J. and Loffler, M. (2006) *FEBS J.*, **273,** 3183-3191.

44. Copeland, R. A., Marcinkeviciene, J., Haque, T. S., Kopcho, L. M., Jiang, W., Wang, K., Ecret, L. D., Sizemore, C., Amsler, K. A., Foster, L., Tadesse, S., Combs, A. P., Stern, A. M., Trainor, G. L., Slee, A., Rogers, M. J. and Hobbs, F. (2000) *J. Biol. Chem.*, **275,** 33373-33378.

45. Heikkila, T., Ramsey, C., Davies, M., Galtier, C., Stead, A. M., Johnson, A. P., Fishwick, C. W., Boa, A. N. and McConkey, G. A. (2007) *J. Med. Chem.*, **50,** 186-191.

46. Heikkila, T., Thirumalairajan, S., Davies, M., Parsons, M. R., McConkey, A. G., Fishwick, C. W. and Johnson, A. P. (2006) *Bioorg. Med. Chem. Lett.*, **16,** 88-92.

47. Hurt, D. E., Widom, J. and Clardy, J. (2006) *Acta Crystallogr. D Biol. Crystallogr.*, **62,** 312-323.

48. Malmquist, N. A., Gujjar, R., Rathod, P. K. and Phillips, M. A. (2008) *Biochemistry*, **47,** 2466-2475.

49. Annoura, T., Nara, T., Makiuchi, T., Hashimoto, T. and Aoki, T. (2005) *J. Mol. Evol.*, **60,** 113-127.

50. Palfey, B. A., Björnberg, O. and Jensen, K. F. (2001) *J. Med. Chem.*, **44,** 2861-2864.

51. Wolfe, A. E., Thymark, M., Gattis, S. G., Fagan, R. L., Hu, Y. C., Johansson, E., Arent, S., Larsen, S. and Palfey, B. A. (2007) *Biochemistry*, **46,** 5741-5753.

52. Baumgartner, R., Walloschek, M., Kralik, M., Gotschlich, A., Tasler, S., Mies, J. and Leban, J. (2006) *J. Med. Chem.*, **49,** 1239-1247.

53. Liu, S., Neidhardt, E. A., Grossman, T. H., Ocain, T. and Clardy, J. (2000) *Structure*, **8,** 25-33.

54. Hansen, M., Le Nours, J., Johansson, E., Antal, T., Ullrich, A., Loffler, M. and Larsen, S. (2004) *Protein Sci.*, **13,** 1031-1042.

55. Nørager, S., Jensen, K. F., Björnberg, O. and Larsen, S. (2002) *Structure*, **10,** 1211-1223.

56. Nørager, S., Arent, S., Björnberg, O., Ottosen, M., Lo Leggio, L., Jensen, K. F. and Larsen, S. (2003) *J. Biol. Chem.*, **278,** 28812-28822.

57. Rowland, P., Björnberg, O., Nielsen, F. S., Jensen, K. F. and Larsen, S. (1998) *Protein Sci.*, **7,** 1269-1279.

58. Rowland, P., Nielsen, F. S., Jensen, K. F. and Larsen, S. (1997) *Structure*, **5,** 239-252.

59. Inaoka, D. K., Sakamoto, K., Shimizu, H., Shiba, T., Kurisu, G., Nara, T., Aoki, T., Kita, K. and Harada, S. (2008) *Biochemistry*, **47,** 10881-10891.

60. Pinheiro, M. P., Iulek, J. and Cristina Nonato, M. (2008) *Biochem. Biophys. Res. Commun.*, **369**, 812-817.

61. Rowland, P., Nørager, S., Jensen, K. F. and Larsen, S. (2000) *Structure*, **8,** 1227-1238.

62. Björnberg, O., Gruner, A. C., Roepstorff, P. and Jensen, K. F. (1999) *Biochemistry*, **38,** 2899-2908.

63. Shi, J., Palfey, B. A., Dertouzos, J., Jensen, K. F., Gafni, A. and Steel, D. (2004) *J. Am. Chem. Soc.*, **126,** 6914-6922.

64. Small, Y. A., Guallar, V., Soudackov, A. V. and Hammes-Schiffer, S. (2006) *J. Phys. Chem. B*, **110,** 19704-19710.

65. Ottosen, M. B., Björnberg, O., Nørager, S., Larsen, S., Palfey, B. A. and Jensen, K. F. (2002) *Protein Sci.*, **11,** 2575-2583.

66. Krakow, G. and Vennesland, B. (1961) *J. Biol. Chem.*, **236,** 142-144.

67. Palfey, B. A., Björnberg, O. and Jensen, K. F. (2001) *Biochemistry*, **40,** 4381-4390.

68. Thorpe, C. and Kim, J. J. (1995) *FASEB J.*, **9,** 718-725.

69. Mohsen, A. W., Rigby, S. E., Jensen, K. F., Munro, A. W. and Scrutton, N. S. (2004) *Biochemistry*, **43,** 6498-6510.

70. DeFrees, S. A., Sawick, D. P., Cunningham, B., Heinstein, P. F., Morre, D. J. and Cassady, J. M. (1988) *Biochem. Pharmacol.*, **37,** 3807-3816.

71. Mahmoudian, M., Pakiari, A. H. and Khademi, S. (1992) *Biochem. Pharmacol.*, **43,** 283-287.

72. Hines, V. and Johnston, M. (1989) *Biochemistry*, **28,** 1227-1234.

73. Argyrou, A., Washabaugh, M. W. and Pickart, C. M. (2000) *Biochemistry*, **39,** 10373-10384.

74. Pascal, R. A., Jr. and Walsh, C. T. (1984) *Biochemistry*, **23,** 2745-2752.

75. Fagan, R. L., Jensen, K. F., Björnberg, O. and Palfey, B. A. (2007) *Biochemistry*, **46,** 4028-4036.

76. Fagan, R. L., Nelson, M. N., Pagano, P. M. and Palfey, B. A. (2006) *Biochemistry*, **45,** 14926-14932.

77. Bruice, T. C., Fife, T. H., Bruno, J. J. and Brandon, N. E. (1962) *Biochemistry*, **1,** 7-12.

78. Jordan, D. B., Bisaha, J. J. and Picollelli, M. A. (2000) *Arch. Biochem. Biophys.*, **378,** 84-92.

79. Hines, V. and Johnston, M. (1989) *Biochemistry*, **28,** 1222-1226.

80. Traut, T. W. and Loechel, S. (1984) *Biochemistry*, **23,** 2533-2539.

81. Traut, T. W. and Jones, M. E. (1996) *Prog. Nucleic Acid Res. Mol. Biol.*, **53,** 1-78.

82. Al-Sanna'a, N. A., Van Kuilenburg, A. B., Atrak, T. M., Abdul-Jabbar, M. A. and Van Gennip, A. H. (2005) *J. Inherit. Metab. Dis.*, **28,** 793-796.

83. Fiumara, A., van Kuilenburg, A. B., Caruso, U., Nucifora, C., Marzullo, E., Barone, R., Meli, C. and van Gennip, A. H. (2003) *J. Inherit. Metab. Dis.*, **26,** 407-409.

84. Ho, D. H., Townsend, L., Luna, M. A. and Bodey, G. P. (1986) *Anticancer Res.*, **6,** 781-784.

85. Kimura, M., Sakata, S. F., Matoba, Y., Matsuda, K., Kontani, Y., Kaneko, M. and Tamaki, N. (1998) *J. Nutr. Sci. Vitaminol. (Tokyo)*, **44,** 537-546.

86. Shiotani, T. and Weber, G. (1981) *J. Biol. Chem.*, **256,** 219-224.

87. Podschun, B., Wahler, G. and Schnackerz, K. D. (1989) *Eur. J. Biochem.*, **185,** 219-224.

88. Rosenbaum, K., Schaffrath, B., Hagen, W. R., Jahnke, K., Gonzalez, F. J., Cook, P. F. and Schnackerz, K. D. (1997) *Protein Expr. Purif.*, **10,** 185-191.

89. Porter, D. J., Chestnut, W. G., Taylor, L. C., Merrill, B. M. and Spector, T. (1991) *J. Biol. Chem.*, **266,** 19988-19994.

90. Lu, Z. H., Zhang, R. and Diasio, R. B. (1992) *J. Biol. Chem.*, **267,** 17102-17109.

91. Papamichael, D. (2000) *Stem Cells*, **18,** 166-175.

92. Milano, G. and Etienne, M. C. (1994) *Anticancer Res.*, **14,** 2295-2297.

93. Diasio, R. B. (2001) *Oncology (Williston Park)*, **15,** 21-26; discussion 27.

94. Hull, W. E., Port, R. E., Herrmann, R., Britsch, B. and Kunz, W. (1988) *Cancer Res.*, **48,** 1680-1688.

95. Lu, Z., Zhang, R. and Diasio, R. B. (1993) *Cancer Res.*, **53,** 5433-5438.

96. Lu, Z., Zhang, R. and Diasio, R. B. (1995) *Clin. Pharmacol. Ther.*, **58,** 512-522.

97. Kubota, T. (2003) *Int. J. Clin. Oncol.*, **8,** 127-131.

98. Omura, K. (2003) *Int. J. Clin. Oncol.*, **8,** 132-138.

99. Schnackerz, K. D., Dobritzsch, D., Lindqvist, Y. and Cook, P. F. (2004) *Biochim. Biophys. Acta*, **1701,** 61-74.

100. Collie-Duguid, E. S., Etienne, M. C., Milano, G. and McLeod, H. L. (2000) *Pharmacogenetics*, **10,** 217-223.

101. Fleming, R. A., Milano, G., Thyss, A., Etienne, M. C., Renee, N., Schneider, M. and Demard, F. (1992) *Cancer Res.*, **52,** 2899-2902.

102. Van Kuilenburg, A. B., Van Lenthe, H., Tromp, A., Veltman, P. C. and Van Gennip, A. H. (2000) *Clin. Chem.*, **46,** 9-17.

103. van Kuilenburg, A. B., Haasjes, J., Richel, D. J., Zoetekouw, L., Van Lenthe, H., De Abreu, R. A., Maring, J. G., Vreken, P. and van Gennip, A. H. (2000) *Clin. Cancer Res.*, **6,** 4705-4712.

104. Brito, R. A., Medgyesy, D., Zukowski, T. H., Royce, M. E., Ravandi-Kashani, F., Hoff, P. M. and Pazdur, R. (1999) *Oncology*, **57 Suppl 1,** 2-8.

105. Dobritzsch, D., Ricagno, S., Schneider, G., Schnackerz, K. D. and Lindqvist, Y. (2002) *J. Biol. Chem.*, **277,** 13155-13166.

106. Dobritzsch, D., Schneider, G., Schnackerz, K. D. and Lindqvist, Y. (2001) *EMBO J.*, **20,** 650-660.

107. Hagen, W. R., Vanoni, M. A., Rosenbaum, K. and Schnackerz, K. D. (2000) *Eur. J. Biochem.*, **267,** 3640-3646.

108. Rosenbaum, K., Jahnke, K., Curti, B., Hagen, W. R., Schnackerz, K. D. and Vanoni, M. A. (1998) *Biochemistry*, **37,** 17598-17609.

109. Yokota, H., Fernandez-Salguero, P., Furuya, H., Lin, K., McBride, O. W., Podschun, B., Schnackerz, K. D. and Gonzalez, F. J. (1994) *J. Biol. Chem.*, **269,** 23192-23196.

110. Bruschi, M. and Guerlesquin, F. (1988) *FEMS Microbiol. Rev.*, **4,** 155-175.

111. Podschun, B. (1992) *Biochem. Biophys. Res. Commun.*, **182,** 609-616.

112. Podschun, B., Cook, P. F. and Schnackerz, K. D. (1990) *J. Biol. Chem.*, **265,** 12966-12972.

113. Podschun, B., Jahnke, K., Schnackerz, K. D. and Cook, P. F. (1993) *J. Biol. Chem.*, **268,** 3407-3413.

114. Porter, D. J., Chestnut, W. G., Merrill, B. M. and Spector, T. (1992) *J. Biol. Chem.*, **267,** 5236-5242.

115. Rosenbaum, K., Jahnke, K., Schnackerz, K. D. and Cook, P. F. (1998) *Biochemistry*, **37,** 9156-9159.

116. Sprinzl, M., Steegborn, C., Hubel, F. and Steinberg, S. (1996) *Nucleic Acids Res.*, **24,** 68-72.

117. Bishop, A. C., Xu, J., Johnson, R. C., Schimmel, P. and de Crecy-Lagard, V. (2002) *J. Biol. Chem.*, **277,** 25090-25095.

118. Xing, F., Martzen, M. R. and Phizicky, E. M. (2002) *RNA*, **8,** 370-381.

119. Xing, F., Hiley, S. L., Hughes, T. R. and Phizicky, E. M. (2004) *J. Biol. Chem.*, **279,** 17850-17860.

120. Dalluge, J. J., Hashizume, T., Sopchik, A. E., McCloskey, J. A. and Davis, D. R. (1996) *Nucleic Acids Res.*, **24,** 1073-1079.

121. Noon, K. R., Guymon, R., Crain, P. F., McCloskey, J. A., Thomm, M., Lim, J. and Cavicchioli, R. (2003) *J. Bacteriol.*, **185,** 5483-5490.

122. House, C. H. and Miller, S. L. (1996) *Biochemistry*, **35,** 315-320.

123. Alexandrov, A., Chernyakov, I., Gu, W., Hiley, S. L., Hughes, T. R., Grayhack, E. J. and Phizicky, E. M. (2006) *Mol. Cell*, **21,** 87-96.

124. Kuchino, Y. and Borek, E. (1978) *Nature*, **271,** 126-129.

125. Kato, T., Daigo, Y., Hayama, S., Ishikawa, N., Yamabuki, T., Ito, T., Miyamoto, M., Kondo, S. and Nakamura, Y. (2005) *Cancer Res.*, **65,** 5638-5646.

126. Park, F., Gajiwala, K., Noland, B., Wu, L., He, D., Molinari, J., Loomis, K., Pagarigan, B., Kearins, P., Christopher, J., Peat, T., Badger, J., Hendle, J., Lin, J. and Buchanan, S. (2004) *Proteins*, **55,** 772-774.

127. Savage, D. F., de Crecy-Lagard, V. and Bishop, A. C. (2006) *FEBS Lett.*, **580,** 5198-5202.

128. Rider, L. W., Ottosen, M. B., Gattis, S. G. and Palfey, B. A. (2009) *J. Biol. Chem.*, In Press.

Chapter 2
Mechanism of Flavin Reduction in Class 2 Dihydroorotate Dehydrogenases

Dihydroorotate dehydrogenases (DHODs) are flavin-containing enzymes that catalyze the oxidation of dihydroorotate (DHO) to orotate (Figure 2-1), the only redox

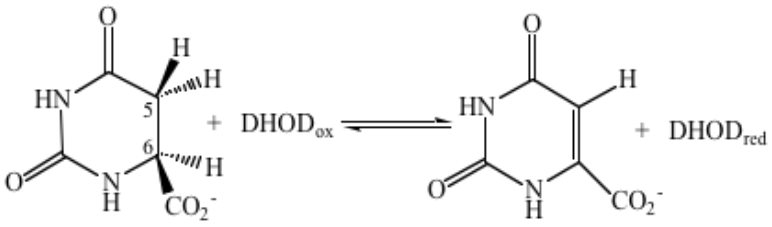

Figure 2-1: Reductive Half-Reaction of DHODs

step in the *de novo* synthesis of pyrimidines. DHODs fall into two broad classes on the basis of sequence (1). Class 1 enzymes are cytosolic enzymes that use cysteine as an active site base. This class is further divided into two subclasses, 1A and 1B (2, 3). Class 1A enzymes contain only FMN as a prosthetic group and use fumarate as the oxidizing substrate (3). Class 1B enzymes have a second protein subunit that contains an iron-sulfur cluster and an FAD in addition to a subunit that resembles the Class 1A

enzymes (2). Class 2 enzymes, in comparison, are membrane bound, are oxidized by ubiquinone (4) and use a serine as the active site base. Class 1 DHODs are found mostly in Gram-positive bacteria while Class 2 DHODs are found in the majority of Gram-negative bacteria and eukaryotes.

The oxidation of DHO involves both a deprotonation and a hydride transfer, forming the α,β-unsaturated carbonyl moiety of the product orotate. Oxidations that form α,β-unsaturated carbonyl compounds (or the reverse reaction) are catalyzed by a number of flavin-containing enzymes (5). In reactions such as these, the slightly acidic proton α to the carbonyl (for DHOD, the C5 *pro-S* hydrogen of DHO (6)) is removed by an active site base (either serine in Class 2 enzymes or cysteine in Class 1 enzymes) and the β-hydrogen (for DHOD, the hydrogen on C6 of DHO) is transferred to N5 of the isoalloxazine of the flavin as a hydride or hydride equivalent. Structures of such enzymes show that N5 of the flavin is in van der Waals contact with the hydride donor/acceptor and the active site base (or acid) is positioned correctly for deprotonation/protonation at the site α to the carbonyl. Residues with hydrogen bonding capabilities are generally present in the active site to stabilize possible charge development. DHODs - with four asparagines and a threonine or serine providing hydrogen bonds of potential catalytic importance - possess these characteristics (Figure

2-2), making them excellent model systems for investigating mechanisms in flavin-enone reactions.

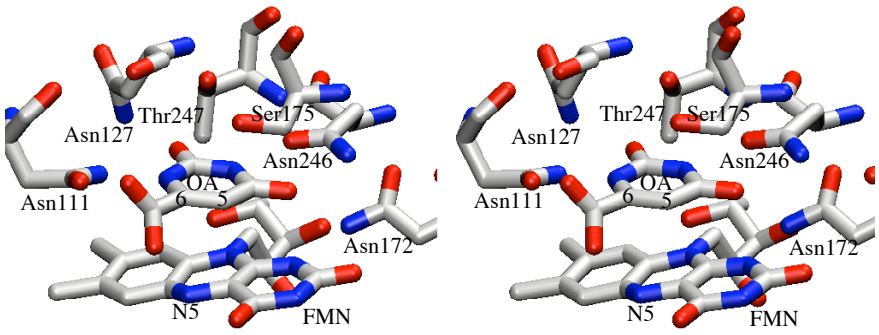

Figure 2-2: Stereo View of the Pyrimidine Binding-Site of *E. coli* DHOD

Orotate (OA) is stacked against the flavin with N5 of FMN, the site of hydride transfer, in van der Waals contact with C6 of orotate. Ser175, the active site base, is positioned correctly for deprotonation of C5. Four Asn side chains and one Thr side chain are present in the active site and could potentially help to stabilize the formation of a charged intermediate.

During the oxidation of DHO, the two C-H bonds of DHO could break at the same time in a concerted mechanism, or they could break sequentially in a stepwise mechanism. To address the question of whether the oxidation of DHO is stepwise or concerted, kinetic isotope effects on flavin reduction were determined in anaerobic stopped-flow experiments using DHO deuterated at the 5-position, the 6-position, or both the 5- and 6-positions. Isotope effects were determined for two Class 2 enzymes – those

from *Escherichia coli* and from *Homo sapiens*. We found that if hydrogen-tunneling effects are small, Class 2 enzymes oxidize DHO in a stepwise mechanism.

Experimental Procedures

Overexpression and Purification of DHODs

The expression plasmid for *E. coli* DHOD was the gift of Professor Kaj Frank Jensen (University of Copenhagen). The expression plasmid for a construct of the *H. sapiens* enzyme with a deletion of the N-terminal membrane-inserting hydrophobic sequence (residues 1-29) was a gift from Professor Lizbeth Hedstrom (Brandeis University). Dihydroorotate dehydrogenases from *E. coli* and *H. sapiens* were overexpressed and purified according to published procedures (7, 8).

Synthesis of deuterium-labeled DHO

Deuterium-labeled DHO was synthesized from L-dihydroorotic acid (Sigma) or orotic acid (Aldrich) according to the procedures of Pascal and Walsh (6), and characterized by mass spectrometry and ^{1}H-NMR. Proton NMR showed less than 4% contamination by protium in all compounds synthesized. Representative NMR spectra can be found in Appendix A.

Instrumentation

Absorbance spectra were obtained using a Shimadzu UV-2501PC scanning spectrophotometer. Stopped-flow experiments were performed at 4 ^{o}C using a Hi-Tech Scientific KinetAsyst SF-61 DX2 stopped-flow spectrometer controlled by KinetAsyst 3 software for Windows. NMR spectra were taken on a Bruker Avance DRX-500 spectrometer.

Preparation of anaerobic solutions

Enzyme solutions for rapid reaction studies were made anaerobic in glass tonometers by repeated cycles of evacuation and equilibration over an atmosphere of purified argon (9). Substrate solutions were made anaerobic by bubbling solutions with purified argon within the syringes that were to be loaded onto the stopped-flow instrument.

pH Dependence of the Reduction of Human DHOD

The pH dependence of the reductive half-reaction of the human DHOD was studied using buffers ranging from pH 6 to 11.3. The enzyme, in 3 mM KP_i, 150 mM KCl, 10% glycerol, 0.1 mM EDTA, pH 6.66, was mixed with 0.1 M buffer (KP_i pH 6 -

7.7; Tris-HCl pH 7.8 - 8.9; CHES pH 9.0 - 10.2; CAPS pH 10.3 - 11.3) at the pH of interest which also included 150 mM KCl, 10% glycerol, 0.1 mM EDTA and contained concentrations of DHO ranging from 0 to 4 mM (0 to 2 mM final concentrations after mixing). Control experiments showed that the rate of equilibration of the enzyme with the new pH of the buffer after the pH-jump was much more rapid than the reduction reaction. Absorbance traces at 470 nm or 550 nm were fit to either two or three exponentials depending on whether biphasic or triphasic exponential decays were observed, using KinetAsyst 3 (Hi-Tech Scientific), pro Fit (Quantum Soft), or Program A (Rong Chang, Chung-Jin Chiu, Joel Dinverno, and David P. Ballou, University of Michigan). In all cases, the apparent rate constant for reduction was determined by fitting directly to Equation 1 using KaleidaGraph (Synergy Software).

$$k_{obs,1} = \frac{k_{red}[DHO]}{K_d + [DHO]} \qquad (1)$$

Here, k_{red} is the rate constant of flavin reduction and K_d is the apparent dissociation constant of DHO. The pH dependence of the rate constant for the reduction was fit to Equation 2 using pro Fit (Quantum Soft), where $k_{red,max}$ represents the reduction rate constant at the high-pH extreme.

$$\log k_{red} = \log\left[\frac{10^{-pH} k_{red,\max}}{10^{-pK_a} + 10^{-pH}}\right] \qquad (2)$$

Simulating Kinetic Traces

Kinetic traces were simulated by the using a 4th-order Runge-Kutta algorithm implemented in Berkeley Madonna X, version 8.1β15. Values of rate constants satisfying the exact solution of the rate constant for a two-step reaction (Equation 3) were obtained by grid-searches in Microsoft Excel using the OptWorks plug-in from PiBlue Software.

$$k_{obs} = \frac{k_1 + k_2 + k_3 + k_4 - \sqrt{\left(k_1 + k_2 + k_3 + k_4\right)^2 - 4\left(k_1k_3 + k_2k_4 + k_1k_4\right)}}{2} \qquad (3)$$

Kinetic Isotope Effects in Human and *E. coli* DHOD

Kinetic isotope effects were studied at three pH values – pH 6.5, 8.5, and 10.5. At pH 6.5 and 8.5, the enzyme in 0.1 M buffer (KP_i pH 6.5 and Tris-HCl pH 8.5) was mixed with solutions of DHO ranging from 0 to 4 mM in the same buffer. At pH 10.5, the enzyme in 0.1 M Glycine was mixed with solutions of DHO made anaerobic in ddH_2O (pH 6.5) to remove the possibility of base catalyzed exchange at the C5 position of DHO (10). Reaction traces were collected at 470 nm in the case of human DHOD or 475 nm in the case of *E. coli* DHOD and were analyzed as described above. KIEs were calculated

by dividing the k_{red} determined for protio-DHO by the k_{red} determined for each labeled substrate.

Results

Reduction of *H. sapiens* DHOD

The kinetics of the reductive half-reaction of the Class 2 DHOD from *H. sapiens* were studied at various pH values in anaerobic stopped-flow experiments. Enzyme was mixed with DHO in the absence of an oxidizing substrate so that only the reductive half-reaction could occur. DHO binds to the enzyme in the dead-time of the stopped-flow instrument, causing a large red shift in the FMN absorbance peak. This shift – from 456 nm to 470 nm – seen in the enzyme-substrate complex is similar to that previously observed for DHOD-DHO or DHOD-orotate complexes in the *E. coli* enzyme as well as in Class 1A DHODs from both *Lactococcus lactis* and *Enterococcus faecalis* (1, 11-13). After the formation of the enzyme-substrate complex, flavin absorbance decreases rapidly as DHO is oxidized in the first observable kinetic phase (Figure 2-3). The reduced enzyme-orotate complex formed in this reaction has a charge-transfer band extending to long wavelengths, which indicates stacking of orotate with the reduced FMN. This is seen as an increase in absorbance at 550 nm (Figure 2-3). The loss of this

charge-transfer absorbance, corresponding to product dissociation, occurs slowly. Between these two phases, we occasionally observed a small decrease at 470 nm (less than 10% of the change corresponding to the main phase of flavin reduction), which was

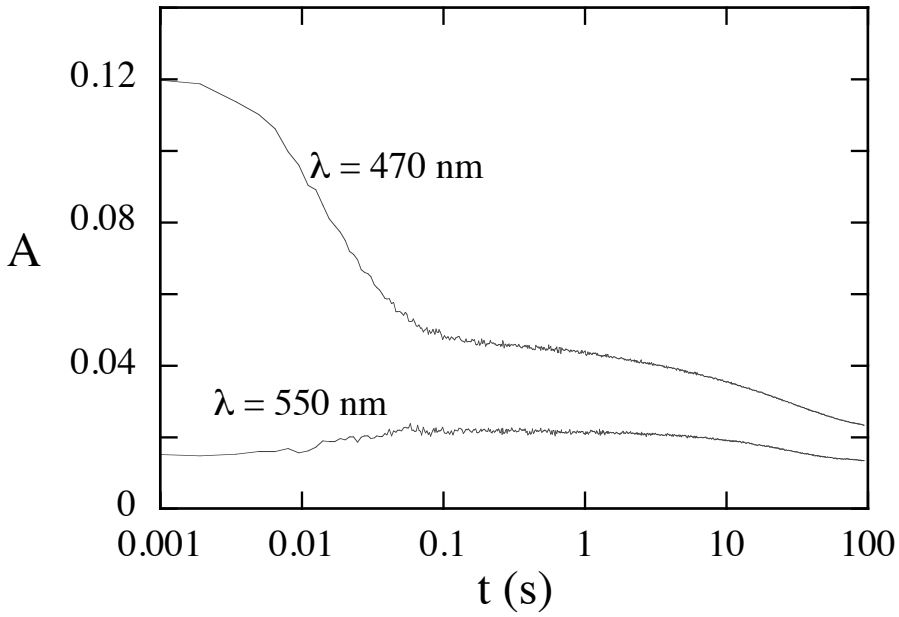

Figure 2-3: Reduction of H. sapiens DHOD

Anaerobic DHOD (11 μM after mixing) was mixed with DHO (final concentration 2 mM) in 0.1 M Tris, pH 8.7, at 4°C in a stopped-flow spectrometer. Note that reaction traces are displayed on a logarithmic time scale. At 470 nm, flavin reduction is seen as a rapid decrease in absorbance and orotate dissociation is seen as a small and slow decrease in absorbance. At 550 nm, flavin reduction is seen as an increase in absorbance while orotate dissociation is seen as a decrease in absorbance.

not observed at 550 nm. It is not clear what this phase represents, but we speculate that it was caused by the consumption of a small amount of contaminating oxygen, or by a small amount of damaged enzyme, or by the reduction of contaminating free FMN.

Many flavoenzymes have flavin reductase activity (V. Massey, personal communication). Regardless of its origin, this reaction phase was always well-resolved – generally at least an order of magnitude slower than the main phase of flavin reduction and one or two orders of magnitude faster than orotate dissociation – so that it did not interfere with the analysis of the other phases.

Absorbance traces collected at 470 nm were fit to three exponentials and traces collected at 550 nm were fit to two exponentials. The observed rate constants obtained for the first phase in these fits describe the time-dependence of the DHO-oxidized enzyme complex reacting to the orotate-reduced enzyme complex, modulated by the fraction of enzyme that has DHO bound. At saturating DHO, the observed rate constant will depend only on the reaction – or reactions, if there are unresolved intermediates – leading from the DHO complex to the orotate complex. The equilibrium of this reaction lies far towards reduced flavin (11); therefore, if the reaction occurs in a single step (a concerted reaction), the reverse reaction is negligibly slow and the observed rate constant at saturation will represent the rate constant for flavin reduction. If the reaction is stepwise, then the limiting observed rate constant will be a function of the rate constants of each step. At both wavelengths investigated, the observed rate constant of the first

phase, representing flavin reduction, varied hyperbolically with DHO concentration, allowing the overall rate constant for flavin reduction (k_{red}) to be determined. At pH 8.7 and 4 ^{o}C, k_{red} was 52 ± 1 s^{-1} and a K_d for DHO of 31 ± 2 μM was found. The observed rate constant for the dissociation of the charge-transfer complex, observed at 550 nm, decreased from a value of ~0.2 s^{-1} at low DHO concentrations (3.75 μM) to a limiting value of ~0.023 s^{-1} at high DHO concentrations (500 μM) (data not shown). This behavior is diagnostic for a unimolecular reaction step – in this case orotate release – followed by a bimolecular reaction – binding of DHO to free reduced enzyme (Figure 2-4). Thus the reduced human enzyme also makes a tightly bound orotate complex like that previously reported for the *E. coli* enzyme (11), where orotate dissociation is only possible to a significant extent in the presence of a high concentration of DHO, which acts as a competing ligand.

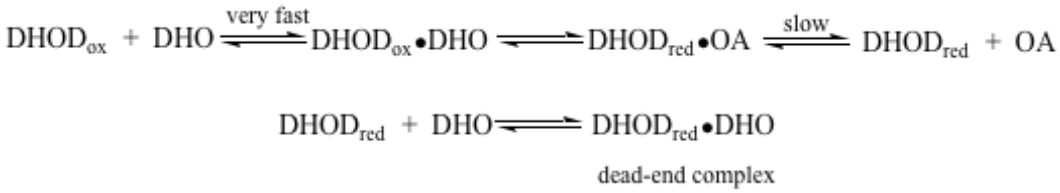

Figure 2-4: Reductive Half-Reaction Kinetic Scheme for Human DHOD

DHO binding is extremely rapid. Following the chemical step, OA release is slow. Due to the high concentration of DHO remaining following the reaction, the free reduced enzyme forms a dead-end complex with DHO.

The rate constant for flavin reduction was determined for pH values ranging from 6 to 11.3 in pH-jump stopped-flow experiments, where weakly buffered anaerobic enzyme solutions were mixed with anaerobic solutions of DHO containing concentrated buffer. Control experiments showed that the enzyme equilibrated rapidly with the new buffer, giving rates identical to those obtained in reactions starting with enzyme at the target pH. The rate constant for flavin reduction increased with pH from a value of 0.07 s^{-1} at pH 6 to about 80 s^{-1} at pH 9 (Figure 2-5), where there is a break in the log plot, indicating a pK_a. These data were fit to Equation 2, giving a pK_a value controlling reduction of 9.30 ± 0.03 and a maximum rate constant for reduction of 230 ± 30 s^{-1}. The reduction rate constant of the *E. coli* DHOD has been previously studied and was found to also increase with pH to a similar limiting value (360 ± 20 s^{-1}), above a pK_a at 9.5 (11). The dissociation constant of DHO from the human enzyme also varied with pH, increasing from a value of 4.6 μM at pH 7.2 to a value of 330 μM at pH 11.3, with no plateau, suggesting that deprotonation of the amide nitrogen of DHO prevents binding. This behavior is qualitatively similar to that of the *E. coli* enzyme (11).

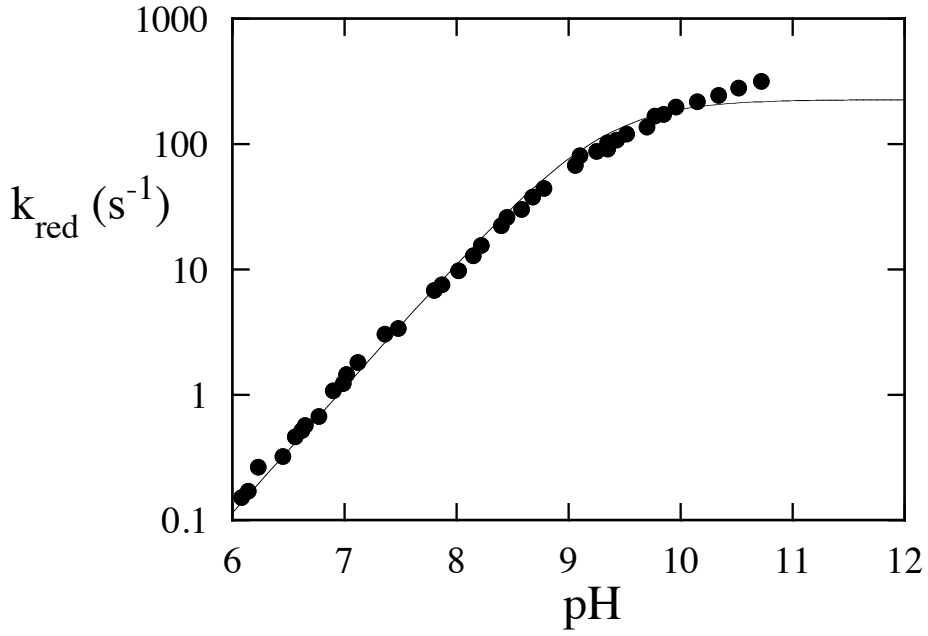

Figure 2-5: pH Dependence of Flavin Reduction in *H. sapiens* DHOD

The limiting rate constants for reduction (k_{red}) were obtained from pH-jump stopped-flow experiments as described in the text. The plot was fit to Equation 2 giving a pK_a value of 9.30 ± 0.03 and maximum rate constant for flavin reduction at high pH of 230 ± 30 s^{-1}.

Kinetic Isotope Effects on Flavin Reduction

Because the oxidation of DHO might occur via either concerted or stepwise mechanisms, double kinetic isotope effects were measured to determine which mechanism is operational for the *E. coli* and the *H. sapiens* DHODs. Anaerobic stopped-flow experiments were conducted by mixing *E. coli* DHOD with DHO in the absence of an oxidizing agent, ensuring that only the reductive half-reaction would occur. Reactions were carried out at 4 °C, which slowed the reduction sufficiently so that it could be

observed. Similar to the human enzyme, DHO binding caused a large red shift in the flavin absorbance spectrum of *E. coli* DHOD as was previously reported (11).

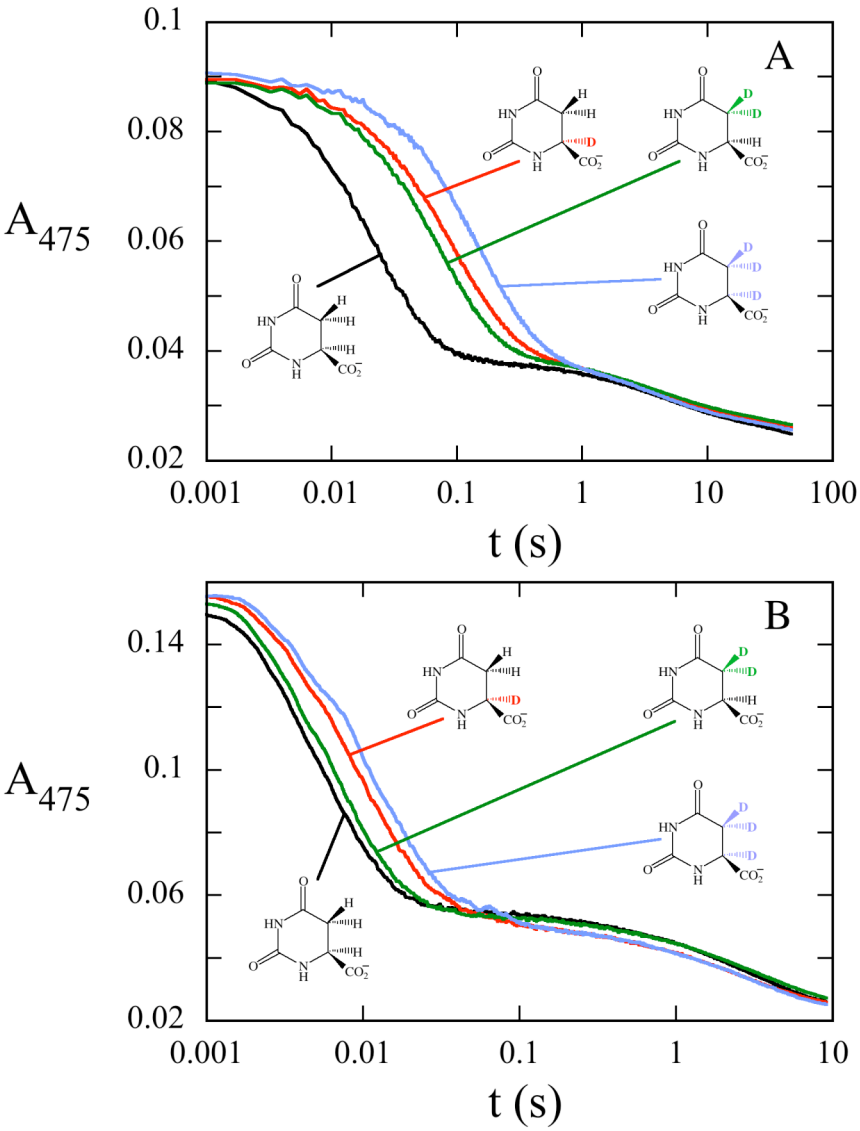

Figure 2-6: Reduction of *E. coli* DHOD with Labeled and Unlabeled DHO at 475 nm

(A) Anaerobic DHOD (final concentration 7.41 μM) was mixed with anaerobic substrate (final concentration 200 μM) at 4 °C in a stopped-flow spectrometer at pH 8.5. (B) Anaerobic DHOD (final concentration 13.3 μM) was mixed with anaerobic substrate (final concentration 200 μM) at pH 10.5. Note that the reaction traces are shown on a logarithmic time scale. Protio-DHO is shown in black, 5,5-$^{2}H_2$ DHO is shown in green, 6-^{2}H DHO is shown in red, and 5,5,6-$^{2}H_3$ DHO is shown in periwinkle.

Reactions were monitored at 475 nm and were biphasic. The fast reaction phase, corresponding to flavin reduction, was over within ~100 ms, while product dissociation was much slower. Absorbance traces at 475 nm (Figure 2-6) were fit to two exponentials. Observed rate constants for reduction varied hyperbolically with DHO concentration, allowing k_{red} to be determined. Kinetic isotope effects (KIEs) were obtained by dividing the k_{red} determined for protio-DHO by the k_{red} determined for deuterated DHO.

Table 2-1: Reduction Rate Constants and KIEs for *E. coli* DHOD[a]

	pH 6.5		pH 8.5		pH 10.5	
Compound	k_{red} (s^{-1})	KIE	k_{red} (s^{-1})	KIE	k_{red} (s^{-1})	KIE
DHO	0.882 ± 0.004		40 ± 2		242 ± 3	
5,5-$^2H_2$ DHO	0.276 ± 0.005	3.2 ± 0.2	14 ± 0.2	2.9 ± 0.2	221 ± 2	1.09 ± 0.02
6-^2H DHO	0.203 ± 0.007	4.4 ± 0.3	11.2 ± 0.1	3.6 ± 0.2	127 ± 3	1.90 ± 0.07
5,5,6-$^2H_3$ DHO	0.120 ± 0.007	7.4 ± 0.7	6.8 ± 0.1	5.9 ± 0.4	121 ± 2	1.99 ± 0.09

[a]Reductive rate constants were obtained from the value at saturating DHO concentration as explained in Experimental Methods. The highest concentration of DHO used (after mixing) was 200 μM at pH 6.5 and 8.5 (more than 40 times K_d) and 4 mM at pH 10.5 (more than 80 times K_d).

KIEs were determined for the *E. coli* DHOD at two pH values below the pK_a of 9.5 observed for reduction (11). At pH 6.5, using 5,5-$^2H_2$ DHO, a KIE of 3.2 ± 0.2 was found (Table 2-1), and a KIE of 4.4 ± 0.3 was obtained using 6-^2H DHO. The double

KIE determined using 5,5,6-$^2H_3$ DHO was found to be 7.4 ± 0.7. Similar values were obtained at pH 8.5 (Table 2-1). Interestingly, at pH 10.5, above the observed pK_a (~9.5) for the *E. coli* enzyme (11), essentially no KIE (1.09 ± 0.02) was observed using 5,5-$^2H_2$ DHO, although the KIEs observed using either 6-^2H DHO or 5,5,6-$^2H_3$ DHO were both about 2-fold. No isotope effect was seen on the rate of charge-transfer disappearance at any pH studied, consistent with the assignment of this phase as the dissociation of orotate. Significant kinetic isotope effects were also observed for the *H. sapiens* enzyme at pH 8.0 (Table 2-2), similar to those observed for the *E. coli* enzyme at both pH 6.5 and 8.5, with values for both 5,5-$^2H_2$ DHO and 6-^2H DHO of around 4-fold and for 5,5,6-$^2H_3$ DHO of around 8-fold.

Table 2-2: Reduction Rate Constants and KIEs for *H. sapiens* DHOD at pH 8.0[a]

Compound	k_{red} (s^{-1})	KIE
DHO	10.9 ± 0.1	
5,5-$^2H_2$ DHO	2.62 ± 0.04	4.15 ± 0.09
6-^2H DHO	2.88 ± 0.04	3.77 ± 0.08
5,5,6-$^2H_3$ DHO	1.37 ± 0.02	8.0 ± 0.2

[a]Reductive rate constants were obtained from the value at saturating DHO concentration as explained in Experimental Methods. The highest concentration of DHO used was 200 μM after mixing (more than 40 times K_d).

Deuterium isotope effects were also used to determine whether DHO was a "sticky" substrate for the *E. coli* enzyme. If the reaction of DHO with FMN were much faster than its dissociation from the complex with oxidized enzyme (*i.e.*, if it is a "sticky" substrate), then an equimolar mixture of labeled and unlabeled DHO would form equal populations of complexes with and without deuterium, and each of these would subsequently react faster than DHO dissociation. In such a situation, two phases of flavin reduction – a fast phase corresponding to protio-DHO and a slow phase corresponding to deutero-DHO – would be observed. On the other hand, if DHO dissociates rapidly compared to its reaction with FMN, then only one phase of flavin reduction would be observed because oxidized enzyme would continually equilibrate with the pool of isotopically mixed DHO. When *E. coli* DHOD was mixed with a solution containing 400 μM *protio*-DHO and 400 μM of 5,5,6-$^{2}H_3$ DHO at pH 8.5, 4 °C, only one reaction phase was observed for flavin reduction (Figure 2-7), showing that DHO dissociates rapidly compared to flavin reduction. Simulations showed that two phases would be observed for a commitment factor (the ratio of the reduction rate constant to the DHO dissociation rate constant) as low as 0.45 when mixing DHOD with a solution of both *protio*- and 5,5,6-$^{2}H_3$ DHO.

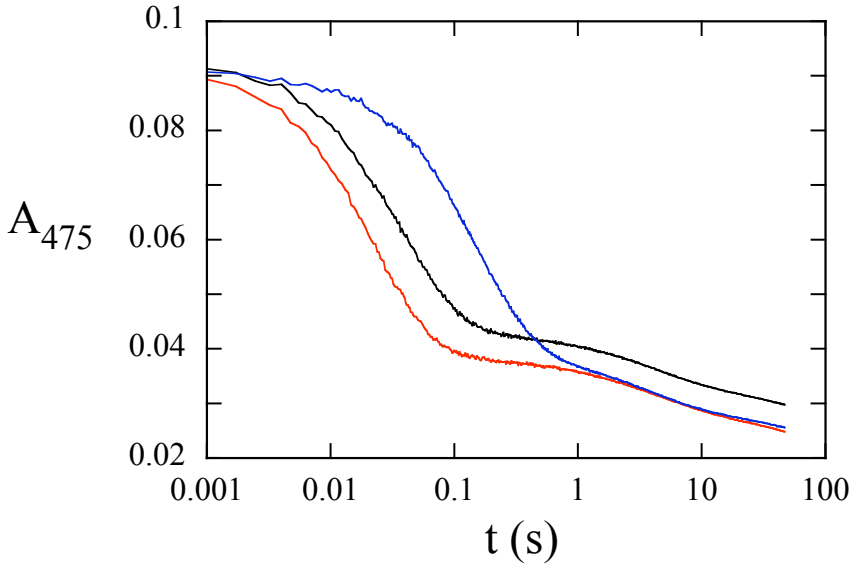

Figure 2-7: Rapid Equilibrium Binding of DHO

E. coli DHOD (7.4 μM) was mixed with 200 μM DHO (red), 200 μM 5,5,6-$^2H_3$ DHO (blue), or a mixture of 200 μM DHO and 200 μM 5,5,6-$^2H_3$ DHO (black). All concentrations are for solutions after mixing. Note the logarithmic timescale. Flavin reduction by the isotopic mixture occurs in one phase.

Discussion

All DHODs oxidize DHO to orotate by transferring a hydride or a hydride equivalent from C6 of DHO to the flavin and by deprotonating C5 of DHO with an enzyme side-chain. An issue central to the mechanism is the timing of the two C-H bond cleavages. These could be concerted, with both C-H bonds breaking in a single transition state, or stepwise, with each C-H bond breaking in separate transition states. Double kinetic isotope effects can be used to distinguish between concerted or stepwise mechanisms for flavin reduction. The Rule of the Geometric Mean states that, in the absence of large quantum effects, perturbations to a partition function caused by isotopic

substitutions at a particular site are independent of isotopic substitutions at other sites (14). Therefore, if both C-H bonds break in a concerted mechanism (*i.e.*, a single transition state), then the product of the two single isotope effects (obtained by comparing 5,5-$^{2}H_2$ DHO and 6-^{2}H DHO with the *protio*-DHO) will equal the observed double KIE (obtained by comparing 5,5,6-$^{2}H_3$ DHO with the *protio*-DHO). Below the observed pK_a for reduction (9.5 in the *E. coli* enzyme), the product of the two single-site KIEs is much greater than the KIE measured for 5,5,6-$^{2}H_3$ DHO (Table 2-3). Therefore, we conclude that if quantum mechanical tunneling is not significant, the mechanism of flavin reduction is stepwise.

Table 2-3: Analysis of KIEs

E. coli	5,5-$^{2}H_2$ DHO	6-^{2}H DHO	predicted double KIEs	5,5,6-$^{2}H_3$ DHO
pH 6.5	3.2 ± 0.2	4.4 ± 0.3	13.9 ± 1.8	7.4 ± 0.7
pH 8.5	2.9 ± 0.2	3.6 ± 0.2	10.5 ± 1.3	5.9 ± 0.4
pH 10.5	1.09 ± 0.02	1.90 ± 0.07	2.1 ± 0.1	1.99 ± 0.09
H. sapiens				
pH 8.0	4.15 ± 0.09	3.77 ± 0.08	15.5 ± 0.6	8.0 ± 0.2

An alternate interpretation of our KIE data is that the oxidation of DHO is concerted but that there is a significant contribution from hydrogen tunneling. If the

cleavage of each C-H bond is coupled to the other by significant tunneling, then substituting one hydrogen with deuterium will impair the ability of both hydrogens to tunnel. Isotopic substitution at the second site will, therefore, have a smaller additional impact on the rate when the first site is already substituted with deuterium, and the Rule of the Geometric Mean will not be obeyed, as observed with our results.[1] Our data do not address the possibility of tunneling in hydrogen transfer. Quantum mechanical tunneling sometimes causes very large isotope effects, but the KIEs observed here were not unusually large, so that by this criterion, tunneling need not be invoked. However, there are numerous instances of tunneling that do not exhibit unusually large KIEs, so that the magnitude of the KIE is not a decisive criterion (15). Therefore, in the absence of other data, no conclusion can be drawn yet concerning the importance of quantum mechanical tunneling in the reduction of the Class 2 DHODs.

If the oxidation of DHO by Class 2 DHODs is actually stepwise, two reaction phases for flavin reduction in the stopped-flow experiments might be expected. However, only one phase of reduction is observed, *i.e.*, no spectral intermediates or lags

[1] It is also worth noting that the possibility of tunneling need not be limited to a concerted reaction. In the putative stepwise mechanism described above, hydrogen tunneling would also be possible in one or both of the transition states. However, such a scenario would not alter the interpretation.

are detected during the reaction. This is not inconsistent with behavior possible for a two-step reversible reaction sequence. If the net flux of intermediates through the first kinetic step is significantly slower than that through the second step, no intermediates would be visible and the process would appear as a single exponential. One detailed example of this can be found in Appendix B.

Our kinetic data do not allow the determination of the order of the bond breaking in the oxidation of DHO, *i.e.,* deprotonation followed by hydride transfer or *vice versa* (Figure 2-8), and the published crystal structures do not provide a basis for making this distinction either. If deprotonation at C5 occurs first, then the reaction would proceed via an enolate intermediate that could be stabilized through hydrogen bonds in the active site. Two conserved asparagine side-chains (172 and 246 in the *E. coli* enzyme) are ideally positioned within hydrogen bonding distance of the O on C4 of the pyrimidine (Figure 2-2) (16). These residues could stabilize the negative charge that would form on this O in a manner similar to the oxyanion "hole" of serine proteases. The other possible order of bond cleavage – hydride transfer from C6 to the flavin followed by deprotonation at C5 – leads to an iminium intermediate. An asparagine residue (111 in the *E. coli* enzyme) is located within hydrogen bonding distance of N1 of DHO (Figure 2-2) (16) and could potentially stabilize this intermediate.

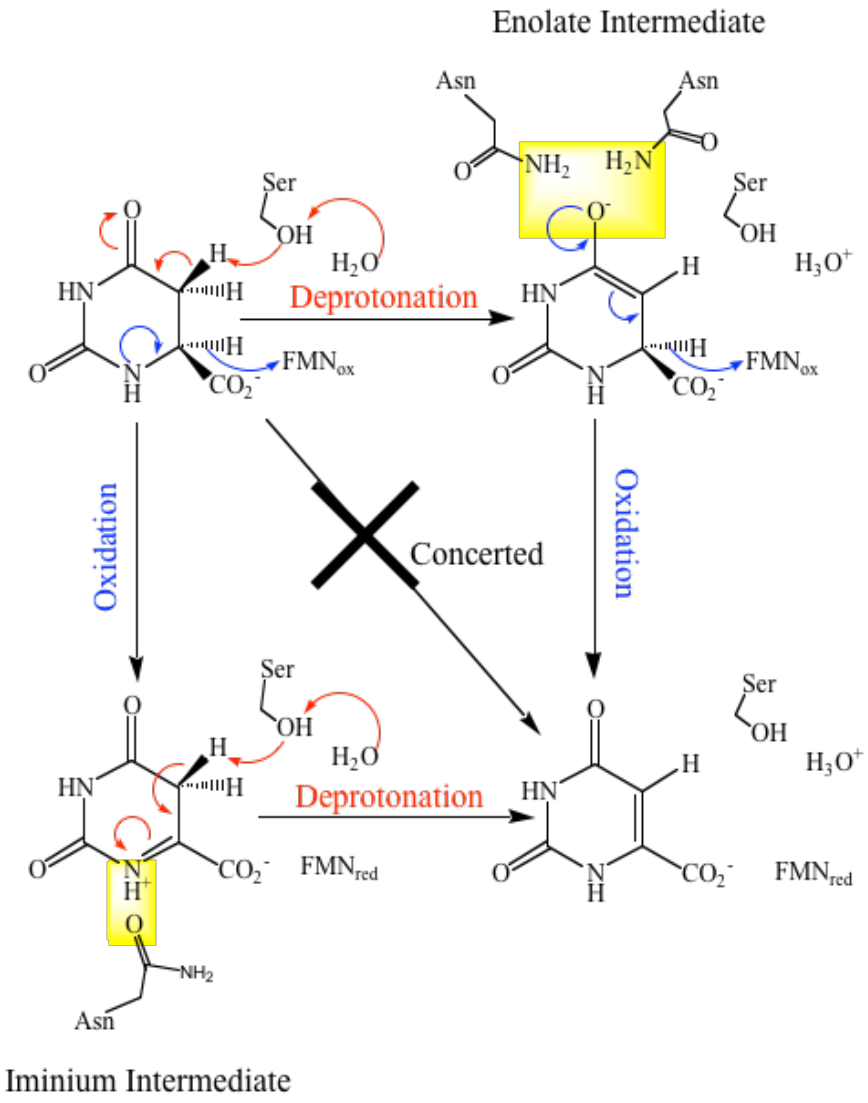

Figure 2-8: Possible Mechanisms of DHO Oxidation in Class 2 DHODs

Without tunneling, a concerted oxidation of DHO (upper-left corner) to orotate (lower-right corner) is not compatible with our data, but two possible stepwise mechanisms are still possible. If deprotonation precedes hydride transfer, then an enolate intermediate would form that could be stabilized by two conserved asparagines. If hydride transfer (oxidation) precedes deprotonation, an iminium intermediate would form that could hydrogen bond with another conserved asparagine. Note that in both mechanisms, the active site base (serine) is a component in a proton-relay system allowing the transient generation of the alkoxide (not shown) even at pH values below its pK_a. Deprotonation is shown by red arrows, and oxidation is shown by blue arrows. Hydrogen bonds that could stabilize each intermediate are highlighted by yellow boxes.

The acid/base chemistry necessary in Class 2 DHODs has presented a dilemma. The base that deprotonates C5 of DHO is serine (Ser175 in the *E. coli* enzyme and Ser215 in the human enzyme). The side-chain of free serine has a high pK_a (~13.6) (17), but the pK_a observed for reduction of the Class 2 DHODs is ~9.5. This is too low to be the thermodynamic pK_a for an unactivated serine residue. However, crystal structures show that in Class 2 DHODs, the environment of the serine is somewhat hydrophobic and no residues such as histidines are nearby to activate the serine (16, 18). It was suggested that the serine was activated by a hydrogen bond to a water molecule that is in turn hydrogen bonded to the OH of a threonine residue and stacked on the aromatic ring of a phenylalanine residue (16, 18). These residues are highly conserved in Class 2 DHODs. However, this arrangement, which allows fewer hydrogen bonds to the serine hydroxyl than would be available in bulk water, is unlikely to lower the pK_a. Empirical calculations of the perturbation of the pK_a using the program PROPKA (19) agree with this assessment, predicting a slight increase in the pK_a of the base due to the protein environment, rather than a decrease.

A stepwise reaction mechanism for DHO oxidation allows the apparent pK_a of 9.5 to be explained. The lack of a KIE at the C5 position of DHO (the proton donor in the reaction) above the pK_a of reduction shows that this bond cleavage no longer affects the

observed rate.[2] At pH 10.5, deprotonation at C5 occurs quickly enough that it no longer contributes to the overall rate of flavin reduction, explaining the lack of an isotope effect using 5,5-$^2H_2$ DHO. Therefore, the observed pK_a of ~9.5 in Class 2 DHODs does not represent the actual thermodynamic pK_a of the active site serine. Instead, this is a "kinetic" pK_a, shifted "outward" from its thermodynamic value which might even exceed the standard value of ~13.6 (17). If the actual pK_a of the serine is high, as our data suggest, then it is the neutral serine side chain that must deprotonate DHO. Forming a doubly protonated positively charged serine oxygen would be very unfavorable. Instead, we propose that the active site serine is deprotonated at the same time it receives a proton from DHO (Figure 2-8), thus acting as a component in a proton-relay system rather than as a classic general base. Crystal structures of Class 2 enzymes show that the serine is accessible to the solvent through a short tunnel (Figure 2-9), although the carbonyl oxygen of the serine residue blocks direct solvent access and would have to move to

[2] The variation of the KIE with pH for reduction by 6-^{2}H DHO, from 4.4 at pH 6.5 to 1.9 at pH 10.5, should also be noted, indicating additional kinetic complexity masking KIEs at higher pH values. This may indicate that another step, such as a conformational change, becomes coupled to the reduction reaction at high pH, partially masking the isotope effect. Alternatively, the deprotonation of ionizable groups at the active site, such as Lys66 (in *E. coli*; 100 in human), which hydrogen bonds to the carboxylate of the pyrimidine ligand, Lys217 (in *E. coli*; 217 in human), which hydrogen bonds to the flavin at N1 and C2O, or N3 of FMN (pK_a 9.5 in aqueous solution), might change the intrinsic isotope effect for hydride transfer.

allow proton transfer. Alternatively, a network of hydrogen bonds formed by the active site serine, an internal water, and threonine (16, 18) communicates directly with the solvent. Therefore, a proton transfer network responsible for deprotonating DHO is feasible and consistent with all available data.

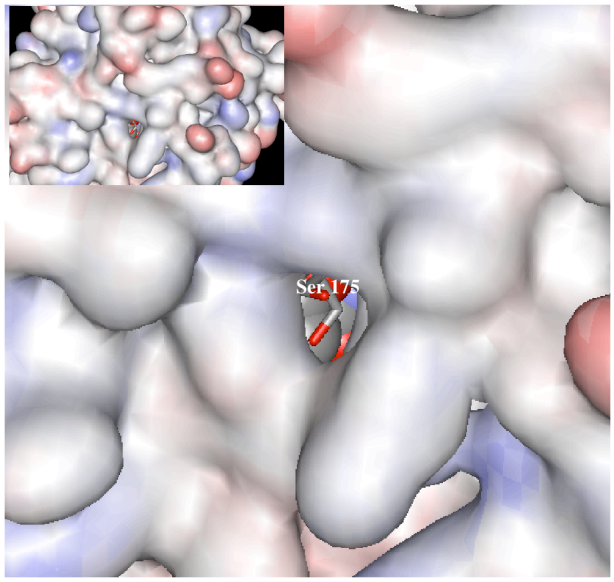

Figure 2-9: Surface of *E. coli* DHOD

Surface of *E. coli* DHOD showing the tunnel connecting the active site serine to the bulk solvent. Inset: view of the full protein.

The question of whether DHO oxidation by DHODs is stepwise or concerted has been addressed previously by steady-state kinetics for other examples of Class 1A, 1B, and 2 enzymes (6, 20, 21). It was suggested that the Class 2 enzyme from bovine liver mitochondria utilized a concerted mechanism (21), which differs from our findings that

Class 2 DHODs utilize a stepwise mechanism. We cannot explain this discrepancy, but note that these authors acknowledged that large errors in their determinations left open the possibility that the mechanism was actually stepwise.

Both the *E. coli* and *H. sapiens* DHODs utilize a stepwise mechanism for flavin reduction (barring large quantum effects) and a kinetic pK_a of ~9.5 is observed in both enzymes. Since all Class 2 enzymes appear to be structurally similar and have high sequence homology, it is likely that these features are true of all Class 2 DHODs. Interestingly, analogous stopped-flow data suggest that Class 1A DHODs utilize a concerted mechanism (22) in contrast to an earlier study on the Class 1A enzyme from *Crithidia fasciculata* (6). Structures of the Class 1A DHOD from *L. lactis* have been solved (1), and they show a high degree of similarity to the structures of the Class 2 enzymes, especially with regard to pyrimidine-protein and flavin-protein interactions. However, the Class 1A enzymes use a cysteine as the active site base, which may be responsible for the difference in mechanism. The structural basis for the possible mechanistic differences in these two classes of enzymes remains an intriguing question.

References

1. Rowland, P., Nielsen, F. S., Jensen, K. F., and Larsen, S. (1997) *Structure*, **5**, 239-252.

2. Nielsen, F. S., Andersen, P. S., and Jensen, K. F. (1996) *J. Biol. Chem.*, **271**, 29359-29365.

3. Nagy, M., Lacroute, F., and Thomas, D. (1992) *Proc. Natl. Acad. Sci. U. S. A.*, **89**, 8966-8970.

4. Jones, M. E. (1980) *Annu. Rev. Biochem.*, **49**, 253-279.

5. Palfey, B. A., and Massey, V. (1998) *Comprehensive Biological Catalysis, volume III/Radical Reactions and Oxidation/Reduction*, Academic Press, New York.

6. Pascal, R. A., Jr., and Walsh, C. T. (1984) *Biochemistry*, **23**, 2745-2752.

7. Björnberg, O., Gruner, A. C., Roepstorff, P., and Jensen, K. F. (1999) *Biochemistry*, **38**, 2899-2908.

8. Neidhardt, E. A., Punreddy, S. R., McLean, J. E., Hedstrom, L., and Grossman, T. H. (1999) *J. Mol. Microbiol. Biotechnol.*, **1**, 183-188.

9. Palfey, B. A. (2003) Time Resolved Spectral Analysis, in *Kinetic Analysis of Macromolecules* (Johnson, K. A., Ed.), Oxford University Press, New York.

10. Argyrou, A. and Washabaugh, M. W. (1999) *J. Am. Chem. Soc.*, **121**, 12054-12062.

11. Palfey, B. A., Björnberg, O., and Jensen, K. F. (2001) *Biochemistry*, **40**, 4381-4390.

12. Marcinkeviciene, J., Jiang, W., Locke, G., Kopcho, L. M., Rogers, M. J., and Copeland, R. A. (2000) *Arch. Biochem. Biophys.*, **377**, 178-186.

13. Larsen, J. N., and Jensen, K. F. (1985) *Eur. J. Biochem.*, **151**, 59-65.

14. Bigeleisen, J. (1955) *J. Chem. Phys.*, **23**, 2264-2267.

15. Basran, J., Masgrau, L., Sutcliffe, M. J., and Scrutton, N. S. (2006) Solution and Computational Studies of Kinetic Isotope Effects in Flavoprotein and Quinoprotein Catalyzed Substrate Oxidations as Probes of Enzymatic Hydrogen Tunneling and Mechanism, in *Isotope Effects in Chemistry and Biology* (Kohen, A. and Limbach, H.- H., Eds.) pp 671-689, CRC Press Taylor & Francis Group.

16. Nørager, S., Jensen, K. F., Björnberg, O., and Larsen, S. (2002) *Structure*, **10**, 1211-1223.

17. Bruice, T. C., Fife, T. H., Bruno, J. J., and Brandon, N. E. (1962) *Biochemistry*, **1**, 7-12.

18. Liu, S., Neidhardt, E. A., Grossman, T. H., Ocain, T., and Clardy, J. (2000) *Structure*, **8**, 25-33.

19. Liu, H., Roberston, A. D., and Jensen, J. H. (2005) *Proteins*, **61**, 704-721.

20. Argyrou, A., Washabaugh, M. W., and Pickart, C. M. (2000) *Biochemistry*, **39**, 10373-10384.

21. Hines, V., and Johnston, M. (1989) *Biochemistry*, **28**, 1227-1234.

22. Fagan, R. L., Jensen, K. F., Björnberg, O. and Palfey, B. A. (2007) *Biochemistry*, **46,** 4028-4036.

Chapter 3
Mechanism of Flavin Reduction in the Class 1A Dihydroorotate Dehydrogenase from *Lactococcus lactis*

Dihydroorotate dehydrogenase (DHOD) is a flavin-containing enzyme that catalyzes the only redox reaction in the pyrimidine biosynthetic pathway - the conversion of dihydroorotate (DHO) to orotate (OA; Figure 3-1). DHODs have been categorized into two broad classes based on sequence, Class 1 and Class 2 (1). Class 2 DHODs are membrane-bound proteins. This class of enzymes uses serine as an active site base and is oxidized by ubiquinone (2). Class 1 DHODs, in comparison, are cytosolic proteins which

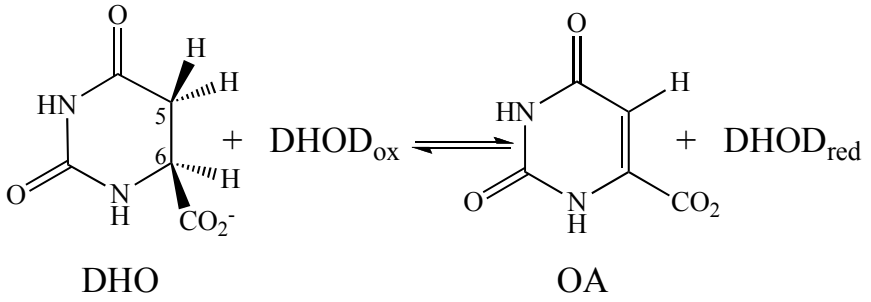

Figure 3-1: Reductive Half-Reaction of DHODs

contain cysteine as their active site base. This class of enzymes has been further divided into two subclasses. Class 1A enzymes are homodimers that are oxidized by fumarate

(3). Class 1B enzymes are $\alpha_2\beta_2$ heterotetramers, which contain not only FMN (like all other DHODs), but also an iron-sulfur cluster and FAD, where the enzyme is oxidized by NAD (4).

Several pathogens including *Enterococcus faecalis* and *Trypanosoma cruzi* express Class 1A DHODs, while humans have Class 2 enzymes, making Class 1A DHODs inviting drug targets. Genetic studies have shown that DHOD is essential for the survival of *T. cruzi* (5), validating the idea that inhibitors specific for Class 1A enzymes could treat diseases. Most DHOD inhibitors discovered to date are directed at the hydrophobic quinone binding pocket found in Class 2 DHODs – not the pyrimidine binding site (6). Class 1A DHODs, however, do not have a quinone-binding pocket to target. Specifically targeting the pyrimidine binding site of Class 1A DHODs would appear to be difficult because the structure of the pyrimidine binding site in Class 1A and Class 2 DHODs is nearly identical (7-9). However, functional rather than structural differences between the pyrimidine binding sites may exist that could be exploited in drug design. Thus, determining the differences between the mechanisms utilized by these classes of enzymes should aid in the design of class-specific inhibitors.

In all classes of DHODs, DHO is converted to OA by breaking two C-H bonds. The reaction involves both a deprotonation and a hydride transfer. During the oxidation

of DHO, the C5 *pro-S* hydrogen of DHO (10) is removed by an active site base, either cysteine in Class 1 enzymes or serine in Class 2 enzymes. The hydrogen on C6 of DHO is transferred to N5 of the isoalloxazine of the flavin as a hydride or hydride equivalent. The oxidation of DHO to OA could occur via a concerted mechanism, where both C-H bonds break simultaneously, or a stepwise mechanism, where the C-H bonds break sequentially. Double kinetic isotope effects (KIEs) can determine which mechanism is operational. Class 2 DHODs from *Escherichia coli* and *Homo sapiens* have been previously studied in stopped-flow experiments. With those enzymes, the KIEs suggested either a stepwise mechanism, or a concerted mechanism with quantum mechanical tunneling (11). In this paper, we examine the Class 1A enzyme from *L. lactis* and find that the oxidation of DHO by this enzyme is concerted and the active site cysteine acts as a classic general base.

Experimental Procedures

Overexpression and Purification of DHODs

The wild-type *L. lactis* DHOD, the Cys130Ser mutant, and the Cys130Ala mutant were expressed from the plasmid pFN1 (1, 12). The enzymes were expressed in SØ6645 cells as previously described (12). The cells overexpressing the proteins were harvested

by centrifugation (4,000 rpm for 25 minutes at 4 ^{o}C). Enzyme was purified either according to the published procedure (12) or by the following method. Cells were resuspended in 20 mM Bis-Tris pH 6.5 buffer containing 10% glycerol, lysed by sonication, and the cell debris was removed by centrifugation at 16,000 rpm for 20 minutes at 4 ^{o}C. Addition of 50% ammonium sulfate (313 g/L) to the cleared lysate precipitated proteins other than the recombinantly expressed DHOD. Precipitated proteins were removed by centrifugation at 16,000 rpm for 20 minutes at 4 ^{o}C. The bright yellow supernatant containing the enzyme was dialyzed overnight in 3 L of 20 mM Bis-Tris pH 6.5 buffer containing 10% glycerol to remove the salt. The dialyzed enzyme was then filtered with a 0.45 μm syringe-filter and applied to a Q-Sepharose fast-flow resin (Sigma-Aldrich) previously equilibrated in 20 mM Bis-Tris pH 6.5 buffer containing 10% glycerol. The enzyme was eluted with a linear gradient from 0 – 500 mM NaCl in 20 mM Bis-Tris pH 6.5 buffer containing 10% glycerol. The fractions containing enzyme were pooled, concentrated and stored at -80 °C after diluting with glycerol to 50% (v/v). For use in experiments, the enzyme was exchanged into the appropriate buffer using Econo-Pac 10DG disposable desalting columns (Bio-Rad).

Synthesis of deuterium-labeled DHO

Deuterium-labeled DHO was synthesized from L-dihydroorotic acid (Sigma) or orotic acid (Aldrich) according to the procedures of Pascal and Walsh (13) and characterized by ^{1}H-NMR. Synthetic DHOs were found to be >94% isotopically pure. Representative NMR spectra can be found in Appendix A.

Instrumentation

Absorbance spectra were obtained using a Shimadzu UV-2501PC scanning spectrophotometer. Stopped-flow experiments were performed at 4 °C using a Hi-Tech Scientific KinetAsyst SF-61 DX2 stopped-flow spectrophotometer. NMR spectra were taken using a Bruker Avance DRX-500 spectrometer.

Preparation of anaerobic solutions

Enzyme solutions for rapid reaction studies were made anaerobic in glass tonometers by repeated cycles of evacuation and equilibration over an atmosphere of purified argon as previously described (14). Substrate solutions were made anaerobic within the syringes that were to be loaded onto the stopped-flow instrument by bubbling solutions with purified argon. Slow reactions were performed in anaerobic cuvettes (15)

and monitored in a standard scanning spectrophotometer. These reaction mixtures were also made anaerobic by repeated evacuation and equilibration with purified argon.

pH Dependence of the Reduction of the Wild-Type DHOD from *L. lactis*

The pH dependence of the reductive half-reaction of the wild-type DHOD from *L. lactis* was studied from pH 6.47 – 10.36 (MOPS pH 6.47 – 7.96; TAPS pH 8.58; CHES pH 9.3 – 10.36). The anaerobic enzyme equilibrated in the buffer of interest (50 mM buffer adjusted to 50 mM ionic strength with KCl) was mixed with various concentrations of DHO (up to 8 mM before mixing) in the same buffer. Reaction traces were collected at both 475 nm and 550 nm. Kinetic traces were fit to either two or three exponentials with Program A (Rong Chang, Chung-Jin Chiu, Joel Dinverno and David P. Ballou, University of Michigan). The reduction rate constant (k_{red}) was determined from the limiting value of the observed rate constant at infinite DHO concentration obtained by fitting k_{obs} vs. DHO concentration to a hyperbola in Kaleidagraph (Synergy, Inc.). The pK_a value controlling reduction was determined by fitting the pH dependence of the reduction rate constant to Equation 1,

$$k_{red} = \frac{k_{red,limiting}}{1 + 10^{(pK_a - pH)}} \qquad (1)$$

where $k_{red,\ limiting}$ is the limiting value of the reduction rate constant at high pH.

Determination of Spectral Intermediates

Anaerobic enzyme equilibrated in 100 mM Tris-HCl, 0.1 mM EDTA, pH 8.5 was mixed with 4 mM DHO in the same buffer. Absorbance spectra were collected from 350 to 700 nm for 0.4 seconds with an integration time of 1.5 milliseconds using a diode-array detector. Absorbance spectra of intermediates were calculated in SpecFit/32 (Spectrum Software Associates) via singular value decomposition using a two-step model. Anaerobic enzyme was mixed with buffer containing no DHO to obtain the spectrum of fully oxidized enzyme.

Kinetic Isotope Effects in Wild-Type DHOD

Double deuterium isotope effects were measured at pH 7.0 and 8.5. Anaerobic enzyme equilibrated in the buffer of interest (either 40 mM KP_i, pH 7.0 or 50 mM Tris, pH 8.5) was mixed with various concentrations (up to 8 mM before mixing) of labeled and unlabeled DHO. Reaction traces were collected at 475 and 550 nm and k_{red} values were determined as described above. KIEs were calculated by dividing the k_{red} determined for protio-DHO by the k_{red} determined for each labeled substrate.

DHO Binding to the Cys130Ala and Cys130Ser Mutants

The reductive half-reaction of the Cys130Ala mutant was excruciatingly slow, allowing the direct aerobic titration of the enzyme with DHO to determine a dissociation constant. The enzyme equilibrated in the buffer of interest was titrated with DHO in the same buffer. The buffers used for this pH dependence were the same as those described for wild-type reduction experiments. After the titration was complete, the titration mixture was filtered (Centricon 30) to remove enzyme and the extent of reaction was determined from the orotate concentration in the filtrate (ε_{280} = 7.52 mM^{-1} cm^{-1}). In the time course of an experiment (~30 minutes), the reaction had not proceeded to an appreciable extent (less than 5%). The reductive half-reaction of the Cys130Ser mutant was faster than that of the Cys130Ala mutant. Therefore, aerobic titrations for this mutant were performed in the stopped-flow spectrophotometer, allowing spectra to be scanned within 10 s of mixing. For both mutants, the differences in flavin absorbance caused by binding of DHO were plotted against DHO concentration, and the data were fit to a hyperbola in Kaleidagraph (Synergy, Inc.) to determine the K_d.

pH Dependence on the Reductive Half-Reactions of Cys130Ala and Cys130Ser

In the active site base mutants, flavin reduction did not occur on a stopped-flow time scale; therefore, all reductive half-reactions were measured using a standard scanning spectrophotometer under anaerobic conditions at pH values ranging from 6.47 to 10.36. Anaerobic enzyme equilibrated in a particular buffer (same buffers used for the pH dependence of the reduction of the wild-type enzyme) was mixed with a saturating concentration of DHO (from 2 to 10 mM; always $\geq$ 10x K_d) and spectra were taken at intervals until flavin reduction was complete. Since flavin reduction was extremely slow in the Cys130Ala mutant, reduction reactions were performed at 25 °C. For the Cys130Ser mutant, reduction reactions were performed at 4 °C to facilitate comparison with the wild-type. Reduction rate constants were determined by fitting the absorbance traces at 475 nm to either one or two exponentials. Since a saturating DHO concentration was used in each experiment, the k_{obs} obtained from fitting the exponential traces is equivalent to k_{red}.

Kinetic Isotope Effects on Flavin Reduction in the Cys130Ser Mutant

Deuterium isotope effects were also determined for the Cys130Ser mutant. The extremely slow rate of the Cys130Ala mutant prevented the determination of KIEs for

this mutant. Anaerobic Cys130Ser DHOD in 50 mM TAPS, 50 mM ionic strength, pH 8.5, 4 °C was mixed with 3 mM substrate (either labeled or unlabeled) and spectra were taken at intervals until flavin reduction was complete. Kinetic traces at 475 nm were fit to a single exponential to give k_{red}. Reduction with each substrate was repeated a minimum of three times and the k_{red} values obtained were averaged. The averaged k_{red} values were used to determine the KIE by dividing k_{red} calculated for protio-DHO by the k_{red} calculated for each labeled substrate.

Results

Reduction of the Class 1A DHOD

Our goal was to determine the mechanism of FMN reduction by DHO. Stopped-flow methods provide the most direct window to observe this chemistry because large spectral changes accompany the reaction. Often, steady-state kinetics are used to address such questions, but in an enzyme as complex as DHOD, the reduction could be obscured by other processes. The catalytic cycle of DHOD consists of two half-reactions. In the reductive half-reaction – the focus of this study – the enzyme-bound flavin is reduced by DHO. In the oxidative half-reaction, the reduced enzyme is oxidized by fumarate. Reactions other than flavin reduction, such as fumarate reduction or product dissociation,

could be partly or completely rate-determining in turnover, masking the chemistry of interest. Therefore, rather than study the mechanism in the steady-state, we elected to study flavin reduction directly by only observing the reductive half-reaction – the conversion of DHO to OA and concomitant reduction of the enzyme.

The reductive half-reaction of the Class 1A DHOD from *L. lactis* was studied by mixing anaerobic oxidized enzyme with anaerobic DHO in the absence of an oxidizing substrate. All experiments were conducted at 4 °C to sufficiently slow the reaction so it could be observed. Absorbance spectra were collected using a diode-array detector from 350 to 700 nm over the course of 0.4 seconds (Figure 3-2A). Singular-value decomposition indicated one reaction intermediate; therefore, data were fit to a two-step model to calculate spectra. DHO binds to the enzyme in the dead-time of the stopped-flow instrument causing a large red-shift in flavin absorbance (Figure 3-2B). This shift in the flavin peak (from 456 nm to 475 nm) seen in the enzyme-substrate complex is similar to that previously observed for DHOD-DHO complexes in the Class 2 enzymes from *E. coli* (16) and *H. sapiens* (11). After formation of the enzyme-substrate complex, flavin absorbance at 475 nm decreases rapidly as DHO is oxidized. The reduced enzyme-OA complex formed in this reaction has a charge-transfer band extending to long wavelengths which indicates stacking of OA with the reduced FMN. This is seen as an

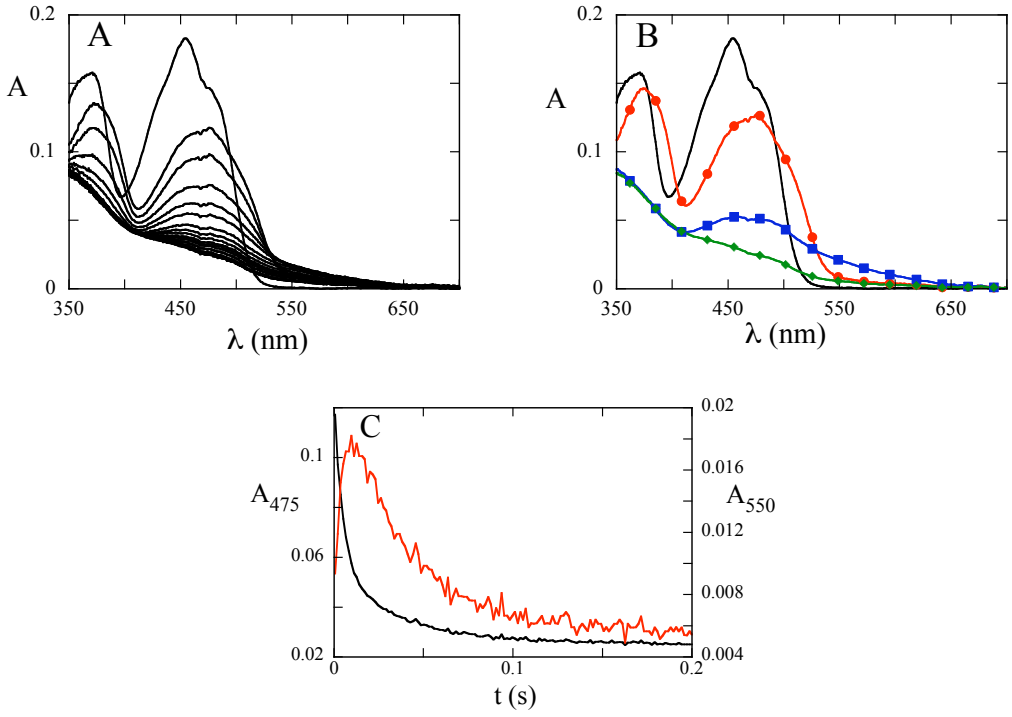

Figure 3-2: Spectral Changes During Reductive Half-Reaction

(A) Anaerobic DHOD (15.9 μM after mixing) was mixed with DHO (2 mM after mixing) in 0.1 M Tris-HCl, 0.1 mM EDTA, pH 8.5, at 4 °C in a stopped-flow spectrophotometer and spectra were collected with a diode-array over 0.4 seconds. The starting spectrum of fully oxidized DHOD was collected by mixing anaerobic DHOD with anaerobic buffer. (B) Intermediates were calculated from the data in (A) by singular-value decomposition and fitting to a two-step model in SpecFit (Spectrum Software Associates). Oxidized DHOD is shown in black. A large red-shift in flavin absorbance is seen in the Michaelis complex (red), which reacts to yield the reduced enzyme-product complex having a charge-transfer band extending to long wavelengths (blue). OA dissociation gives enzyme with the final spectrum (green). (C) Single-wavelength data from (A) are plotted as a function of time. At 475 nm (black), the peak of the Michaelis complex, a biphasic decrease in flavin absorbance is seen. At 550 nm (red), flavin reduction is seen as an increase in absorbance followed by a decrease caused by OA dissociation.

increase in absorbance at 550 nm (Figure 3-2B). This charge-transfer band is also observed in Class 2 DHODs (16). The charge-transfer absorbance of the reduced enzyme

is lost upon product dissociation producing the spectrum of the reduced enzyme (Figure 3-2B)[1].

Rate constants for the reductive half-reaction were determined from absorbance traces at either 475 nm or 550 nm. At 475 nm a large decrease in absorbance representing flavin reduction is followed by a small decrease in absorbance representing product dissociation (Figure 3-2C). At 550 nm, flavin reduction is accompanied by an increase in absorbance while OA dissociation is seen as a decrease in absorbance (Figure 3-2C). Rate constants for both flavin reduction and product dissociation were determined by fitting to sums of exponentials. At either wavelength, the observed rate constant of the first phase, representing flavin reduction, varied hyperbolically with DHO concentration, allowing the rate constant for flavin reduction (k_{red}) and the K_d to be determined. At pH 8.5 and 4 ^oC, k_{red} was 157 ± 4 s^{-1} and K_d was 240 ± 30 μM. The rate constant of charge-transfer disappearance was 25 ± 2 s^{-1}. Sometimes, a final small phase was observed that showed no concentration dependence. It is not clear what this phase represents, but we speculate that it was caused by the consumption of a small amount of

[1] Occasionally, the enzyme did not fully reduce in the time frame of a stopped-flow experiment, but instead stopped with half of the oxidized flavin remaining. The origin of this apparent half-sites reactivity in the homodimeric enzyme is not known, but has been observed before (17, 18). Regardless of whether the enzyme reduced completely or only halfway, the rate constants and spectral changes were identical.

contaminating oxygen. Regardless of its origin, this reaction phase was well-resolved – always being at least an order of magnitude slower than product release.

pH Dependence of the Reductive Half-Reaction

The reductive half-reaction of *L. lactis* DHOD was studied from pH 6.47 – 10.36 in anaerobic stopped-flow experiments. Enzyme at the pH of the experiment was mixed with various concentrations of DHO at the same pH. During the course of these experiments, it was noticed that higher ionic strengths increased the observed rates of reduction (data not shown), consistent with previously published data that showed higher ionic strength favored increased activity in this enzyme (19). Because of this, all buffers used to determine the pH dependence had a constant ionic strength of 50 mM. At each pH, the observed rate constant for reduction varied hyperbolically with DHO concentration, allowing the determination of both the reduction rate constant and the K_d of DHO. The reduction rate constant increased with pH until reaching a limiting value of 270 ± 10 s^{-1} (Figure 3-3). The pH profile gave a pK_a controlling reduction of 8.3 ± 0.1. This pK_a is consistent with crystal structures which indicate that the active site base is Cys130. The K_d of DHO (~200 μM) was essentially independent of pH until pH 9, whereupon it increased with pH showing no sign of a plateau, reaching a value of 1 mM

at the highest pH value studied, 10.36. The loss of affinity of DHO at high pH could be due to the deprotonation of N3 of DHO or lysine 43 (which makes a salt-bridge to the pyrimidine in the crystal structure) (*7*). The rate constant for product dissociation from the reduced enzyme (loss of charge-transfer absorbance) varied randomly between 22 – 35 s^{-1} at all pH values studied above 7.5. Below pH 7.5, the rate of flavin reduction was slower than 22 s^{-1}, changing the rate-limiting step of the overall reaction from product release to flavin reduction, preventing the observation of the charge-transfer complex.

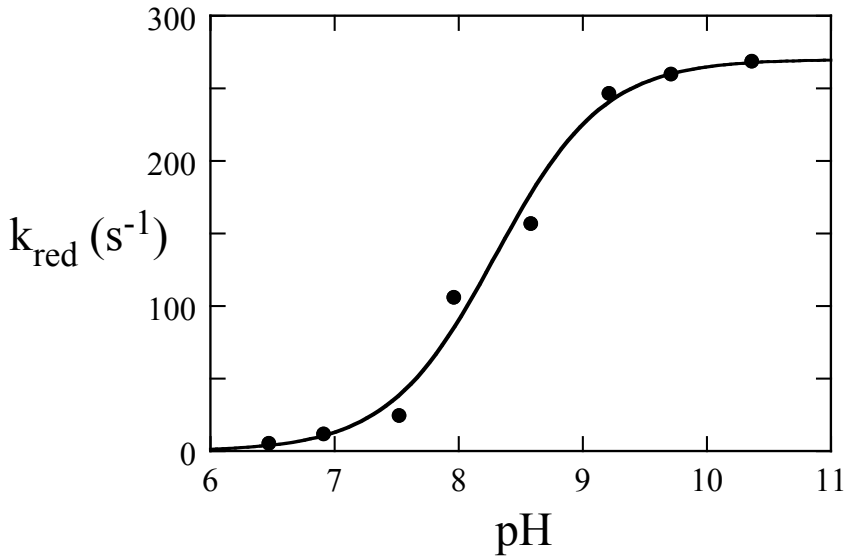

Figure 3-3: pH Dependence of Flavin Reduction in Class 1A DHOD from *L. lactis*

The limiting rate constants for reduction (k_{red}) were obtained from stopped-flow experiments at 4° C as described in the text. The plot was fit to Equation 1 giving a pK_a value of 8.3 ± 0.1 and maximum rate constant for flavin reduction at high pH of 270 ± 10 s^{-1}.

Active Site Base Mutants

The importance of the active site base in the reduction of DHOD was investigated by studying the reactions of Cys130Ala (where the active site base is removed) and Cys130Ser (where the active site base is replaced by the active site base utilized in Class 2 DHODs). Reduction of the flavin was very slow in both mutants; however, the binding of DHO to both mutants caused an immediate red-shift in the flavin absorbance as seen in wild type. The slow reaction allowed the K_d of DHO to be determined by direct aerobic titration for the Cys130Ala mutant, as the extent of reaction over the course of the titration was negligible. In this mutant, the K_d of DHO (~200 μM) was unaffected by pH until pH 9.35 was reached. A maximum K_d value of ~400 μM was found at pH 10.22, the highest pH evaluated. To determine the K_d of DHO for the Cys130Ser mutant, aerobic DHO titrations were performed in the stopped-flow spectrophotometer, allowing spectra to be scanned within 10 s of mixing. Similar to the wild-type enzyme, the K_d of DHO in the Cys130Ser mutant remained around 200 μM until pH 9 was reached. At that point, the K_d increased with no sign of plateau to a maximum value of 600 μM at pH 10.3, the highest pH value investigated.

The reductive half-reaction of both mutants was studied at saturating DHO concentration ($\geq$ 10x K_d). Upon addition of DHO, the flavin absorption peak

immediately shifted from 456 to 475 nm as seen in the wild-type enzyme (Figure 3-4). Slow flavin reduction was observed following addition of DHO. No charge-transfer complex was observed because the rate of product release is not changed by the active site base mutation; however, the rate of reduction is significantly reduced, preventing the accumulation of the charge-transfer complex.

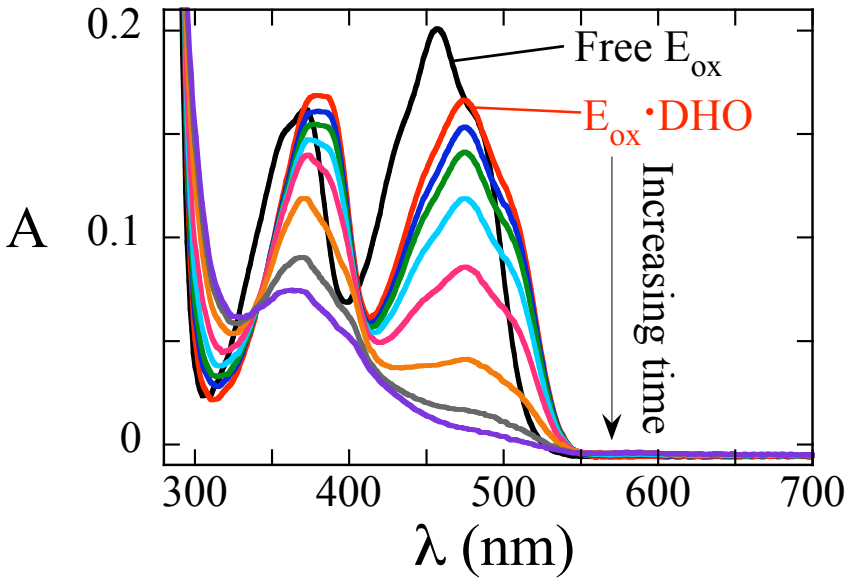

Figure 3-4: Reduction of Cys130Ser *L. lactis* DHOD

10.4 μL of 250 mM DHO was added to 1.29 mL of 16.7 μM Cys130Ser in 50 mM MOPS, 50 mM ionic strength, pH 7.5 at 4 °C in an anaerobic cuvette. Immediately upon mixing, the flavin absorbance undergoes a red-shift from 456 to 475 nm (red) as seen in wild-type enzyme. Flavin absorbance then decreases slowly with time. For clarity, only selected spectra are shown. As the reaction proceeds, anionic semiquinone was produced, as evidenced by peaks/shoulders at 370 and 400 nm (prominent in the orange and grey spectra). The final spectrum shown was taken 44 hours after mixing.

During the course of reduction, both mutant enzymes formed anionic semiquinone as evidenced by peaks/shoulders at 370 and 400 nm (Figure 3-4). The semiquinone produced during the reduction was ultimately consumed - however, at a very slow rate, requiring several days, and therefore reactions were not routinely followed to completion. In some cases, the kinetic traces at 475 nm fit to a single exponential, while in other cases the traces required an extra phase for good fits. In those cases, the two observed rates were close, only differing by ~3-fold, with the second phase apparently related to semiquinone reduction. It is not clear why this phase is not always resolved, but semiquinone was always detected. Semiquinone production required the presence of DHO. Simply reducing the enzyme in the absence of DHO with a xanthine/xanthine oxidase reducing system (20) or dithionite did not produce semiquinone. Furthermore, using DHO concentrations in vast excess of the K_d (100x) resolved the reaction traces into two phases without changing the observed rate constant of the first phase, suggesting that differential DHO binding to the semiquinone and reduced forms of the enzyme changes their reactivities. Our data suggest that following 2-electron reduction, the hydroquinone reacts with the unreacted oxidized enzyme forming semiquinone (Figure 3-5). This could occur by several conceivable intra- and

intermolecular mechanisms. A detailed dissection of these finding is beyond the scope of this work.

$$DHOD_{ox} + DHO \longrightarrow DHOD_{ox}{\bullet}DHO \longrightarrow DHOD_{red}{\bullet}OA \longrightarrow DHOD_{red} + OA$$

$$DHOD_{ox}{\bullet}DHO + DHOD_{red} \text{ (with or without DHO)} \longrightarrow 2 \text{ Semiquinone}$$

Figure 3-5: Kinetic Scheme of Cys130Ser Mutant DHOD Reductive Half-Reaction

The effect of pH on the reduction rate constant of the Cys130Ser mutant was studied at saturating DHO concentrations at 4 °C. The rate constant increased with pH from 9.9 x 10^{-6} s^{-1} at pH 6.47 to 0.03 s^{-1} at pH 10.36 (Figure 3-6) but did not show a pK_a. The rate of reduction observed with the Cys130Ser mutant was four orders of magnitude lower than the rate obtained using wild-type DHOD at pH 10.36, and the difference between the rates was even larger at lower pH values.

The pH dependence on the reduction of the Cys130Ala mutant was also studied. This reaction was even slower than that of the Cys130Ser mutant, so rate constants were determined at 25 °C instead of 4 °C using saturating DHO concentrations (≥10x K_d). Below pH 7.7, the protein was not stable and would precipitate after about twenty hours, preventing the determination of the rate constant for reduction. From pH 7.7 – 10.2, the

rate constant increased from 3.8 x 10^{-5} s^{-1} to 9.6 x 10^{-4} s^{-1} but never reached an accessible pK_a (Figure 3-6).

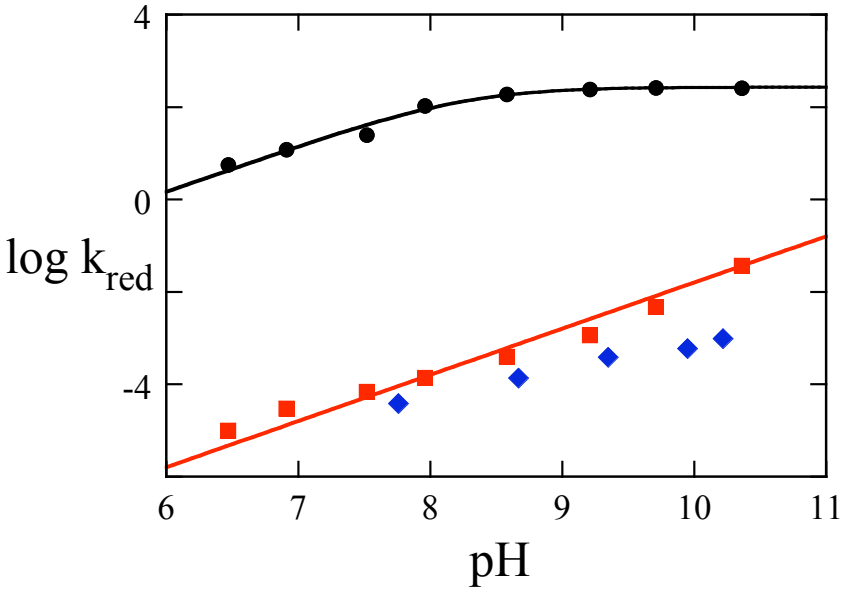

Figure 3-6: pH Dependence of Wild-Type and Mutant DHODs

The limiting rate constants for reduction (k_{red}) of the Cys130Ser mutant (red squares) were obtained at 4 °C as described in the text and Figure 3-3; those for the Cys130Ala mutant (blue diamonds) were obtained at 25 °C. Neither mutant shows an accessible pK_a in the pH range investigated and both mutants reduced extremely slowly. The pH dependence of the wild-type enzyme, previously shown in Figure 3-3, is also shown in this figure (black circles) for comparison.

Kinetic Isotope Effects

The oxidation of DHO could occur either by a concerted or a stepwise mechanism. To determine which mechanism is utilized by the wild-type Class 1A DHOD from *L. lactis*, kinetic isotope effect experiments were conducted using DHO

labeled at either the 5-position, the 6-position, or both the 5- and 6-positions. Absorbance traces at 475 nm (Figure 3-7) were fit to three exponentials. The fast phase, corresponding to flavin reduction, varied hyperbolically with DHO concentration allowing the rate constant for reduction to be determined. Kinetic isotope effects (KIEs) were obtained by dividing the k_{red} determined for protio-DHO by the k_{red} determined for deuterated DHO.

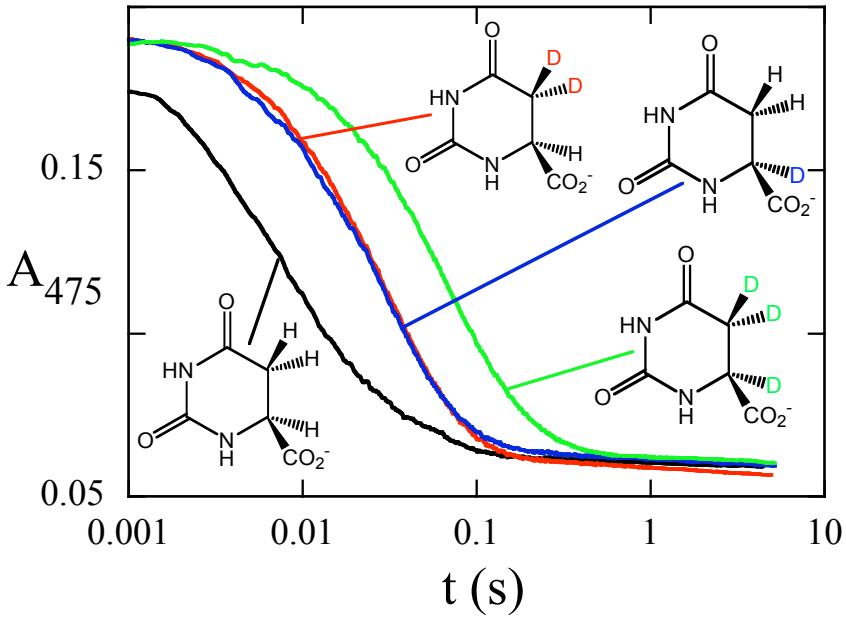

Figure 3-7: Reduction of Wild-Type DHOD with Labeled and Unlabeled DHO

Anaerobic DHOD (final concentration 15 µM) was mixed with anaerobic substrate (final concentration 2 mM) at pH 8.5. Note that the reaction traces at 475 nm are shown on a logarithmic time scale. Protio-DHO is shown in black, 5,5-$^{2}H_2$ DHO is shown in red, 6-^{2}H DHO is shown in blue, and 5,5,6-$^{2}H_3$ DHO is shown in green. The traces were adjusted by adding a constant to matching final absorbance. Note that time is on a logarithmic scale.

KIEs were determined for the wild-type enzyme at pH 7.0 and 8.5. At pH 7.0, using 5,5-$^2H_2$ DHO, a KIE of 1.83 ± 0.04 was found (Table 3-1), and a KIE of 2.21 ± 0.04 was obtained using 6-^2H DHO. The double KIE determined using 5,5,6-$^2H_3$ DHO was found to be 4.3 ± 0.2. The KIE values obtained at pH 8.5 using 5,5-$^2H_2$ DHO, 6-^2H DHO, and 5,5,6-$^2H_3$ DHO were 2.2 ± 0.1, 2.9 ± 0.1, and 5.8 ± 0.3 respectively.

Table 3-1: Reduction Rate Constant and KIEs for Wild-Type DHOD[a]

	pH 7.0		pH 8.5	
Compound	k_{red} (s^{-1})	KIE	k_{red} (s^{-1})	KIE
DHO	12.0 ± 0.1		164 ± 3	
5,5-$^2H_2$ DHO	6.5 ± 0.1	1.83 ± 0.04	73 ± 2	2.2 ± 0.1
6-^2H DHO	5.44 ± 0.06	2.21 ± 0.04	57 ± 2	2.9 ± 0.1
5,5,6-$^2H_3$ DHO	2.77 ± 0.08	4.3 ± 0.2	28.3 ± 0.3	5.8 ± 0.3

[a]The k_{red} values used to calculate the KIE were obtained from the value at saturating DHO concentration as explained in Experimental Procedures. The highest concentration of DHO used was 4 mM after mixing (about 20 times K_d).

Double deuterium isotope effects were also used to study the mechanism of DHO oxidation in the *L. lactis* Cys130Ser mutant DHOD.[2] Anaerobic Cys130Ser DHOD was mixed with saturating concentrations (≥ 10x K_d) of labeled and unlabeled substrate as

[2] Isotope effect experiments were not conducted with the Cys130Ala mutant due to the extremely slow rate of flavin reduction.

described in Experimental Procedures. Kinetic traces at 475 nm (Figure 3-8) were fit to a single exponential to give k_{red} values. At pH 8.5, KIE values of 2.56 ± 0.14, 1.65 ± 0.13 and 4.57 ± 0.58 were obtained for DHO deuterated the 5-position, 6-position and 5- and 6-positions respectively (Table 3-2).

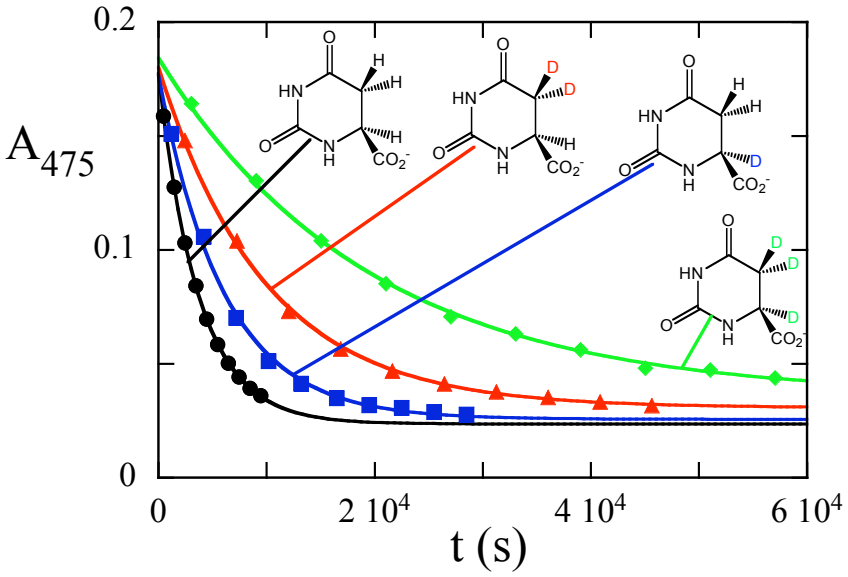

Figure 3-8: Reduction of Cys130Ser Mutant with Labeled and Unlabeled DHO

Anaerobic DHOD (final concentration 15 µM) was mixed with anaerobic substrate (final concentration 2 mM) at 4 °C in a scanning spectrophotometer at pH 8.5 and spectra were scanned at intervals as in Figure 3-4. Absorbance traces at 475 nm were extracted from the data and fit to single exponentials to obtain rate constants. Protio-DHO is shown in black, 5,5-$^2H_2$ DHO is shown in red, 6-^2H DHO is shown in blue, and 5,5,6-$^2H_3$ DHO is shown in green. Most points were omitted for clarity; the curves are the fits to the complete data set. Note that time is on a linear scale.

Table 3-2: Reduction Rate Constants and KIEs for the Cys130Ser Mutant at H 8.5[a]

Compound	k_{red} (s^{-1})	KIE
DHO	$2.61 \times 10^{-4} \pm 9 \times 10^{-6}$	
5,5-$^2H_2$ DHO	$1.02 \times 10^{-4} \pm 2 \times 10^{-6}$	2.56 ± 0.14
6-^2H DHO	$1.58 \times 10^{-4} \pm 7 \times 10^{-6}$	1.65 ± 0.13
5,5,6-$^2H_3$ DHO	$5.71 \times 10^{-5} \pm 5.3 \times 10^{-6}$	4.57 ± 0.58

[a]The k_{red} values used to calculate the KIE were determined by averaging values from fits of at least three separate traces obtained at saturating (≥ 10x K_d) DHO concentrations at 4 °C; errors reported are the standard deviations on the averaged rate constants.

Discussion

DHODs are flavin-containing enzymes that catalyze the oxidation of DHO to OA with the concomitant reduction of the FMN prosthetic group. We studied the mechanism of flavin reduction in the Class 1A DHOD from *L. lactis* in detail, looking at the pH dependence of reduction as well as the double kinetic isotope effects associated with DHO oxidation. To further investigate the importance of the active site base, two base- mutants were also studied – Cys130Ala (where the active site base has been removed) and Cys130Ser (where the active site base has been switched to the base utilized in Class 2 DHODs).

Upon binding of DHO to the wild-type Class 1A DHOD, the flavin absorbance undergoes a dramatic red-shift. Similar red-shifts are seen for the binding of several

ligands to all oxidized DHODs investigated. Substrates, such as DHO or dihydrooxonate, products, such as orotate or oxonate, or non-reactive inhibitors, such as 3,5-dihydroxybenzoate cause this red shift upon binding (16, 18, 21). Spectra of flavoproteins often undergo large shifts when reaction intermediates are formed (22). However, this red-shifted spectrum is not that of a chemical intermediate, because products and inhibitors give the same shift but cannot react with oxidized enzyme. Ligand binding to flavoproteins often causes charge-transfer bands (22). However, the red-shift cannot be the formation of charge-transfer absorbance because charge-transfer transitions require an electron-rich donor to be in contact with the electron-deficient flavin, but the binding of electron-poor ligands such as OA cause the red-shift. It is possible that the close proximity of the dipole of the ligands to the flavin causes this shift. It is not surprising that this shift occurs in all classes of DHODs, given the very similar structures of the active sites in these enzymes. Both classes of DHODs contain four highly conserved asparagine residues (7-9) that have been shown to interact with OA in the product complex crystal structures and the remainder of the active site is also nearly identical in the two classes of enzymes (Figure 3-9).

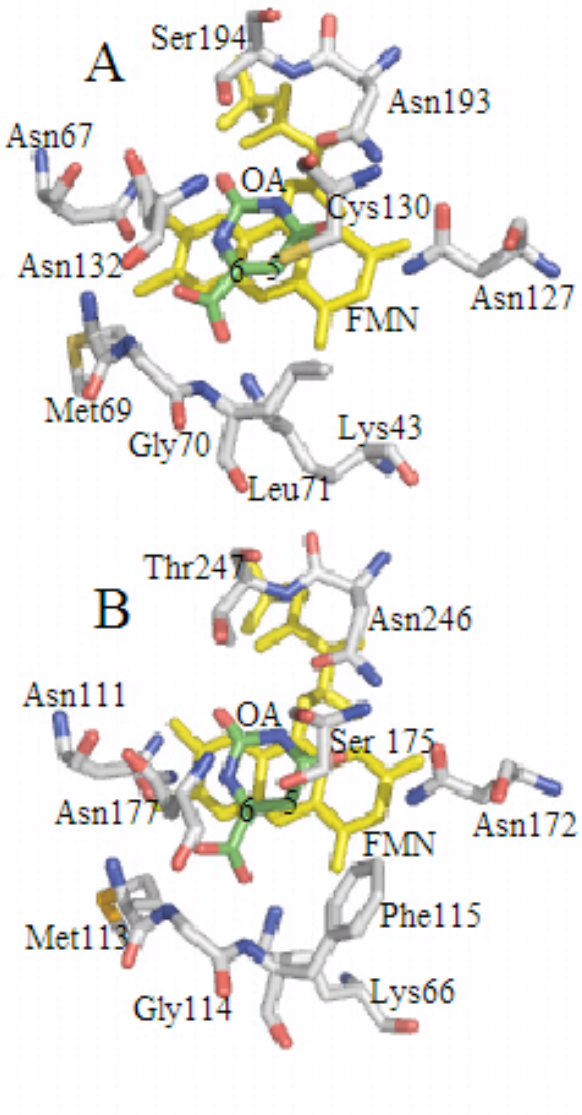

Figure 3-9: Pyrimidine-Binding Pockets of Class 1A and Class 2 DHODs

The flavin, OA, and key active site residues are shown for the Class 1A enzyme from *L. lactis* (A) and the Class 2 enzyme from *E. coli* (B). Note the similar OA-protein interactions, the proximities of the active site bases to the 5-position of OA, and the propinquities of the 6-position of OA to N5 of FMN in both structures. Coordinates were taken from PDB files 2dor and 1f76.

The rate of flavin reduction is pH-dependent in the Class 1A DHOD from *L. lactis*. In this enzyme, Cys130 is acting as a general base to deprotonate C5 of DHO.

The pK_a controlling reduction (~8.3) is similar to that of unperturbed cysteine, suggesting that the cysteine is not activated by other active site residues. This is expected from crystal structures, which show nothing in the active site that would activate the cysteine. Our finding is also consistent with previously published work that used chemical modification to investigate the pK_a of this enzyme (1). When the active site base was mutated to either alanine or serine the originally observed pK_a (~8.3) is no longer observed, providing further evidence for the assignment of the pK_a to residue Cys130. The lack of an observable pK_a in the Cys130Ser mutant is consistent with our conclusion that the active site does not provide large electrostatic perturbations to lower the pK_a of the base. Serine has a pK_a of 13.6 in aqueous solution (23). If the enzyme had lowered the pK_a by ~3 units or more the shift would have been detected.

The oxidation of DHO requires the deprotonation of the *pro-S* hydrogen on C5 of DHO and the transfer of the C6 hydrogen to the flavin as a hydride or hydride equivalent. The reaction could occur either by a concerted mechanism (both C-H bonds break at the same time) or by a stepwise mechanism (the C-H bonds break sequentially). Double kinetic isotope effects can be used to distinguish between concerted or stepwise mechanisms for flavin reduction. The Rule of the Geometric Mean states that in the absence of large quantum effects, perturbations to a partition function caused by isotopic

substitutions at a particular site are independent of isotopic substitutions at another site (24). Therefore, if both C-H bonds break in a concerted mechanism (*i.e.*, a single transition state), then the product of the two single isotope effects, obtained by multiplying the KIE obtained with 5,5-$^2H_2$ DHO and 6-^2H DHO, will equal the observed double KIE, obtained with 5,5,6-$^2H_3$ DHO. At both pH values investigated, the Rule of the Geometric Mean is obeyed within experimental error (Table 3-3). This rules out major tunneling effects and we conclude that the oxidation of DHO by the Class 1A DHOD from *L. lactis* is concerted (Figure 3-10).

Table 3-3: Analysis of KIEs

L. lactis WT	5,5-$^2H_2$ DHO	6-^2H DHO	predicted double KIEs[a]	5,5,6-$^2H_3$ DHO
pH 7.0	1.83 ± 0.04	2.21 ± 0.04	4.0 ± 0.2	4.3 ± 0.2
pH 8.5	2.2 ± 0.1	2.9 ± 0.1	6.5 ± 0.6	5.8 ± 0.3
Cys130Ser				
pH 8.5	2.56 ± 0.14	1.65 ± 0.13	4.22 ± 0.56	4.57 ± 0.58

[a]The Rule of the Geometric Mean predicts that the double KIE equal the product of each single KIE if the reaction occurs in a single transition state (23).

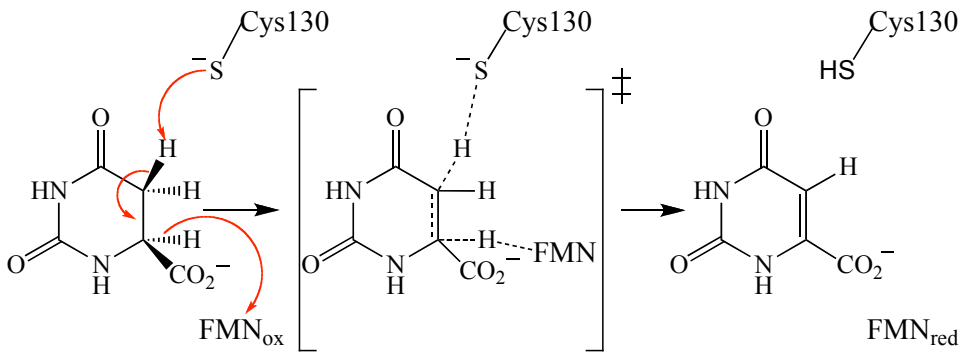

Figure 3-10: Mechanism of DHO Oxidation by the Class 1A DHOD from *L. lactis*

The conversion of DHO to OA occurs via a single transition state in which the active site base, cysteine, deprotonates DHO as the hydride is transferred to the flavin.

The question of whether the flavin of DHOD is reduced in a concerted or stepwise mechanism has been addressed previously for the Class 1A enzyme from *Crithidia fasciculata* (13). In contrast to our work, that study concluded that DHO oxidation was stepwise, based on a steady-state kinetic analysis of multiple deuterium isotope effects. We offer two possible explanations for these different conclusions. First, it is possible that there is variation of the reaction mechanisms within Class 1A DHODs. However, all other biochemical properties of DHODs segregate according to the phylogenetic classification. Alternatively, the different conclusions could have a chemical rationale. At the time the steady-state analysis was performed, it had not yet been shown that the Class 1A DHODs use fumarate as the oxidizing substrate and dissolved oxygen was used instead. Most reduced flavoenzymes will reduce O_2 even if it is not the physiological

substrate; its reaction with DHOD does not require the participation of an active site acid. The bimolecular rate constant observed for the oxidation of the Cys130Ser mutant by O_2 is nearly identical to that of the wild-type (Palfey, unpublished data). The rate of exchange of the protons derived from DHO between a reduced Class 1A enzyme and solvent has been shown to be slow relative to catalysis (24). Thus, when oxygen rather than fumarate is used as the oxidizing substrate, the active site cysteine, which acted as a base in the reductive half-reaction, will very likely remain protonated or deuterated after flavin oxidation. It must be deprotonated prior to the next turnover with DHO, and a significant isotope effect can be expected because fractionation factors of thiols are generally ~0.5 or less (25). Therefore, in steady-state kinetics using O_2 as the oxidizing substrate, isotope effects from deprotonation of the active site cysteine could also contribute to the observed isotope effects. Such a possibility was not considered.

Changing the active site base did not alter the concerted mechanism. The Cys130Ser DHOD mutant obeyed the Rule of the Geometric Mean (Table 3-3) just as the wild-type. The Class 2 DHODs from *E. coli* and *H. sapiens* do not obey the Rule of the Geometric Mean, leading to the conclusion that Class 2 DHODs utilize either a stepwise mechanism, or a concerted mechanism with significant quantum mechanical tunneling (11). Therefore, the identity of the active site base is not responsible for the difference in

mechanism between the two classes despite the otherwise nearly identical active site structures (Figure 3-9). Subtle dynamic features may be in play in these two classes of enzymes that determine the mechanism of DHO oxidation.

The value of the KIE for deprotonating DHO barely increased when the active site cysteine was mutated to serine (Table 3-3), suggesting that the extent of proton transfer did not change markedly between the two transition states. However, the value of the KIE for hydride transfer decreased almost two-fold due to the mutation, indicating a lower extent of hydride transfer at the transition state in the mutant enzyme. The different KIEs, measured under the same conditions, clearly indicate changes in transition state structures between the wild-type and mutant enzymes, although the mechanism of DHO oxidation is concerted in both enzymes.

We have detected a significant difference in the mechanisms of the two classes of DHODs, but the basis of this difference is not yet clear. The measurement of other isotope effects, such as heavy atom effects, should allow the structures of the different transition states to be deduced. Differences in transition state structures might open the possibility for designing class-specific inhibitors for various DHODs.

References

1. Björnberg, O., Rowland, P., Larsen, S., and Jensen, K. F. (1997) *Biochemistry*, **36**, 16197-16205.

2. Jones, M. E. (1980) *Annu. Rev. Biochem.*, **49**, 253-279.

3. Nagy, M., Lacroute, F., and Thomas, D. (1992) *Proc. Natl. Acad. Sci. U. S. A.*, **89**, 8966-8970.

4. Nielsen, F. S., Andersen, P. S., and Jensen, K. F. (1996) *J. Biol. Chem.*, **271**, 29359-29365.

5. Annoura, T., Nara, T., Makiuchi, T., Hashimoto, T., and Aoki, T. (2005) *J. Mol. Evol.*, **60**, 113-127.

6. Palfey, B. A., Björnberg, O., and Jensen, K. F. (2001) *J. Med. Chem.*, **44**, 2861-2864.

7. Rowland, P., Björnberg, O., Nielsen, F. S., Jensen, K. F., and Larsen, S. (1998) *Protein Sci.*, *7*, 1269-1279.

8. Nørager, S., Jensen, K. F., Björnberg, O., and Larsen, S. (2002) *Structure*, **10**, 1211-1223.

9. Liu, S., Neidhardt, E. A., Grossman, T. H., Ocain, T., and Clardy, J. (2000) *Structure*, **8**, 25-33.

10. Blattmann, P., and Retey, J. (1972) *Eur. J. Biochem.*, **30**, 130-137.

11. Fagan, R. L., Nelson, M. N., Pagano, P. M., and Palfey, B. A. (2006) *Biochemistry*, **45**, 14926 - 14932.

12. Nielsen, F. S., Rowland, P., Larsen, S., and Jensen, K. F. (1996) *Protein Sci.*, **5**, 852-856.

13. Pascal, R. A., Jr., and Walsh, C. T. (1984) *Biochemistry*, **23**, 2745-2752.

14. Palfey, B. A. (2003) Time resolved spectral analysis, in *Kinetic analysis of macromolecules* (Johnson, K. A., Ed.) pp 203-227, Oxford University Press, New York.

15. Williams, C. H., Jr., Arscott, L. D., Matthews, R. G., Thorpe, C., and Wilkinson, K. D. (1979) *Methods in Enzymology*, **62**, 185-198.

16. Palfey, B. A., Björnberg, O., and Jensen, K. F. (2001) *Biochemistry*, **40**, 4381-4390.

17. Shi, J., Dertouzos, J., Gafni, A., Steel, D., and Palfey, B. A. (2006) *Proc. Natl. Acad. Sci. U. S. A.*, **103**, 5775-5780.

18. Nørager, S., Arent, S., Björnberg, O., Ottosen, M., Lo Leggio, L., Jensen, K. F., and Larsen, S. (2003) *J. Biol. Chem.*, **278**, 28812-28822.

19. Ottosen, M. B., Björnberg, O., Nørager, S., Larsen, S., Palfey, B. A., and Jensen, K. F. (2002) *Protein Sci.*, **11**, 2575-2583.

20. Massey, V. (1990) in *Flavins and Flavoproteins* (Curti, B., Ronchi, S., and Zanetti, G., Eds.) pp 59-66, Walter de Gruyter, Berlin, Germany.

21. Björnberg, O., Jordan, D. B., Palfey, B. A., and Jensen, K. F. (2001) *Arch. Biochem. Biophys.*, ***391***, 286-294.

22. Palfey, B. A., and Massey, V. (1998) Flavin-dependent enzymes, in *Comprehensive biological catalysis, volume iii/radical reactions and oxidation/reduction* (Sinnott, N., Ed.) pp 83-154, Academic Press, New York.

23. Bruice, T. C., Fife, T. H., Bruno, J. J., and Brandon, N. E. (1962) *Biochemistry*, **1**, 7-12.

24. Bigeleisen, J. (1955) *J. Chem. Phys.*, **23**, 2264-2267.

Chapter 4
Roles in Binding and Chemistry for Conserved Active Site Residues in the Class 2 Dihydroorotate Dehydrogenase from *E. coli*

Dihydroorotate dehydrogenases (DHODs) are flavin-containing enzymes that catalyzes the fourth step (the only redox step) in the *de novo* synthesis of pyrimidines - the conversion of dihydroorotate (DHO) to orotate (OA). DHODs have been categorized into two broad classes based on sequence (1). Several properties of the enzymes segregate nicely into these classes. Class 2 DHODs are membrane-bound enzymes that are oxidized by ubiquinone (2). Class 1 enzymes are cytosolic proteins that have been further divided into two subclasses. Class 1A enzymes are homodimers that are oxidized by fumarate (3). Class 1B enzymes are $\alpha_2\beta_2$ heterotetramers that contain a subunit that resembles the Class 1A enzymes and a second subunit that contains FAD and an iron-sulfur cluster, allowing the enzyme to be oxidized by NAD (4). Class 1 DHODs are found mostly in Gram-positive bacteria, although a few microbial eukaryotes also have Class 1A DHODs, while Class 2 enzymes are found in Gram-negative bacteria and almost all eukaryotes.

The catalytic cycle of DHODs can be studied in two separate half-reactions, allowing the direct observation of the chemistry. The reductive half-reaction involves the oxidation of DHO to OA with the concomitant reduction of the enzyme-bound FMN. The kinetics of the reductive half-reaction has been studied in anaerobic stopped-flow experiments for several Class 2 DHODs (5-7). The spectra of intermediates formed during the reductive half-reaction have been determined (7), allowing a common scheme to be proposed.

Oxidation of DHO breaks two carbon-hydrogen bonds; an active site base deprotonates the C5 *pro-S* hydrogen of DHO (8) and the C6 hydrogen is transferred as a hydride to N5 of the isoalloxazine ring of the flavin. The active site bases differ between classes of DHODs, with Class 1 enzymes using a cysteine and Class 2 enzymes using a serine. The two C-H bonds could break at the same time in a concerted mechanism or sequentially in a stepwise mechanism. If a stepwise mechanism is used, there are two possible intermediates. If deprotonation occurred first, an enolate intermediate would form. However, if hydride transfer occurs first, an iminium intermediate would form.

Using DHO deuterated at the 5-, 6-, or both positions in anaerobic stopped-flow experiments, the Class 2 enzyme from *E. coli* was shown to use a stepwise mechanism for DHO oxidation (5). Interestingly, the Class 1A DHOD from *L. lactis* was shown to

use a concerted mechanism (9). Aside from the difference in the active site base, the pyrimidine-binding sites of the two classes are nearly identical (10-13). Even though the main structural difference between the enzymes is the base, the identity of the active base is not responsible for the determining the mechanism of DHO oxidation; the *L. lactis* Cys130Ser mutant enzyme was shown to use a concerted mechanism for DHO oxidation (9).

All DHODs contains a ring of strictly conserved asparagine residues that make extensive interactions with OA in the product complex (Figure 4-1). Also hydrogen-bonding to OA is either a threonine (in Class 2 and 1B enzymes) or a serine (in Class 1A enzymes) that. The roles of these highly conserved residues in the Class 2 enzyme from *E. coli* was investigated by site-directed mutagenesis. The mutations had little effect on the reduction potential of the enzymes, while effects on the kinetics of the reductive half-reaction varied from mild to severe, with the most significant decreases in the rate constant of flavin reduction being observed for the Asn172Ala (removing a hydrogen-bond to the C4 carbonyl) and the Asn111Ala (removing a hydrogen-bond to N1) mutant enzymes. These residues are positioned to stabilize charge build-up that occurs during the stepwise oxidation of DHO by this enzyme.

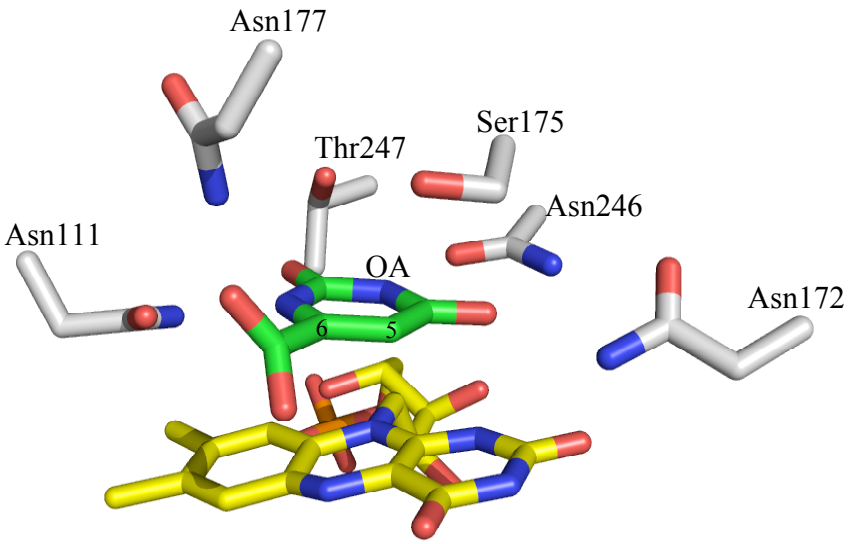

Figure 4-1: Pyrimidine Binding Site of the Class 2 DHOD from *E. coli*

The conserved hydrogen-bonding residues of the pyrimidine binding site are shown along with the active site base (Ser175). OA (green) stacks above the flavin with C6 in van der Waals contact with N5 of FMN and C5 under the active site base. The flavin is shown in yellow. Coordinates taken from 1pdb file f76.

Experimental Procedures

Site-Directed Mutagenesis

Site-directed mutants were made from the previously created pAG-1 expression vector (14) using Stratagene QuikChange II XL mutagenesis kit. Insertion of the correct mutations was checked by sequencing the entire pyrD gene.

Overexpression and Purification of DHODs

Wild-type *E. coli* DHOD and all mutant enzymes were overexpressed in *E. coli* strain SØ6645 (a DHOD deletion strain) as previously described (14). All proteins were purified using previously published procedures (14). All purified enzymes were diluted to 50% (v/v) glycerol and stored at -80 ^{o}C. Enzymes were exchanged into the correct buffer for experiments using Econo-Pac 10DG disposable desalting columns (Bio-Rad).

Instrumentation

Absorbance spectra were obtained using a Shimadzu UV-2501PC scanning spectrophotometer. Stopped-flow experiments were performed at 4 °C using a Hi-Tech Scientific KinetAsyst SF-61 DX2 stopped-flow spectrophotometer.

Preparation of Anaerobic Solutions

Enzyme solutions for rapid-reaction studies were made anaerobic in glass tonometers by repeated cycles of evacuation and equilibration under an atmosphere of purified argon as previously described (15). Substrate solutions were made anaerobic within the syringes that were to be loaded onto the stopped-flow instrument by bubbling solutions with purified argon. Slow reactions were performed in anaerobic cuvettes (16)

and monitored in a standard scanning spectrophotometer. These reaction mixtures were also made anaerobic by repeated evacuation and equilibration with purified argon.

Reduction Potentials

Reduction potentials were determined by the xanthine/xanthine oxidase method of Massey (17). Experiments were preformed in anaerobic cuvettes (16) and monitored in a standard scanning spectrophotometer. 1-Anthraquinone sulfonate (E_m = -225 mV), phenosafranin (E_m = -252 mV), and benzyl viologen (E_m = -350 mV) were used as indicator dyes.

OA Binding to Oxidized DHODs

To increase the solubility of OA, the Tris salt was prepared. The sodium salt of OA from Sigma-Aldrich (31.2 g; 175 mmol) in 500 mL isopropanol was brought to a boil. 24.6 g (203 mmol) of Tris base in 80 mL H_2O was slowly dripped into the solution and the reaction was refluxed overnight. The mixture was then filtered and the solid was dried. The remaining white precipitate was the OA-Tris salt and was soluble in water to at least 400 mM.

The affinity of the oxidized enzymes for OA was determined in aerobic titrations in a standard scanning spectrophotometer. The enzyme equilibrated in 0.1 M Tris-HCl, pH 8.5 was titrated with OA in the same buffer. The differences in flavin absorbance caused by binding of OA were plotted against OA concentration, and the data were fit to a hyperbola in Kaleidagraph (Synergy, Inc.) to determine the K_d.

Reductive Half-Reactions of Mutant DHODs

The reductive half-reaction of all mutant DHODs except Asn172Ala/Asn246Ala were investigated in anaerobic stopped-flow experiments. The experiments were conducted at 4 ^{o}C to facilitate comparison with wild-type. Anaerobic enzyme equilibrated in 0.1 M Tris-HCl, pH 8.5 was mixed with anaerobic DHO in the same buffer (ranging from 40 μM to 300 mM after mixing, depending on the particular mutant). Even at the highest DHO concentrations, the pH of the final mixtures was shown to be within ~0.1 pH units of pH 8.5. Flavin spectral changes were routinely followed at 456 nm, 475 nm, and 550 nm. For the Asn246Ala mutant enzyme, the reaction was also followed at 510 nm. Reaction traces were fit to either two or three exponentials with Program A (R. Chang, C.-J. Chiu, J. Dinverno, and D. P. Ballou, University of Michigan) depending on the number of phases observed. In all cases the

observed rate constant of the phase representing flavin reduction varied hyperbolically with DHO concentration. The reduction rate constant (k_{red}, the limiting value of the observed rate constant at an infinite DHO concentration) and the apparent $K_{d,DHO}$ (the half-saturating concentration) were determined by fitting k_{obs} versus DHO concentration to a hyperbola in Kaleidagraph (Synergy, Inc.).

The reductive half-reaction of the Asn172Ala/Asn246Ala double mutant enzyme was extremely slow. The reaction of this enzyme with DHO was therefore studied using a standard scanning spectrophotometer. Enzyme equilibrated in 0.3 M Tris-HCl, pH 8.5 was mixed with varying concentrations of DHO (40 – 200 mM) in an anaerobic cuvette at either 4 ^{o}C or 25 ^{o}C and spectra were taken at intervals until the flavin was fully reduced. Reaction traces at 453 nm (the maximum flavin absorbance) were extracted and fit to a single exponential.

Kinetic Isotope Effects on Flavin Reduction in Wild-Type and the Asn177Ala Mutant DHOD

Kinetic isotope effects (KIEs) on flavin reduction were determined using 5,5,6-$^{2}H_3$ DHO. Deuterated DHO was synthesized according to published procedures (8). Deuterium content was determined using proton NMR spectroscopy. The synthesized

substrate was found to be >95 % isotopically pure. A representative NMR spectrum can be found in Appendix A.

Anaerobic enzyme equilibrated in 0.1 M Tris-HCl, pH 8.6 was mixed with anaerobic unlabeled or labeled DHO (up to 400 μM after mixing) in the same buffer. Reaction traces were collected at 475 nm. Reaction traces for wild-type DHOD were fit to three exponentials, while reaction traces for the Asn177Ala mutant were fit to two exponentials using Kaleidagraph (Synergy, Inc.), and the reduction rate constant (k_{red}) was determined as described above. KIEs were calculated by dividing the k_{red} obtained with protio-DHO by k_{red} determined with 5,5,6-$^{2}H_3$ DHO.

Results

Reduction Potentials

The reduction potential of wild-type and mutant DHODs was determined using the xanthine/xanthine oxidase method of Massey (17). The Class 2 DHOD from *E. coli* was previously reported to have a reduction potential of -310 mV (7) using the Massey method. The reduction potential was determined again using two different indicator dyes, phenosafranin (E_m = -252 mV) and 1-anthraquinone sulfonate (E_m = -225 mV) (Figure 4-2). In both cases, the reduction potential was found to be ~ -229 mV (Table

4-1). This value is much higher than the previously reported reduction potential and is near the potential reported for the Class 1A DHOD from *L. lactis* (18).

Table 4-1: Reduction Potentials of Wild-Type and Mutant *E. coli* DHODs

Enzyme	Reduction Potential
Wild-Type	-229 mV[a]
Thr247Ser	-229 mV[a]
Thr247Ala	-228 mV[a]
Asn177Ala	-258 mV[b]
Asn172Ala	-255 mV[b]
Asn246Ala	-233 mV[a]
Asn172Ala/Asn246Ala	-233 mV[a]
Asn11Ala	-238 mV[a]
Asn111Asp	-340 mV[c]

[a]Reduction potentials determined using both phenosafranin (E_m = -252 mV) and 1-anthraquinone sulfonate (E_m = -225 mV) and averaged. [b]Reduction potential determined using only phenosafranin. [c]Reduction potential determined using benzyl viologen (E_m = -350 mV).

The reduction potential of most active site mutants was determined by the same method using either phenosafranin, 1-anthraquinone sulfonate, or both as the indicator dye. Most of the mutations had little effect on the potentials (Table 4-1). However, the reduction potentials of the Asn177Ala and the Asn172Ala mutant DHODs were ~25 mV lower than that of wild-type. A major change in reduction potential was observed in the Asn111Asp mutant enzyme. To obtain the potential of this enzyme, benzyl viologen (E_m

= -350 mV) was used as the indicator dye. This enzyme has a potential of -340 mV, over 100 mV lower than the value determined for wild-type.

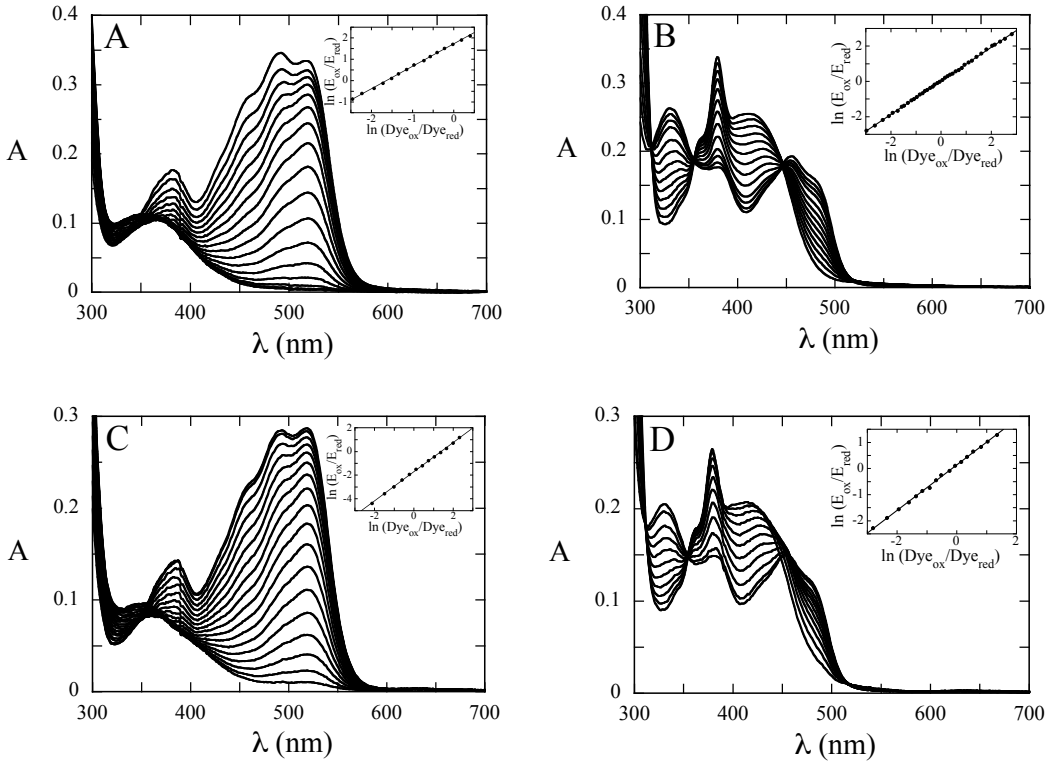

Figure 4-2: Determination of Reduction Potentials

Reduction potentials were determined using the xanthine/xanthine oxidase method of Massey (17). The reduction potential of wild-type *E. coli* DHOD was determined using phenosafranin (A) and 1-anthraquinone sulfonate (B). The reduction potential of the Asn246Ala mutant enzyme was also determined using phenosafranin (C) and 1-anthraquinone sulfonate (D). The insets in each panel show the Nerst plot for determining the potentials.

OA Binding to Oxidized Enzymes

The spectrum of each oxidized enzyme studied was nearly identical to that of wild-type. The Asn111Asp mutant enzyme, where a negative charge was introduced to the active site, exhibited a minor 1 nm red-shift in the maximum flavin absorbance when compared to wild-type. The maximum flavin absorbance of the Asn172Ala/Asn246Ala mutant was at 453 nm, blue-shifted 3 nm compared to wild-type.

A large red-shift is observed upon OA binding to oxidized Class 1A and Class 2 DHODs (14, 18-21). The maximum flavin peak in the *E. coli* DHOD shifts from 456 nm to 475 nm. This spectral change can be used to track OA binding in titration experiments, allowing the determination of OA binding affinity (Figure 4-3). The dissociation constant of OA for the Class 2 DHOD from *E. coli* was previously reported to be 5 μM at pH 8, 25 ^{o}C (14). All the K_d measurements in this work were done at pH 8.5, 25 ^{o}C; therefore, the dissociation constant of wild-type *E. coli* DHOD for OA was determined under these conditions and was found to be 5.5 ± 0.5 μM, essentially identical to the value determined at pH 8.

The effects on OA binding observed in the mutant enzymes varied widely. The conservative mutation, Thr247Ser, had little effect on OA binding (Table 4-2; Figure 4-3). When each of the active site residues that hydrogen-bond to OA in the oxidized

enzyme-OA structure were mutated to alanine, the largest effects were observed at Asn172 (40-fold weakening) and Asn246 (95-fold weakening), the two residues that interact with the C4 carbonyl of OA. All the single alanine mutant enzymes exhibited the signature red-shift associated with OA binding.

Table 4-2: OA Binding to Wild-Type and Mutant Oxidized DHODs at pH 8.5, 25 ^{o}C

Enzyme	K_d (μM)	K_d(mutant)/K_d(Wild-Type)
Wild-Type	5.5 ± 0.5	-
Thr247Ser	10.0 ± 1.2	1.8
Thr247Ala	39.3 ± 1.6	7
Asn177Ala	27.5 ± 1.5	5
Asn172Ala	220 ± 9	40
Asn246Ala	518 ± 29	95
Asn172Ala/Asn246Ala	~ 50,000	~ 9000
Asn111Ala	47.2 ± 0.2	8
Asn111Asp	>> 75,000	>> 14000

When both residues that hydrogen-bond to the C4 carbonyl were mutated to alanine (Asn172Ala/Asn246Ala double mutant), the observed K_d sky-rocketed to ~50 mM. The flavin peak did not shift to 475 nm upon OA binding as seen in wild-type and the alanine single-mutants. Instead a very slight red-shift from 456 nm to 458 nm was observed. No red-shift in the maximum flavin absorbance was observed when the Asn111Asp mutant enzyme was titrated with OA. Due to the limited solubility of OA, the enzyme could only be titrated up to ~75 mM OA. At the highest concentration of

OA, the flavin peak exhibited a slight red-shift. However, saturation of OA could not be reached and a K_d >> 75 mM is therefore estimated.

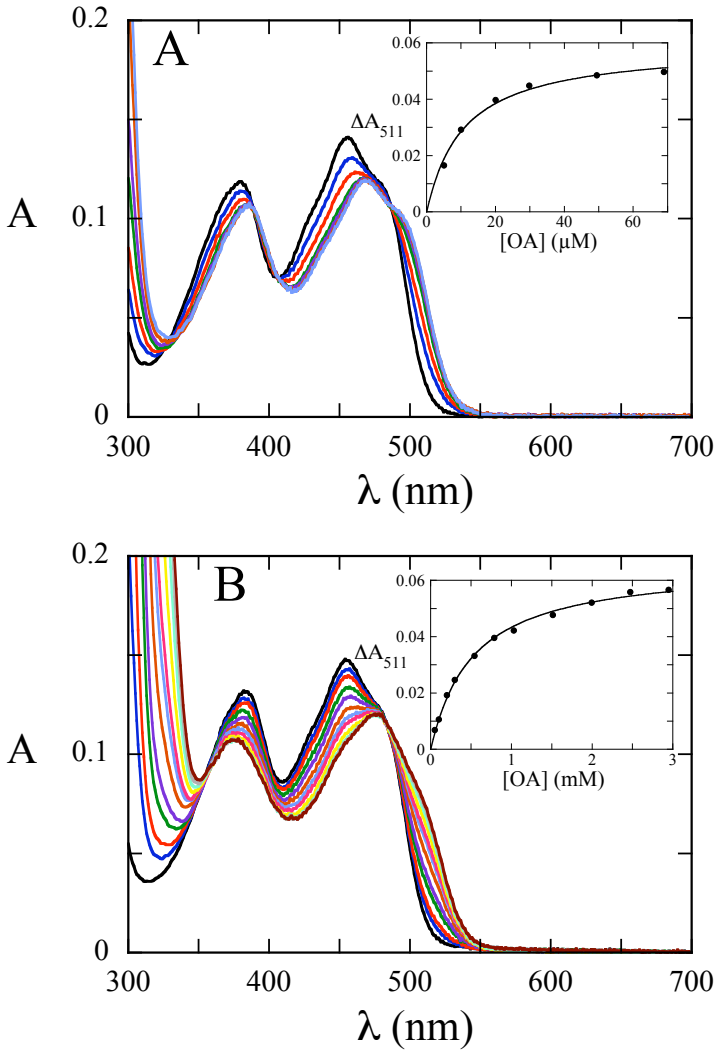

Figure 4-3: OA Binding Titration, pH 8.5, 25 °C

The Thr247Ser mutant enzyme (A) and the Asn246Ala mutant enzyme (B) were titrated aerobically with OA at pH 8.5, 25 °C. The inset shows the maximum change in absorbance due to OA binding as a function of OA concentration. Fitting to a square hyperbola gives the K_d values for OA, 10 ± 1 μM (A) and 520 ± 30 μM (B).

Reductive Half-Reaction of Mutant DHODs

The catalytic cycle of DHODs can be broken down into half-reactions, allowing the individual reactions to be studied in more detail. By studying the reductive half-reaction in the absence of an oxidizing substrate, the oxidation of DHO to OA and concomitant reduction of the enzyme-bound flavin can be observed directly, allowing the determination of the rate constant of the chemical step. The reductive half-reaction of the Class 2 DHOD from *E. coli* has been previously studied (5, 7). Here, we investigated the reductive half-reaction of various active site mutants in anaerobic stopped-flow experiments to better understand the role each residue plays in catalysis. Most mutant enzymes studied fit the same reaction scheme (Figure 4-4) previously proposed for the reductive half-reaction of the wild-type enzyme (7). The data obtained with the Asn246Ala mutant enzyme did not fit this scheme and will be discussed in detail later. A wide range of effects on k_{red} and the apparent K_d for DHO were observed in the mutant enzymes.

Figure 4-4: Reductive Half-Reaction of Wild-Type *E. coli* DHOD

Thr247 Mutant DHODs

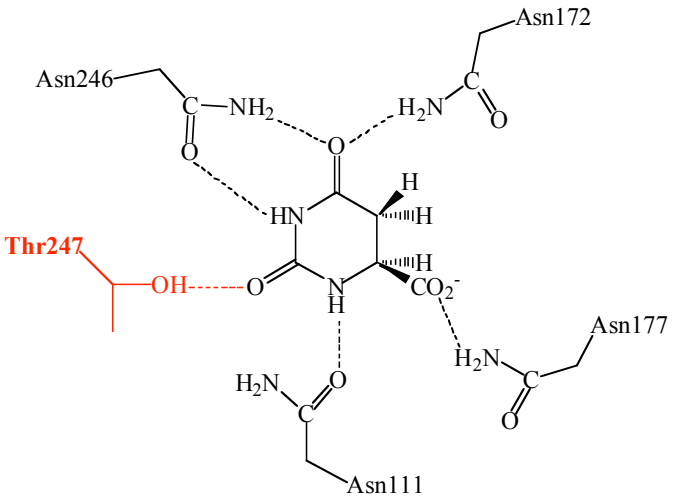

Figure 4-5: Thr247

When Thr247 (Figure 4-5) was mutated to serine, the residue found in Class 1A DHODs, the kinetics of the reductive half-reaction did not differ significantly from wild-type. As seen in wild-type *E. coli* DHOD (7) - and other DHODs (5, 9) - binding of DHO occurred in the dead-time of the stopped-flow instrument and was accompanied by a large-red shift in the maximum flavin absorbance from 456 nm to 475 nm, similar to that caused by OA binding to the oxidized enzyme. Following substrate binding, a large decrease in absorbance at 475 nm with a concomitant increase in absorbance at 550 nm is observed (Figure 4-6A). The absorbance appearing at 550 nm is due to the reduced enzyme-OA complex that forms because of the chemical step. This type of charge-transfer absorbance is common in flavoproteins and results from the electron-deficient

OA stacking against the electron-rich reduced flavin. The observed rate constant of the first phase saturates with increasing DHO concentration giving a reduction rate constant (k_{red}) of 58.8 ± 1.1 s^{-1} and a $K_{d,DHO}$ of 45 ± 5 μM (Table 4-3; Figure 4-6B). These values are very near those reported for wild-type *E. coli* DHOD, k_{red} = 44.7 s^{-1} and $K_{d,DHO}$ = 20 μM (7). The next phase was a smaller decrease in absorbance at 475 nm accompanied by the loss of charge-transfer absorbance at 550 nm. This phase represents product release. The observed rate constant of this phase decreased with increasing DHO concentration to a limiting value of ~0.37 s^{-1} (Figure 4-6C). This behavior was also observed in wild-type enzyme and other Class 2 DHODs and indicates a unimolecular step, OA release, followed by a bimolecular step, DHO binding to the free reduced enzyme. The limiting value of ~0.37 s^{-1} observed in the Thr247Ser mutant enzyme is nearly identical to the value reported for wild-type *E. coli* DHOD (7). Finally, a small slow phase is observed at 475 nm. This phase is also observed in wild-type enzyme and has been suggested to be caused by reduction of a small amount of free flavin (7). The observed rate constant of this phase (~0.02 s^{-1}) is independent of DHO concentration and is much slower, at least an order of magnitude, than the observed rate of any other phase.

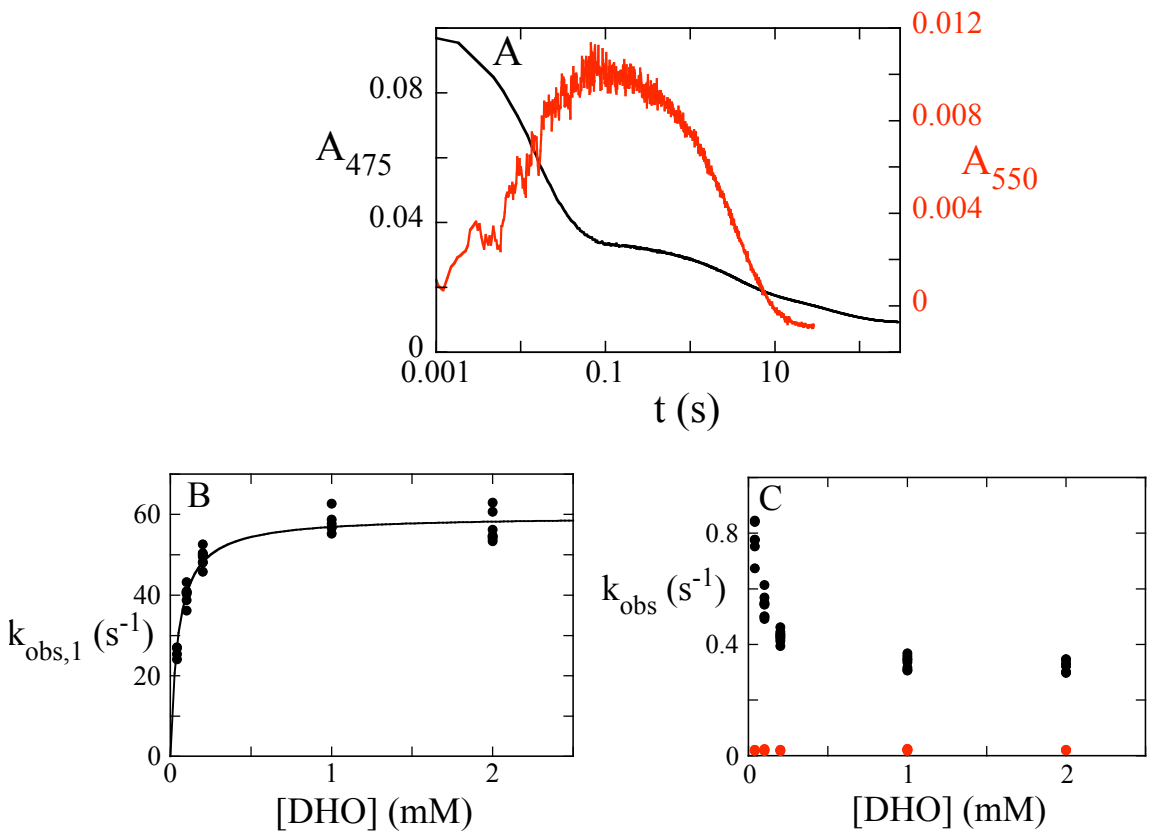

Figure 4-6: Reductive Half-Reaction of Thr247Ser Mutant DHOD

(A) Reaction traces from the reductive half-reaction. At 475 nm (black), the reaction occurs in three phases. The first (large) phase represent the chemical step. The second phase represents product release. At 550 nm (red), flavin reduction is seen as an increase in absorbance and product dissociation is seen as a decrease in absorbance. (B) The observed rate constant of the first phase (flavin reduction) saturates with increasing DHO concentration, giving a reduction rate constant (k_{red}) of 58.8 ± 1.1 s^{-1} and a $K_{d,DHO}$ of 45 ± 5 μM. (C) Concentration dependence of the observed rate constant for the second and third phases. The observed rate constant of the second phase (black), OA release, decreases with increasing DHO concentration, giving a limiting value of 0.37 s^{-1}. The observed rate constant of the final phase (red) is ~0.02 s^{-1} and is independent of DHO concentration.

Table 4-3: Reduction Rate Constants and Apparent $K_{d,DHO}$ for Active Site Mutant DHODs at pH 8.5, 4 °C

Enzyme	$K_{d,DHO}$ (μM)	k_{red} (s^{-1})
Wild-Type[a]	20	46
Thr247Ser	45 ± 5	58.8 ± 1.1
Thr247Ala	198 ± 16	5.52 ± 0.09
Asn177Ala	22 ± 2	0.0586 ± 0.0004
Asn172Ala	278 ± 9	0.00437 ± 0.00002
Asn246Ala	47,000 ± 3,000	0.081 ± 0.002
Asn172Ala/Asn246Ala	~300 mM[b]	~0.002[b]
Asn111Ala	1,040 ± 60	0.0100 ± 0.0001
Asn111Asp	~ 400 mM	~0.1

[a]Data from reference (7). [b]Determined at 25 °C

The Thr247Ala mutant exhibited mild effects on both k_{red} and $K_{d,DHO}$. When this enzyme was mixed with DHO in anaerobic stopped-flow experiments, three phases of reduction were observed at 475 nm, as seen in wild-type and the Thr247Ser mutant. Again, DHO binding occurred in the dead-time of the stopped-flow instrument and caused the signature red-shift in flavin absorbance. The observed rate constant of the first phase, representing flavin reduction, saturated with increasing DHO concentration (Figure 4-7). For the Thr247Ala mutant enzyme, k_{red} was 5.52 ± 0.09 s^{-1} (~8-fold slower than wild-type) and the $K_{d,DHO}$ was 198 ± 13 μM (~10-fold higher than wild-type). The formation of charge-transfer absorbance at 550 nm was observed – although to a lesser extent due to the smaller reduction rate constant. The limiting value observed for product release in the mutant was ~0.7 s^{-1} (Figure 4-7), ~2-fold higher than that observed for

wild-type. Again, a final small phase of reduction was observed at 475 nm. The observed rate constant (~0.025 s^{-1}) of this phase did not vary with DHO concentration. For this enzyme, the difference between spectra scanned immediately after mixing (~1 s)

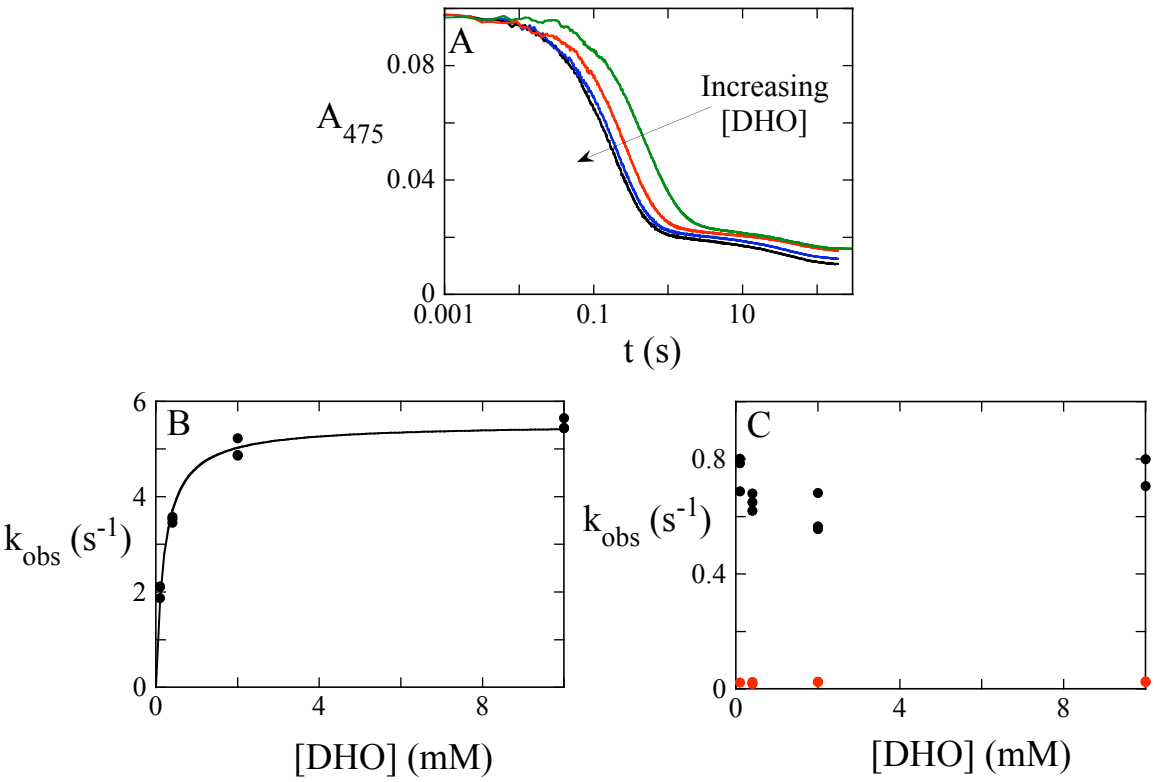

Figure 4-7: Reductive Half-Reaction of the Thr247Ala Mutant DHOD

(A) Reaction traces at 475 nm observed when 8.5 µM enzyme was mixed with DHO ranging from 0.1 – 10 mM. The first phase represents flavin reduction; the second phase represents product release. (B) The observed rate constant of the first phase saturates with increasing DHO concentration, giving a k_{red} of 5.52 ± 0.09 s^{-1} and a $K_{d,DHO}$ of 198 ± 13 µM. (C) The observed rate constant of the second phase (black) decreases with increasing DHO concentration, giving a limiting value of 0.7 s^{-1}. The observed rate constant of the third phase (red) is ~ 0.025 s^{-1} and is independent of DHO concentration.

and well after the reaction (~200 s) clearly showed that the final phase represented the reduction of red-shifted oxidized enzyme, suggesting that enzyme with impaired reactivity is responsible for this final phase.

Asn177Ala DHOD

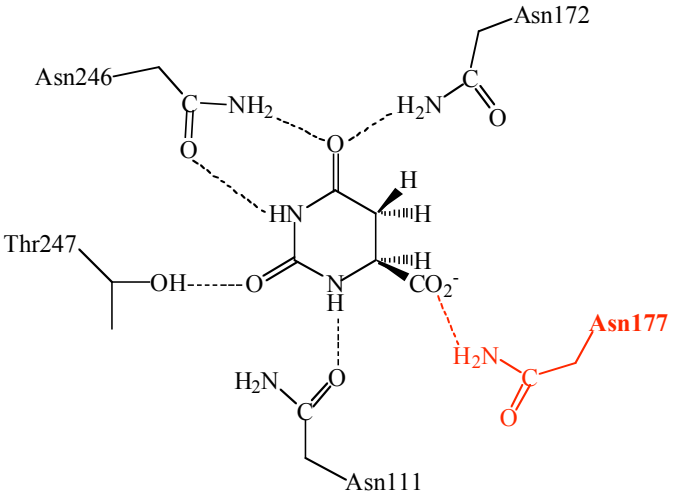

Figure 4-8: Asn177

Asn177 hydrogen-bonds to the carboxylate of DHO (Figure 4-8). This residue is found on the active site loop that has been postulated to control access to the substrate-binding site. This loop must be closed in order for the reaction to take place; the active site base (Ser175) is also on the loop and would not be positioned correctly for proton abstraction unless the loop is closed. When Asn177Ala was mixed with DHO in anaerobic stopped-flow experiments, DHO binding occurred in the dead-time as seen

with the wild-type. However, the shift accompanying DHO binding was not as dramatic. The maximum flavin absorbance shifted to ~470 nm instead of 475 nm as observed in wild-type (7). Two phases of reduction were observed (Figure 4-9A). The first phase accounted for nearly 90% of the total change. The observed rate constant of this phase saturated with increasing DHO concentration (Figure 4-9B). The concentration dependence of this phase and the fact that it represents nearly all the absorbance change lead to the conclusion that it represents flavin reduction. For the Asn177Ala mutant enzyme, k_{red} was found to be 0.0586 ± 0.0004 s^{-1} and $K_{d,DHO}$ was 22 ± 2 μM. Thus, mutation of this conserved asparagine resulted in a 750-fold reduction in k_{red}, with no significant effect on the affinity of DHO. No charge-transfer absorbance at 550 nm was observed with this mutant. It is likely that the rate constant for product dissociation was unaffected by the mutation; with the large decrease in the rate constant for flavin reduction, little reduced enzyme-OA complex would be present. The second phase observed during the reduction accounted for only ~10% of the total absorbance change. The observed rate constant of this phase (~0.085 s^{-1}) was independent of DHO concentration. It is unclear what causes this phase but it could be the result of some damaged enzyme, a small amount of contaminating oxygen, or the reduction of a small amount of free flavin by the reduced enzyme.

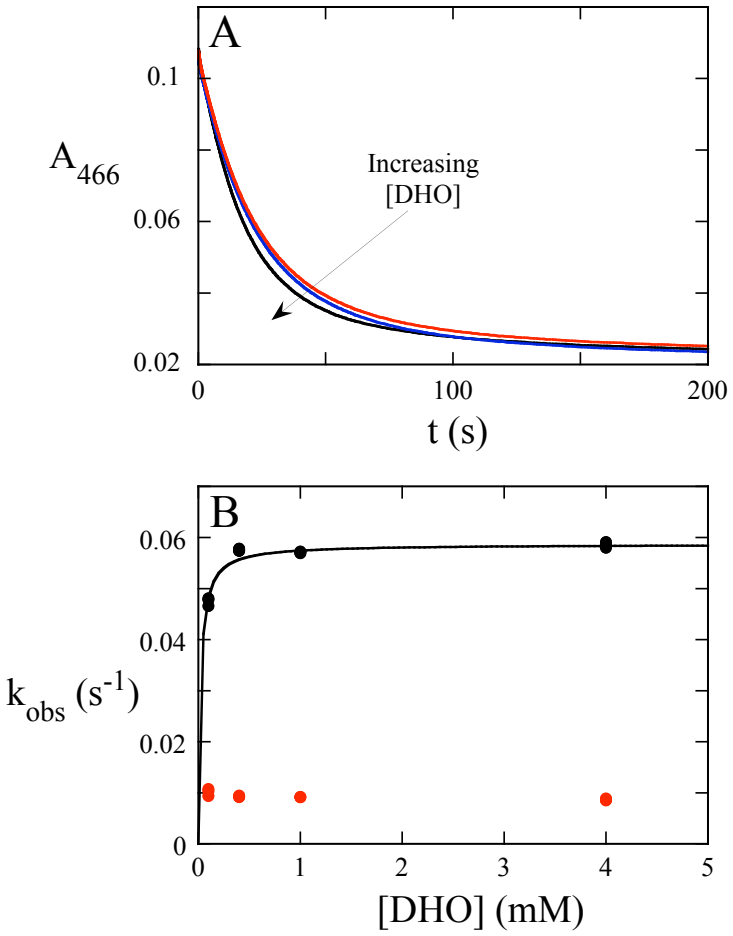

Figure 4-9: Reductive Half-Reaction of the Asn177Ala Mutant DHOD

(A) Reaction traces at 466 nm observed when 8.5 µM enzyme was mixed with DHO ranging from 0.1 to 4 mM. The first phase (large decrease in flavin absorbance) represents flavin reduction. (B) Concentration dependence of the observed rate constants. The first (black) saturates with increasing DHO concentration giving a k_{red} of 0.0586 ± 0.0004 s^{-1} and a $K_{d,DHO}$ of 22 ± 2 µM. The observed rate constant of the second phase (red) is ~0.085 s^{-1} and is independent of DHO concentration.

Asn172Ala DHOD

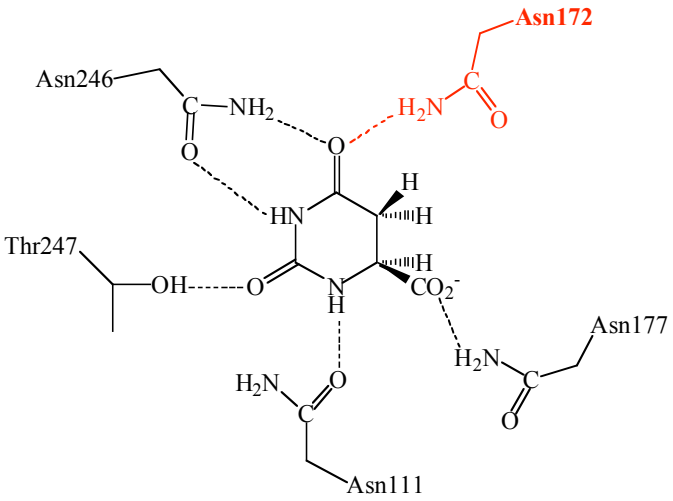

Figure 4-10: Asn172

Asn172 is a strictly conserved active site residue that hydrogen bonds to the C4 carbonyl of OA in structures of the product complex (Figure 4-10). DHO binding to the Asn172Ala mutant occurs quickly, within the dead-time of the stopped-flow instrument, as in other DHODs. The maximum flavin absorbance shifts from 456 nm to ~470 nm upon binding DHO, as is seen in the Asn177Ala mutant enzyme. A single phase of reduction is observed with the Asn172Ala mutant enzyme (Figure 4-11A). The observed rate constant of this phase varied hyperbolically with DHO concentration giving, a k_{red} of 0.00437 ± 0.00002 s^{-1} and a $K_{d,DHO}$ of 278 ± 9 μM (Figure 4-11B). Again, no charge-transfer absorbance at 550 nm was observed, presumably because flavin reduction is slower than product release.

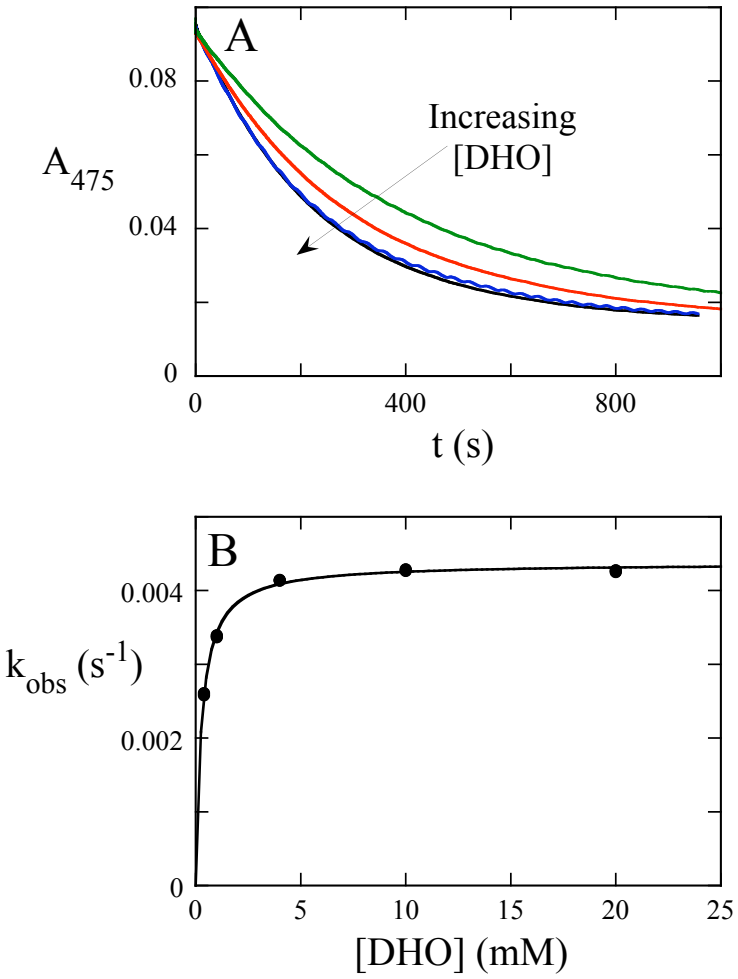

Figure 4-11: Reductive Half-Reaction of the Asn172Ala Mutant DHOD

(A) Reaction traces at 475 nm observed when 9 µM enzyme was mixed with DHO ranging from 0.4 to 20 mM. (B) The observed rate constant varies hyperbolically with DHO concentration giving a k_{red} of 0.004437 ± 0.0002 s^{-1} and a $K_{d,DHO}$ of 278 ± 9 µM.

Asn246Ala DHOD

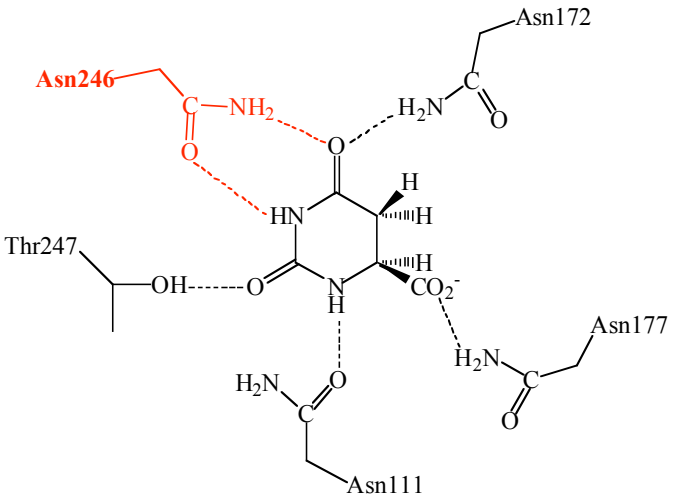

Figure 4-12: Asn246Ala

Asn246 is another conserved active site residue that hydrogen-bonds to the C4 carbonyl and it also hydrogen-bonds to N3 of OA in the product complex (Figure 4-12). The Asn246Ala mutant enzyme was mixed with various concentrations of DHO in anaerobic stopped-flow experiments to investigate its reductive half-reaction. When the Asn246Ala mutant enzyme was mixed anaerobically with low mM concentrations of DHO, no red-shift was observed in the maximum flavin absorbance (Figure 4-13A). However, when using very high concentrations of DHO (40 – 200 mM DHO after mixing), a small red-shift was observed. The reaction traces consisted of three phases at high DHO concentrations. The first observed phase was a mixing artifact caused by the extremely high concentrations of substrate being used; it ended after 5 ms (Figure

4-13B). The second phase was seen as a small decrease in absorbance at 450 nm (Figure 4-13A and B) and a small increase in absorbance at 510 nm. This phase represented the spectral shift associated with substrate binding; the maximum change in absorbance observed when DHO or OA binds to oxidized DHODs occurs at ~510 nm. In all other DHODs studied, DHO binding is extremely fast and the spectral shift is complete in the dead-time of the stopped-flow instrument. The final phase consisted of a large decrease in absorbance at 456 nm and was assigned to flavin reduction (Figure 4-13A and B).

The traces were fit to the sum of three exponentials. The observed rate constant of the first phase – the mixing artifact - is meaningless, but was fit to ensure proper fitting of the other phases in the traces. The observed rate constant of the second phase (~10 s^{-1}), which accompanies the spectral shift caused by DHO binding, was independent of substrate concentration (Figure 4-13C). If this phase simply represented DHO binding to the oxidized enzyme, the dependence on DHO concentration would be linear. Therefore, a more complex scheme is needed. Oxidized enzyme existing in equilibrium between two states – a form that can bind DHO and a form that cannot – could explain this observation if a large proportion of the starting enzyme is in the form incapable of binding DHO (Figure 4-14). Simulations of the reductive half-reaction using this

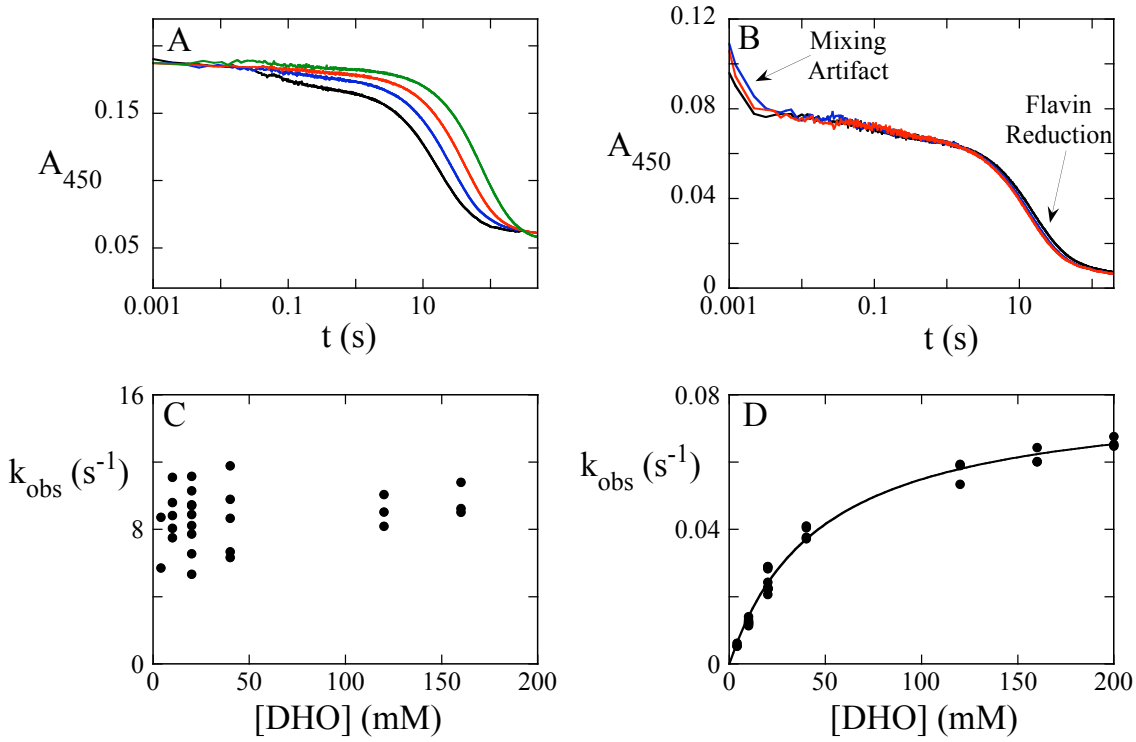

Figure 4-13: Reductive Half-Reaction of the Asn246Ala Mutant DHOD

(A) N246A mutant DHOD (11.5 μM) was mixed with 10 – 40 mM DHO. (B) Reaction traces observed when Asn246Ala DHOD (6 μM) was mixed with 120-200 mM DHO. The mixing artifact is followed by two phases. (C) The observed rate constant of the first phase after the mixing artifact is independent of DHO concentration, with a k_{obs} ~10 s^{-1}. (D) The observed rate constant of the flavin reduction phase saturates with increasing DHO concentration giving a k_{red} of 0.0807 ± 0.0018 s^{-1} and an apparent K_d of DHO of 47 ± 3 mM.

mechanism result in traces very similar to what was observed experimentally. A similar mechanism has been invoked in the reductive half-reaction of α-glycerol phosphate oxidase (22). The observed rate constant of the final phase, representing flavin reduction, varied hyperbolically with DHO concentration giving a k_{red} of 0.081 ± 0.002 s^{-1} and a half-saturating value of 47 ± 3 mM (Figure 4-13D). If the mechanism described above is

correct, then the apparent $K_{d,DHO}$ would be affected by the equilibrium constant of the conformational change, making the actual $K_{d,DHO}$ lower than the observed half-saturating concentration (Equation 1):

$$K_{d,app} = (1 + K_{iso})K_{d,DHO} \qquad (1a)$$

$$K_{iso} = [DHOD_{ox}^{*}]/[DHOD_{ox}] \qquad (1b)$$

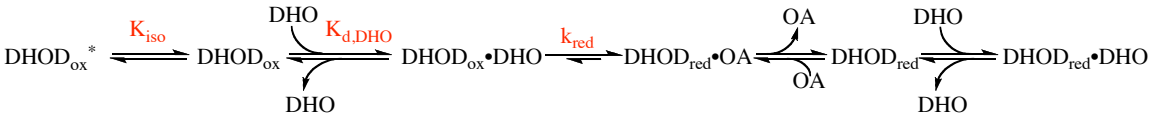

Figure 4-14: Reductive Half-Reaction Scheme of the Asn246Ala Mutant DHOD

K_{iso} is the equilibrium constant for the isomerization step. $K_{d,DHO}$ is the actual dissociation constant of DHO for the enzyme capable of binding DHO.

Asn172Ala/Asn246Ala Double Mutant

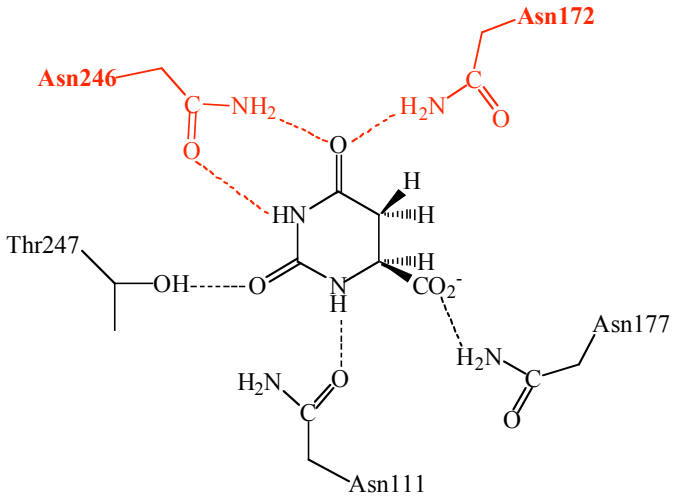

Figure 4-15: Asn172 and Asn246

When both asparagine residues that hydrogen-bond to the C4 carbonyl (Figure 4-15) were mutated to alanine, the reductive half-reaction was excruciatingly slow. The double mutant was mixed with high (up to 200 mM) concentrations of DHO in an anaerobic cuvette and flavin reduction was followed with a standard scanning spectrophotometer. No spectral change occurred when DHO was mixed with the oxidized enzyme. At 4 ^{o}C, the reaction was extremely slow, even when high DHO concentrations were used. With 100 mM DHO, flavin reduction was ~50% complete within 20 hours. After ~2 days, the enzyme began to precipitate, preventing the reaction from being followed to completion. An observed rate constant on the order of 10^{-5} – 10^{-6} s^{-1} is estimated for the reaction. Because the reaction was so slow at 4 ^{o}C, the reaction was studied at 25 ^{o}C. At the higher temperature, flavin reduction was followed to completion (Figure 4-16A). The absorbance change at 453 nm as a function of time was fit to a single exponential to determine an observed rate constant. The observed rate constant increased with DHO concentration; however, saturation was never reached (Figure 4-16B). Fitting the observed rate constants versus DHO concentration gives an estimated k_{red} of 0.002 s^{-1} and a K_d value of ~300 mM, well-above the highest DHO concentration used.

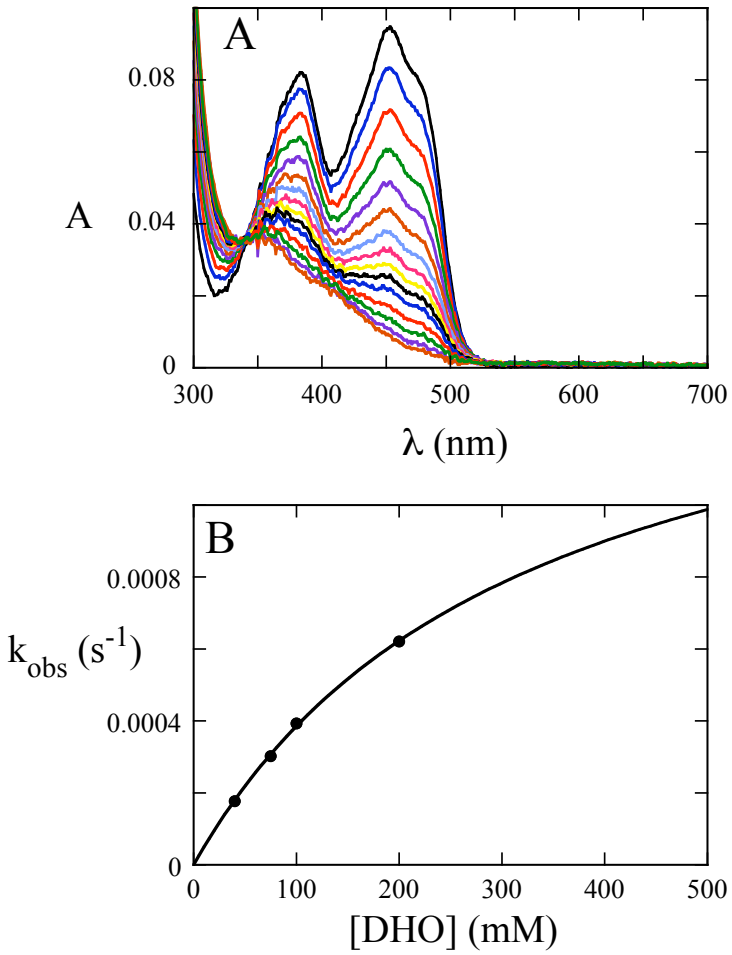

Figure 4-16: Reductive Half-Reaction of the Asn172Ala/Asn246Ala Mutant DHOD

(A) 7.3 μM enzyme was mixed with 100 mM DHO and spectra were collected at intervals for 3.5 hours. Only selected spectra are shown for clarity. (B) The observed rate constant for flavin reduction is plotted as a function of DHO concentration. Saturation was never reached. Fitting the data to a hyperbola gives an estimated k_{red} of 0.002 s^{-1} and a K_d for DHO of ~300 mM.

Asn111 Mutant DHODs

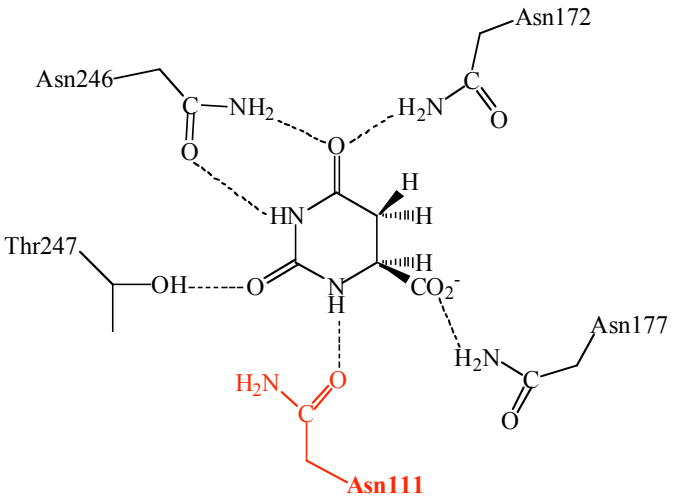

Figure 4-17: Asn111

Asn111 hydrogen-bonds to N1 of OA in the product complex structure and presumably makes a similar interaction with DHO (Figure 4-17). When mutated to alanine, a dramatic reduction in k_{red} was observed. When Asn111Ala was mixed with DHO in anaerobic stopped-flow experiments, DHO binding occurred within the dead-time of the instrument and resulted in ~10 nm red-shift in the maximum flavin absorbance to 466 nm. A single reaction phase followed, representing flavin reduction (Figure 4-18A). The observed rate constant of this phase saturated with increasing DHO concentration giving a k_{red} of 0.0100 ± 0.0001 s^{-1} and a $K_{d,DHO}$ of 1.04 ± 0.06 mM (Figure 4-18B). Thus, the rate constant for flavin reduction decreased ~4,600-fold compared to wild-type and the dissociation constant of DHO increased by ~50-fold.

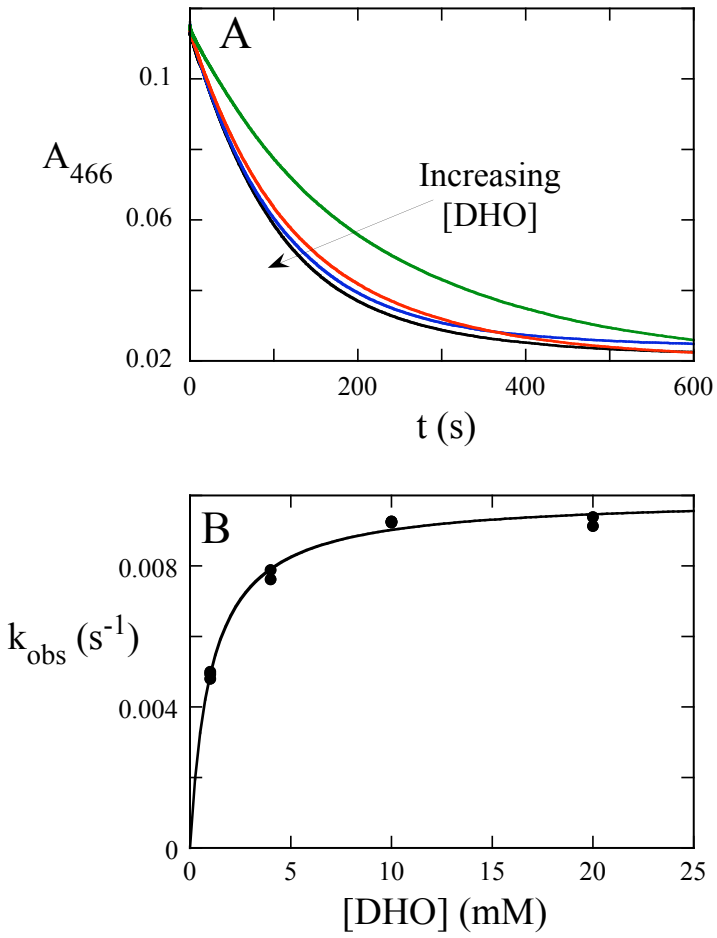

Figure 4-18: Reductive Half-Reaction of the Asn111Ala Mutant DHOD

(A) Reaction traces at 466 nm when Asn111Ala mutant enzyme (9.2 μM) was mixed with DHO ranging from 1 – 20 mM. (B) The observed rate constant varied hyperbolically with DHO concentration giving a k_{red} of 0.00996 ± 0.00013 s^{-1} and a $K_{d,DHO}$ of 1.04 ± 0.06 mM.

The effect of adding a negative charge to the active site was probed using the Asn111Asp mutant. Just like with OA, Asn111Asp bound DHO very weakly. Therefore, extremely high concentrations of DHO (up to 300 mM after mixing) were used. Such high concentrations of substrate resulted in large mixing artifacts that were over within the first 5 ms of the reaction (Figure 4-19A). No shift in the flavin peak was

observed when mixing DHO with Asn111Asp. Only one phase, representing flavin reduction, was observed (Figure 4-19A). The observed rate constant for this phase increased with increasing DHO concentration. Saturation could not be reached, but the concentration dependence appeared nonlinear (Figure 4-19B). The observed rate constants were therefore fit to a hyperbola to give an estimate of the maximum rate constant. A rate constant for flavin reduction in the Asn111Asp mutant of ~0.1 s^{-1} was obtained and the estimated $K_{d,DHO}$ is 400 mM, a value higher than the maximum DHO concentration used experimentally.

Kinetic Isotope Effects

KIEs were used to determine whether a non-chemical step was masking the actual rate of flavin reduction in the mutant enzymes. KIEs were determined using 5,5,6-$^2H_3$ DHO for wild-type and the Asn177Ala mutant DHOD. The K_d of DHO was unaffected by the mutation of Asn177, making it easiest to study with a limited amount of deuterated substrate.

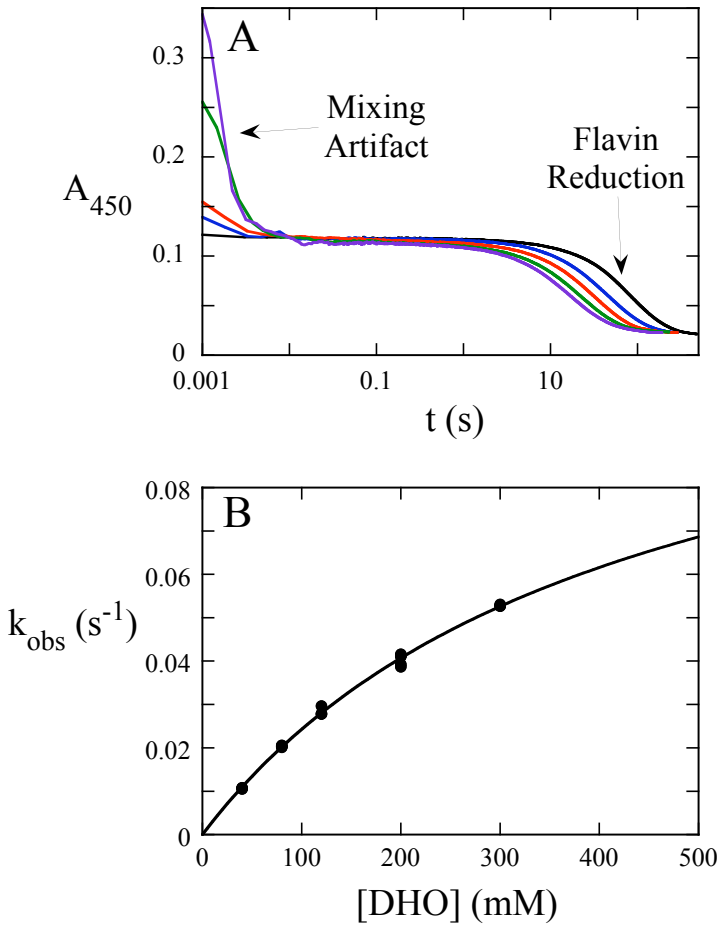

Figure 4-19: Reductive Half-Reaction of the Asn111Asp Mutant DHOD

(A) Reaction traces at 450 nm obtained when 9 μM enzyme was mixed with DHO ranging from 40 – 300 mM. The large mixing artifact is followed by a single phase representing flavin reduction. (B) The observed rate constant for flavin reduction increased with increasing DHO concentration. However, saturation was never reached. The data were fit to a hyperbola to give estimates for k_{red} of 0.1 s^{-1} and $K_{d,DHO}$ of 400 mM.

Reaction traces of wild-type mixed with both protio- and deutero-DHO were similar to those already reported (5, 7) and were fit to three exponentials. The first phase

represented flavin reduction[1]. The observed rate constant of this phase varied hyperbolically with DHO concentration giving a k_{red} of 81.6 ± 2.8 s^{-1} for protio-DHO and 15.5 ± 0.4 s^{-1} for deutero-DHO. The KIE, calculated by dividing the rate constant obtained with protio substrate by that obtained with deutero substrate, was 5.3 ± 0.3 for wild-type *E. coli* DHOD.

The KIE on flavin reduction was also determined for the Asn177Ala mutant protein. When Asn177Ala was mixed with either protio- or deutero- DHO in anaerobic stopped-flow experiments, two phases were observed. The first phase, representing flavin reduction, accounted for more than 90% of the total absorbance change. The observed rate constants of this phase varied hyperbolically with DHO concentration giving a k_{red} of 0.0882 ± 0.001 s^{-1} for protio-DHO and 0.0149 ± 0.0002 s^{-1} for 5,5,6-$^2H_3$ DHO. Therefore, the KIE for the reduction of the Asn177Ala mutant enzyme was 5.9 ± 0.2, essentially the same as that observed for wild-type under these conditions.

---

[1]The temperature was not properly controlled in these experiments and resulted in reaction traces containing a temperature equilibration artifact (~1 s). The highly reproducible artifact was also observed in traces of buffer mixed with buffer and therefore was simply subtracted from all reaction traces. Because of this, the actual temperature of the experiment is unknown. However, the experiments for wild-type and the Asn177Ala mutant enzyme were conducted under identical conditions.

Discussion

DHODs catalyze the conversion of DHO to OA with the concomitant reduction of the enzyme-bound FMN prosthetic group. The pyrimidine-binding pockets of Class 1 and Class 2 DHODs are very similar. Several conserved residues that hydrogen bond to the pyrimidine substrate and product can be found in all DHODs (10-13, 23, 24). The specific roles of these residues in catalysis are unknown. The residues could be involved in binding both DHO and OA. They could also play a role in the chemical conversion of DHO to OA by stabilizing transition states and/or reaction intermediates. To try to better understand the roles these conserved residues play in DHO oxidation, site-directed mutagenesis was used. Some residues have only minor roles in the reductive half-reaction. Other residues appear to be much more important for binding than for chemistry, while some residues were extremely important for chemistry.

None of the mutations appeared to significantly disturb the environment of the flavin. Most of the mutant enzymes studied had reduction potentials nearly identical to that determined for wild-type (Table 4-1), the major exception being the Asn111Asp mutation. The potential of this enzyme was ~100 mV lower than that of wild-type, consistent with the introduction of a negative charge at the active site. In addition, the spectra of all the oxidized mutant enzymes were nearly identical to that of wild-type.

The binding of OA suggests that the pyrimidine-binding site is largely intact in most of the mutants. Although the affinity for OA decreases (Table 4-2), the characteristic flavin spectral change (a red-shift from 456 nm to 475 nm) was usually observed. In the two most dramatic mutations – Asn111Asp, where the charge of the active site was changed, and Asn172Ala/Asn246Ala, where three hydrogen-bonds were removed – the spectral changes were less like wild-type, suggesting more significant perturbations to the active and site and ligand binding, hardly a surprise.

Studying the reductive half-reaction of each mutant enzyme in anaerobic experiments gives information on the rate constant of flavin reduction (k_{red}) and the apparent K_d for DHO. The same KIE on flavin reduction is observed in wild-type and the Asn177Ala mutant enzyme, indicating that the chemical step is not masked by another step, such as a slow isomerization, in these mutant enzymes, i.e., k_{red} truly indicates the rate constant for the chemical step.

Oxidized enzymes can bind both the substrate (DHO) and the product (OA) of the reductive half-reaction. The major difference in these two pyrimidines is their planarity – OA is planar, while DHO is not. When comparing the alanine mutations to wild-type, the range of effects observed on DHO binding was greater than that observed for OA binding (Figure 4-20). When Thr247 was mutated, the K_d for DHO and OA was increased by

nearly the same factor, indicating that Thr247 can bind both ligands equally well. Not only were the effects nearly equal, they were also some of the smallest effects observed in any of the mutant enzymes. Removal of other residues resulted in larger decreases in OA affinity than in DHO affinity. When Asn177 was mutated, no effect was observed on DHO affinity, while the K_d for OA increased ~5-fold. The Asn172Ala mutant enzyme was similar, with the K_d of DHO increased ~14-fold, while the K_d of OA increased ~40-fold. These residues seem more important for binding the planar ligand. In both the Asn246Ala and Asn111Ala mutant enzymes, bigger effects were observed on DHO binding. For example, a ~100-fold increase in the K_d of OA and a ~2000-fold increase in the K_d of DHO were observed in the Asn246Ala mutant enzyme, implying this residue is more important for binding DHO, the non-planar ligand.

The observed effects on the reduction rate constant varied widely. There is no correlation between the observed K_d of DHO and the reduction rate constants (Table 4-3), i.e., the enzymes with the weakest K_d are not necessarily the slowest. For example, the Asn177Ala mutant enzyme had the same apparent K_d as wild-type. However, the reduction rate constant of this mutant was reduced by nearly ~800-fold. Conversely, when Thr247 was mutated to alanine, the reduction rate constant was reduced by only

~8-fold, while the K_d of DHO increased by ~10-fold, so the Thr247Ala mutant enzyme binds DHO ~8-fold worse than the Asn177Ala mutant, but reacts ~80-fold faster.

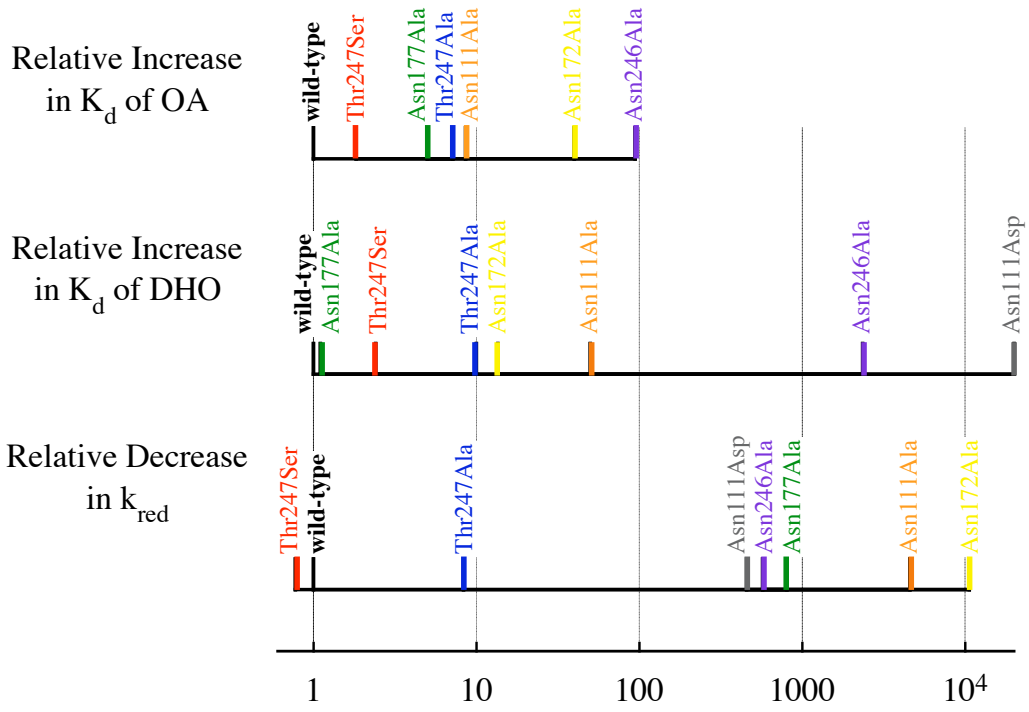

Figure 4-20: Relative Effects of All Mutations

The effects of each mutation on the K_d of OA, the K_d of DHO, and the reduction rate constant with respect to wild-type is shown.

Oxidation of DHO breaks two carbon-hydrogen bonds. An active site base (Ser175 in *E. coli* DHOD) deprotonates C5 of DHO and a hydride is transferred from C6 of DHO to N5 of the isoalloxazine ring of the flavin. Using DHO deuterated at the 5-, 6-, and both the 5- and 6-positions in anaerobic stopped-flow experiments, the *E. coli* DHOD

was shown to use a stepwise mechanism to catalyze this reaction (5). Since DHO oxidation is stepwise in this enzyme, one of two intermediates must form during the reaction (Figure 4-21). If deprotonation occurs first, an enolate intermediate with negative charge on the C4 oxygen would form. If hydride transfer occurs first, an iminium intermediate with positive charge at the N1 position would form. Three of the four strictly conserved asparagine residues in DHOD hydrogen-bond to either the C4 carbonyl (Asn172 and Asn246 in *E. coli* DHOD) or N1 (Asn111 in *E. coli* DHOD) of DHO (Figure 4-1) and therefore are positioned to stabilize this potential charge build-up.

Removal of the hydrogen-bond(s) responsible for stabilizing the charge build-up of the intermediate by mutation to alanine should greatly decrease the rate constant of flavin reduction. Mutation of Asn246 results in only a ~570-fold decrease in the reduction rate constant, while a larger increase (~2,000-fold) in the apparent K_d for DHO is observed, indicating that this residue is more important for binding than for chemistry. Asn246 presumably hydrogen-bonds to both the C4 carbonyl and N3 of DHO. Therefore, replacement with alanine results in the loss of two hydrogen-bonds. If an equal contribution for each bond is assumed, then each hydrogen-bond accounts for ~2.3 kcal mol^{-1} in binding energy. With two hydrogen-bonds missing from the active site, it is

likely that DHO is not held as rigidly in the proper orientation for chemistry. This would cause the observed decrease in reduction rate constant.

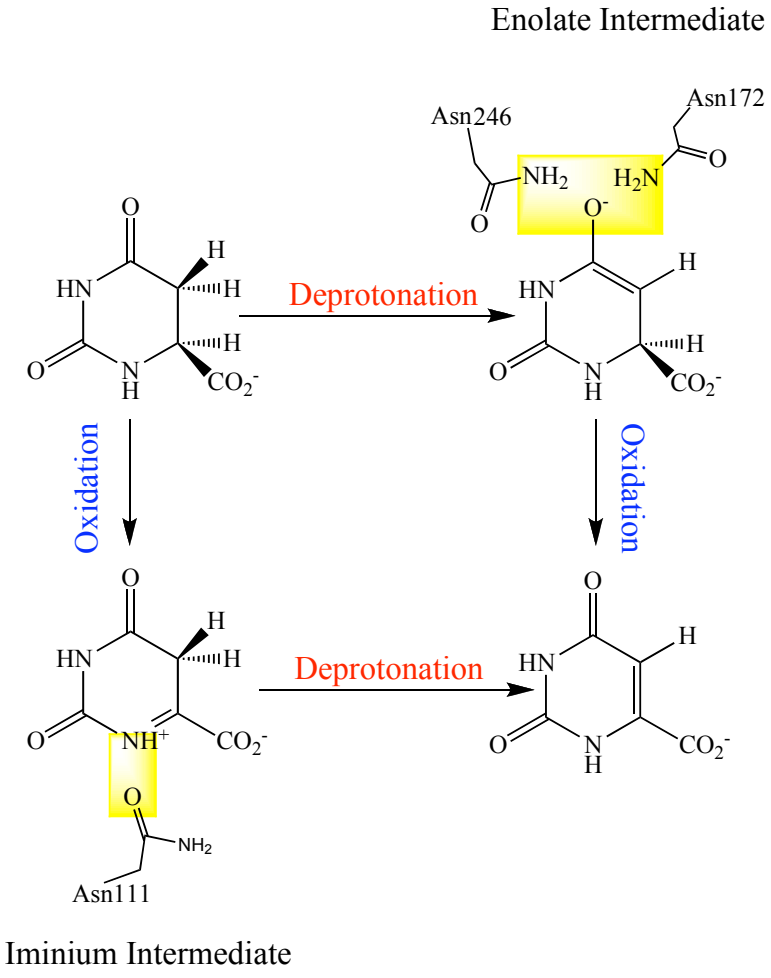

Figure 4-21: Possible Mechanisms of DHO Oxidation

Charge-stabilizing interactions of conserved active site residues are highlighted in yellow. Residues are positioned to stabilize either possible reaction intermediate.

However, mutation of Asn172 results in a large decrease in the reduction rate constant (10,500-fold), with only a minor increase in the K_d for DHO (~14-fold). This means that the hydrogen-bond provided by Asn172 is worth ~1.6 kcal mol^{-1} in binding energy. The large effect on chemistry implies that this residue is important for stabilizing transition states and/or reaction intermediates that form during the reaction. The observed effect supports the formation of an enolate during DHO oxidation. Interestingly, even though both Asn246 and Asn172 hydrogen-bond to the C4 carbonyl of DHO, Asn172 seems to be much more important for chemistry.

Surprisingly, mutation of Asn111 also results in a large decrease in reduction rate constant. In the Asn111Ala mutant enzyme, a ~4600-fold decrease in k_{red} is observed (~2-fold less than the effect observed in the Asn172Ala mutant enzyme). The effect on DHO binding is more significant in the Asn111Ala mutant with a ~50-fold increase in the K_d. This means that the hydrogen-bond contributed by Asn111 is worth ~2.4 kcal mol^{-1} of binding energy, very similar to the contribution of the hydrogen-bonds of Asn246. If an iminium intermediate is forming during DHO oxidation, negative charge near the N1 position of DHO should stabilize the positive charge build-up. Even though DHO binds very weakly to the Asn111Asp mutant enzyme, a reduction rate constant can be estimated. The chemical step in the Asn111Asp mutant enzyme occurs at ~0.1 s^{-1}, about

10-fold faster than in the Asn111Ala mutant, although this rate constant is still ~450-fold slower than wild-type.

With large effects on reduction rate constant being observed when either Asn172 or Asn111 is removed, it is unclear which reaction intermediate is actually forming during DHO oxidation. However, it is clear that some of these conserved asparagine residues are important for chemistry in the Class 2 DHOD from *E. coli*; they are presumably needed to stabilize charge build-up in the active site during the reaction. The mechanism of DHO oxidation has also been studied in the Class 1A DHOD from *L. lactis*. In this instance, the deuterium isotope effects on flavin reduction indicated a concerted mechanism in which both carbon-hydrogen bonds break simultaneously (9). Interestingly, when the analogous asparagine residues in the *L. lactis* DHOD are mutated to alanine, the effects on flavin reduction are very mild, ranging from 40 – 200-fold (Tirupati, B., unpublished data). Thus, the mechanisms of DHO oxidation appear to be different in Class 1A and Class 2 DHODs and so do the affects of losing the active site asparagines. This is very likely due to differences in charge build-up in the active sites. In the Class 1A DHOD, presumably little charge build-up occurs because both bonds break simultaneously, and therefore small effects on the chemical step are observed when the active site asparagines are mutated.

While it seems clear that at least some of the active site asparagines are needed to stabilize charge build-up in the active site, it is still not clear which intermediate is forming in the stepwise oxidation of DHO by the Class 2 DHOD form *E. coli*. If an enolate intermediate is forming, then why is the rate constant of reduction slowed so much by removing a hydrogen-bond to N1 of DHO? The charge build-up of an enolate intermediate is on the opposite end of the molecule. Conversely, why is there such a large affect from losing a hydrogen-bond at the C4 carbonyl if an iminium intermediate is forming? Further work is needed to clarify which intermediate is formed. Heavy-atom isotope effects (^{15}N and ^{13}C) could be used to determine which intermediate is being formed.

The other two conserved active site residues are not positioned to stabilize intermediate formation. Thr247 hydrogen-bonds to the C2 carbonyl. When mutated to alanine, very minor effects are observed on both k_{red} and K_d. This is not surprising as this residue is proposed to bind and position DHO for catalysis, but not to stabilize any reaction intermediates. Asn177, the other strictly conserved asparagine residue, hydrogen-bonds to the carboxylate of DHO. The Asn177Ala mutation only affected the chemical step. This residue is located on the active site loop that is thought to be responsible for allowing access to the active site (11). Our results indicate that Asn177 is

not responsible for binding DHO; that job belongs to the other conserved residues in the active site. It seems more likely that Asn177 is at least partially responsible for closing the active site lid once DHO is bound. The active site base (Ser175) that deprotonates C5 of DHO during the reaction is also on this active site loop. In order for the base to be positioned correctly, the loop must be closed over the active site (11). The decrease in the reduction rate constant upon mutation could be due to the inefficient closing of the active site loop in the absence of the hydrogen-bond between Asn177 and the carboxylate of DHO. It is also likely that Asn177 is needed to help properly position DHO for the reaction once it is initially bound. The reduction in k_{red} observed could be due to improper positioning of DHO in the active.

The removal of each active site hydrogen-bond resulted in differential effects on the binding of DHO, OA, and the reduction of the enzyme-bound flavin. Some residues are more important for substrate binding, while others are extremely important for flavin reduction. Interestingly, the analogous mutations in another phylogenetic class of DHODs resulted in very different effects, suggesting that the conserved residues have different jobs in the different classes of DHODs.

References

1. Björnberg, O., Rowland, P., Larsen, S. and Jensen, K. F. (1997) *Biochemistry*, **36,** 16197-16205.

2. Jones, M. E. (1980) *Annu. Rev. Biochem.*, **49,** 253-279.

3. Nagy, M., Lacroute, F. and Thomas, D. (1992) *Proc. Natl. Acad. Sci. U. S. A.*, **89,** 8966-8970.

4. Nielsen, F. S., Andersen, P. S. and Jensen, K. F. (1996) *J. Biol. Chem.*, **271,** 29359-29365.

5. Fagan, R. L., Nelson, M. N., Pagano, P. M. and Palfey, B. A. (2006) *Biochemistry*, **45,** 14926-14932.

6. Malmquist, N. A., Gujjar, R., Rathod, P. K. and Phillips, M. A. (2008) *Biochemistry*, **47,** 2466-2475.

7. Palfey, B. A., Björnberg, O. and Jensen, K. F. (2001) *Biochemistry*, **40,** 4381-4390.

8. Pascal, R. A., Jr. and Walsh, C. T. (1984) *Biochemistry*, **23,** 2745-2752.

9. Fagan, R. L., Jensen, K. F., Björnberg, O. and Palfey, B. A. (2007) *Biochemistry*, **46,** 4028-4036.

10. Liu, S., Neidhardt, E. A., Grossman, T. H., Ocain, T. and Clardy, J. (2000) *Structure*, **8,** 25-33.

11. Nørager, S., Jensen, K. F., Björnberg, O. and Larsen, S. (2002) *Structure*, **10,** 1211-1223.

12. Rowland, P., Björnberg, O., Nielsen, F. S., Jensen, K. F. and Larsen, S. (1998) *Protein Sci.*, **7,** 1269-1279.

13. Rowland, P., Nørager, S., Jensen, K. F. and Larsen, S. (2000) *Structure*, **8,** 1227-1238.

14. Björnberg, O., Gruner, A. C., Roepstorff, P. and Jensen, K. F. (1999) *Biochemistry*, **38,** 2899-2908.

15. Palfey, B. A. (2003) Time resolved spectral analysis in *Kinetic analysis of macromolecules* (Johnson, K. A.), Oxford University Press, New York.

16. Williams, C. H., Jr., Arscott, L. D., Matthews, R. G., Thorpe, C. and Wilkinson, K. D. (1979) *Methods Enzymol.*, **62,** 185-198.

17. Massey, V. (1990) in *Flavins and flavoproteins* (Curti, B., Ronchi, S. and Zanetti, G.), Walter de Gruyter, Berlin, Germany.

18. Nørager, S., Arent, S., Björnberg, O., Ottosen, M., Lo Leggio, L., Jensen, K. F. and Larsen, S. (2003) *J. Biol. Chem.*, **278,** 28812-28822.

19. Marcinkeviciene, J., Jiang, W., Locke, G., Kopcho, L. M., Rogers, M. J. and Copeland, R. A. (2000) *Arch. Biochem. Biophys.*, **377,** 178-186.

20. Wolfe, A. E., Thymark, M., Gattis, S. G., Fagan, R. L., Hu, Y. C., Johansson, E., Arent, S., Larsen, S. and Palfey, B. A. (2007) *Biochemistry*, **46,** 5741-5753.

21. Zameitat, E., Pierik, A. J., Zocher, K. and Loffler, M. (2007) *FEMS Yeast Res.*, **7,** 897-904.

22. Parsonage, D., Luba, J., Mallett, T. C. and Claiborne, A. (1998) *J. Biol. Chem.*, **273,** 23812-23822.

23. Arakaki, T. L., Buckner, F. S., Gillespie, J. R., Malmquist, N. A., Phillips, M. A., Kalyuzhniy, O., Luft, J. R., Detitta, G. T., Verlinde, C. L., Van Voorhis, W. C., Hol, W. G. and Merritt, E. A. (2008) *Mol. Microbiol.*, **68,** 37-50.

24. Inaoka, D. K., Sakamoto, K., Shimizu, H., Shiba, T., Kurisu, G., Nara, T., Aoki, T., Kita, K. and Harada, S. (2008) *Biochemistry*, **47,** 10881-10891.

Chapter 5
Disruption of the Proton Relay Network in the Class 2 Dihydroorotate Dehydrogenase from *E. coli*

Dihydroorotate dehydrogenases (DHODs) catalyze the fourth step in the *de novo* synthesis of pyrimidines. DHODs are flavin-containing enzymes that convert dihydroorotate (DHO) to orotate (OA) – the only redox step in pyrimidine synthesis. DHODs have been categorized into two broad classes based on sequence (1). Class 2 DHODs are membrane-bound monomers that are oxidized by ubiquinone (2). Class 1 enzymes are cytosolic proteins that have been further divided into two classes. Class 1A enzymes are homodimers that use fumarate as the physiological oxidizing substrate (3). Class 1B DHODs are $\alpha_2\beta_2$ heterotetramers. They contain one subunit that resembles the Class 1A enzymes and a second subunit that contains an iron-sulfur cluster and FAD, allowing the Class 1B DHODs to be oxidized by NAD (4). Class 2 DHODs are found in most eukaryotes and Gram-negative bacteria, while Class 1 enzymes are found mostly in Gram-positive bacteria and in a few microbial eukaryotes.

All DHODs catalyze the same reductive half-reaction, the oxidation of DHO with the concomitant reduction of the enzyme-bound flavin, while the oxidative half-reactions

for each class are different. Structures of Class 2 DHODs have shown that the enzyme contains two separate binding sites for its substrates (5-10). The pyrimidine binding-site is found on the *si* face of the flavin and is very similar in all DHODs. Class 2 enzymes contain an N-terminal domain (not found in Class 1 enzymes) that helps create a tunnel-like pocket leading to the 7,8-dimethyl edge of FMN. This pocket is thought to be the quinone-binding site.

The oxidation of DHO breaks two carbon-hydrogen bonds. An active site base (serine in Class 2 enzymes or cysteine in Class 1 enzymes) deprotonates C5 of DHO and a hydride is transferred from C6 of DHO to N5 of the isoalloxazine ring of the flavin. The reductive half-reaction of the Class 2 DHOD from *E. coli* has been studied in great detail in anaerobic stopped-flow experiments. The rate constant for reduction increased with pH until it plateaued above a pK_a of ~9.5 (11). Structures show that a serine is positioned to deprotonate DHO (7-9). However, there are no obvious structural features that would lower the pK_a so dramatically. Deuterium isotope effects showed that DHO oxidation is stepwise in Class 2 DHODs (12). In addition, using DHO deuterated at the C5 position (the site of deprotonation), the kinetic isotope effect was lost at a pH value above the pK_a (12), leading to the proposal that the observed pK_a in Class 2 DHODs is actually a kinetic pK_a.

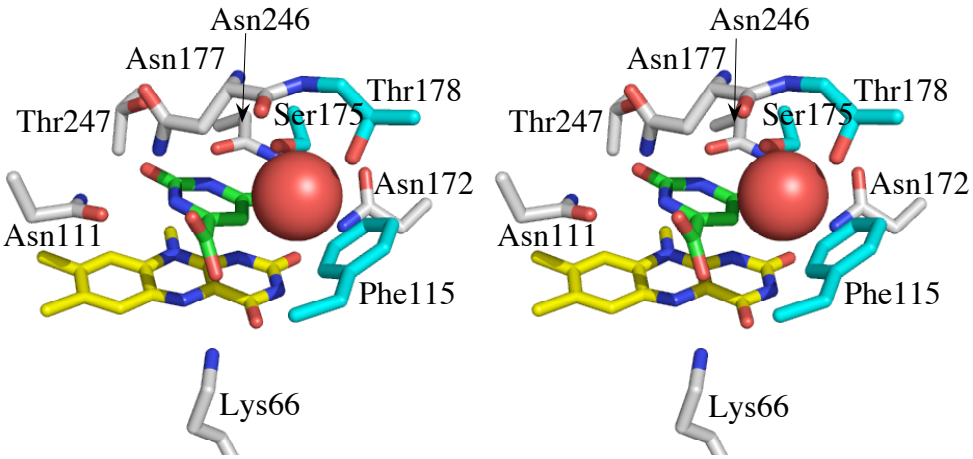

Figure 5-1: Pyrimidine-Binding Site of Class 2 DHODs

The pyrimidine-binding site includes several highly conserved hydrogen-bonding residues that interact with the pyrimidine. In addition, the active site base (Ser175 in the *E. coli* DHOD) is connected to the bulk solvent via a hydrogen-bonding network. A crystallographic water (red ball) sits on Phe115 and hydrogen-bonds to Thr178, residues that are conserved in Class 2 DHODs.

Crystal structures show that the active site base is involved in a hydrogen-bond network with both water molecules and other residues (Figure 5-1). The active site base (Ser175 in the *E. coli* enzyme) hydrogen-bonds to a crystallographic water that is sitting on a phenylalanine (Phe115 in the *E. coli* enzyme) and hydrogen-bonded to a threonine (Thr178 in the *E. coli* enzyme) – residues that are strictly conserved in Class 2 DHODs. This hydrogen-bond network connects the base to bulk solvent through a small tunnel. This network has been proposed to shuttle protons from the active site to bulk solvent and could have a role in activating the serine to act as a base (13).

To investigate the role of this hydrogen-bond network in DHO oxidation, site-directed mutants of the strictly conserved residues were created and the pH dependence of their reductive half-reactions were determined. Blocking the tunnel and/or making the tunnel more hydrophobic impairs reduction and supports the proposed role of this hydrogen-bonding network in reduction.

Experimental Procedures

Site-Directed Mutagenesis

Site-directed mutants were made from the previously created pAG-1 expression vector (14) using the Stratagene QuikChange II XL mutagenesis kit. Insertion of the correct mutations was checked by sequencing the entire pyrD gene.

Overexpression and Purification

All mutant enzymes were overexpressed from the pAG-1 plasmid in SØ6645 *E. coli* cells (14). The enzymes were purified according to the published procedure (14). Purified enzyme was diluted to 50% (v/v) glycerol and stored at -80 ^{o}C. Before use, enzymes were exchanged into the appropriate buffer using Econo-Pac 10DG disposable desalting columns (Bio-Rad).

Instrumentation

Absorbance spectra were obtained using a Shimadzu UV-2501PC scanning spectrophotometer. Stopped-flow experiments were performed at 4 °C using a Hi-Tech Scientific KinetAsyst SF-61 DX2 stopped-flow spectrophotometer.

Preparation of Anaerobic Solutions

Enzyme solutions for rapid reaction studies were made anaerobic in glass tonometers by repeated cycles of evacuation and equilibration over an atmosphere of purified argon as previously described (15). Substrate solutions were made anaerobic within the syringes that were to be loaded onto the stopped-flow instrument by bubbling solutions with purified argon. Slow reactions were performed in anaerobic cuvettes (16) and monitored in a standard scanning spectrophotometer. These reaction mixtures were also made anaerobic by repeated evacuation and equilibration with purified argon.

Reduction Potentials

Reduction potentials were determined by the xanthine/xanthine oxidase method of Massey (17). Experiments were preformed in anaerobic cuvettes (16) and monitored in a

standard scanning spectrophotometer. Phenosafranin (E_m = -252 mV) was used as the indicator dye.

OA Binding to Oxidized Mutants

The dissociation constant of OA was determined in aerobic titrations in a standard scanning spectrophotometer. The enzyme equilibrated in 0.1 M Tris-HCl, pH 8.5 was titrated with OA in the same buffer. The differences in flavin absorbance caused by binding were plotted against OA concentration, and the data were fit to a hyperbola in Kaleidagraph (Synergy, Inc.) to determine the K_d.

pH Dependence of the Reduction of Mutant DHODs

The reductive half-reactions of the Thr178 and Phe115 mutant enzymes were studied in anaerobic stopped-flow experiments at 4 ^{o}C. In most cases, the enzyme was equilibrated in 0.1 M buffer (pH 6 – 7.5, KP_i; pH 7.5 – 9, Tris-HCl; pH 9 – 9.5, CHES; pH 10 – 11.5, CAPS) and was mixed with varying concentrations of DHO in the same buffer. For the Phe115Leu mutant enzyme, double-mixing pH-jump experiments were conducted at pH values higher than 10.5 due to enzyme instability. In these cases, the enzyme, equilibrated in 5 mM KP_i, pH 7, was mixed with 0.2 M buffer (pH 10.5-11.5,

CAPS) and allowed to age for 2 s. Then the enzyme was mixed with varying concentrations of DHO in 0.1 M buffer (pH 10.5-11.5, CAPS). In all cases, reaction traces were collected at 475 nm and 550 nm. In almost all instances, the reaction traces were fit to sums of exponentials in Program A (Rong Chang, Chung-Jin Chiu, Joel Dinverno and David P. Ballou, University of Michigan). The reduction rate constant (k_{red}) was determined from the limiting value of the observed rate constant at infinite DHO concentration obtained by fitting k_{obs} vs. DHO concentration to a hyperbola in Kaleidagraph (Synergy, Inc.). For the Phe115Leu mutant enzyme at pH 8.5, the reaction traces could not easily be fit to sums of exponentials and were therefore analyzed by global fitting in Berkeley Madonna. The pK_a value controlling reduction in each mutant enzyme was determined by fitting the pH dependence of the reduction rate constant to Equation 1, where $k_{red,limiting}$ is the limiting value of the reduction rate constant at high pH.

$$k_{red} = \frac{k_{red,limiting}}{1 + 10^{(pK_a - pH)}} \qquad (1)$$

Reduction of the flavin in the Ser175Ala mutant DHOD was very slow at 4 ^{o}C; therefore, it was studied at 25 ^{o}C. The same buffers described above were used to investigate the pH dependence of flavin reduction in this enzyme. Below pH 9, flavin

reduction was slow enough to be monitored using a standard scanning VIS/UV spectrophotometer. Enzyme equilibrated in the buffer of interest was mixed with either 1 or 2 mM DHO in an anaerobic cuvette and spectra were taken at intervals until flavin reduction was complete. Reactions traces at 475 nm were extracted and fit to a single exponential. The observed rate constant at each DHO concentration was the same, indicating saturation. Since a saturating DHO concentration was used in each experiment, the k_{obs} obtained from fitting the exponential traces is equivalent to k_{red}. Above pH 9, the reductive half-reaction was investigated in anaerobic stopped-flow experiments. Anaerobic enzyme was mixed with varying concentrations of anaerobic DHO. Reaction traces were collected at 475 nm and fit to a single exponential. The reduction rate constant (k_{red}) was determined from the limiting value of the observed rate constant at infinite DHO concentration obtained by fitting k_{obs} vs. DHO concentration to a hyperbola in Kaleidagraph (Synergy, Inc.).

Results

Reduction Potentials

The reduction potential of the enzyme-bound flavin was determined by the method of Massey (17). The reduction potential of wild-type *E. coli* DHOD is reported

as -310 mV in the literature (11). The potential was also determined using both phenosafranin (E_m = -252 mV) and 1-anthraquinone sulfonate (E_m = -225 mV) and found to be -229 mV. The reduction potential of each mutant was determined using phenosafranin as the indictor dye (Table 5-1; Figure 5-2). The only mutation to not affect the potential was Phe115Ala. In this mutant enzyme, the potential was -229 mV. All other mutations lowered the reduction potential. The biggest effects were seen in the Ser175Ala, Thr178Ala, and Thr278Val mutant enzymes, with these enzymes having reduction potentials near -270 mV, ~40 mV lower than wild-type.

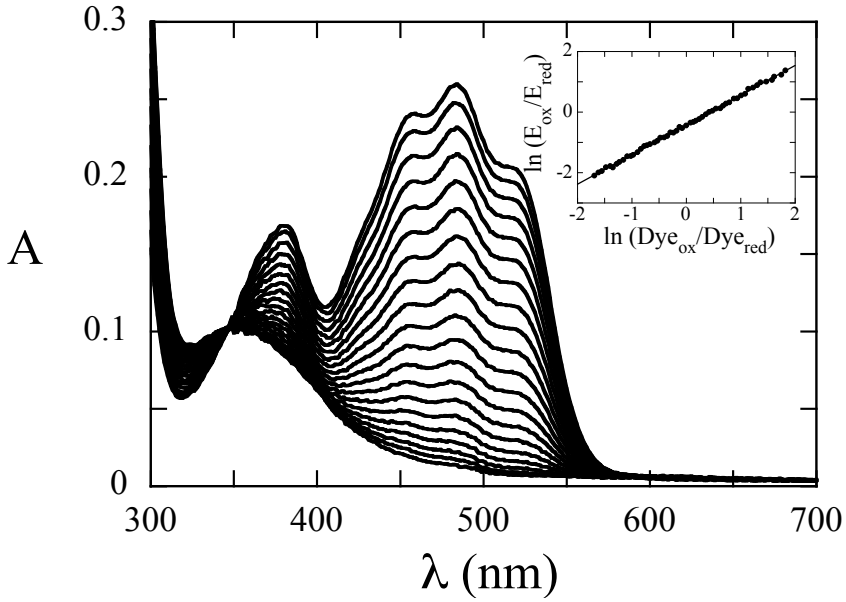

Figure 5-2: Determination of the Reduction Potential of Phe115Leu Mutant DHOD

Phenosafranin was used as an indicator dye to determine the reduction potential. The inset shows the Nerst plot for determining the potential.

Table 5-1: Reduction Potentials of Mutant DHODs

Enzyme	Reduction Potential
Wild-Type	-229 mV
Ser175Ala	-267 mV
Thr178Ser	-249 mV
Thr178Ala	-269 mV
Thr178Val	-264 mV
Phe115Ala	-229 mV
Phe115Leu	-245 mV
Phe115Trp	-258 mV

OA Binding

Oxidized DHOD from *E. coli* has a maximum flavin absorbance peak at 456 nm. The spectrum of all oxidized mutant enzymes was essentially identical to wild-type. Ligand binding often causes spectral perturbation in flavoenzymes. OA binding to oxidized DHODs causes a large red-shift in the maximum flavin absorbance peak (14, 18-21). In the Class 2 enzyme from *E. coli*, this shift is from 456 nm to 475 nm (14). By tracking this spectral change, the dissociation constant for OA could be determined in aerobic titration at pH 8.5, 25 ^{o}C (Figure 5-3). No significant affects on K_d were observed for any mutant (Table 5-2).

Table 5-2: Binding of OA to Oxidized Mutant DHODs, pH 8.5, 25 °C

Enzyme	K_d (μM)
Wild-Type	5.5 ± 0.5
Ser175Ala	15 ± 1
Thr178Ser	6.5 ± 0.8
Thr178Ala	12 ± 1
Thr178Val	7 ± 1
Phe115Ala	8.0 ± 0.5
Phe115Leu	3.7 ± 0.3
Phe115Trp	3.2 ± 0.3

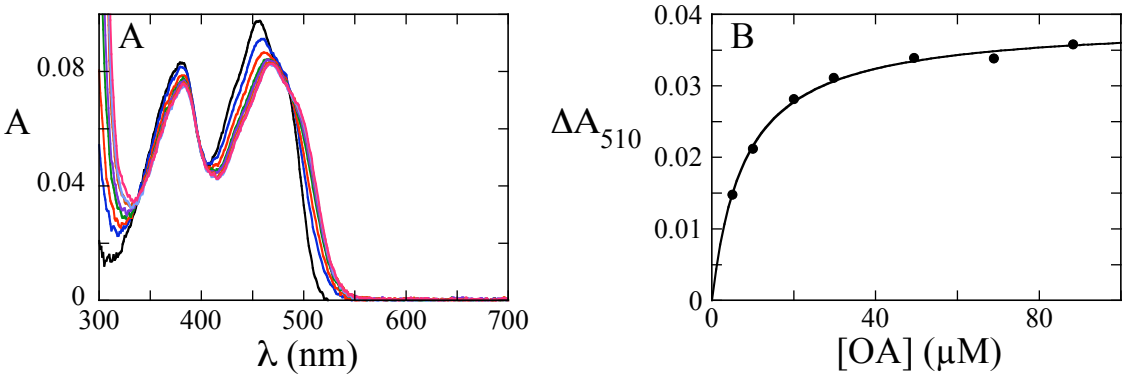

Figure 5-3: OA Binding Titration, pH 8.5, 25 °C

(A) The Phe115Ala mutant DHOD was titrated aerobically with OA. Upon OA Binding, the maximum flavin peak shifts to the red. (B) The maximum change in absorbance due to OA binding as a function of OA concentration. Fitting to a square hyperbola gives the K_d value for OA, 8.0 ± 0.5 μM.

pH Dependence of Flavin Reduction

The reductive half-reaction of the Class 2 DHOD from *E. coli* has been studied in great detail in anaerobic stopped-flow experiments (11, 12). To probe the role of

conserved residues in a hydrogen-bonding network connecting the active site base to bulk solvent, site-directed mutagenesis was used. Thr178, which hydrogen-bonds to a crystallographic water in this network, was replaced by serine, alanine, and valine (the residue found in Class 1A DHODs, which do not contain this network). The water sits on Phe115, which was replaced by alanine, leucine (the residue found in Class 1A DHODs), and tryptophan. The reductive half-reaction of each of these mutant enzymes was studied in anaerobic stopped-flow experiments.

The spectral changes observed during the reductive half-reaction are identical to those observed in wild-type (11, 12). In all cases, DHO binding was very rapid and occurred in the dead time of the stopped-flow instrument. DHO binding was accompanied by a large shift in the flavin peak, from 456 nm to 475 nm. This spectral shift resembles the shift observed upon OA binding. The first observable phase is the chemical step, i.e., reduction of the enzyme-bound flavin. Flavin reduction is pH-dependent. If flavin reduction is faster than product dissociation, the concentration of the reduced enzyme-orotate complex is large enough to be seen spectroscopically. When this occurs, flavin reduction is seen as a large decrease in absorbance at 475 nm with a concomitant increase in absorbance at 550 nm (Figure 5-4A). The 550 nm absorbance is

due to a charge-transfer interaction between the electron-rich reduced flavin and the electron-deficient OA. The next observed phase represents product dissociation and is accompanied by a decrease in absorbance at both 475 nm and 550 nm (Figure 5-4A). When flavin reduction is slower than product release, the reduced enzyme-OA complex does not accumulate and only flavin reduction is observed. Often, a small final well-resolved phase representing less than 10% of the total absorbance change is observed at 475 nm (Figure 5-4A). This phase is also observed in wild-type (11). It is unclear what this phase represents. It has been suggested that this phase could be due to the reduction of a small contaminating amount of free flavin (11).

The reaction traces obtained at 475 nm and 550 nm were fit to sums of exponentials. The observed rate constant for flavin reduction saturated with increasing DHO concentrations. The reduction rate constant (k_{red}) is the rate constant at infinite DHO concentration determined by fitting the observed rate constant versus DHO concentration plot to a hyperbola (Figure 5-4B). The half-saturating value gives the apparent K_d of DHO. The observed rate constant of the second phase decreased with increasing DHO concentration (Figure 5-4C) as seen in wild-type (11). The observed

rate constant of the third phase was independent of DHO and at least order of magnitude smaller than the rate constants of any other phases (Figure 5-4C).

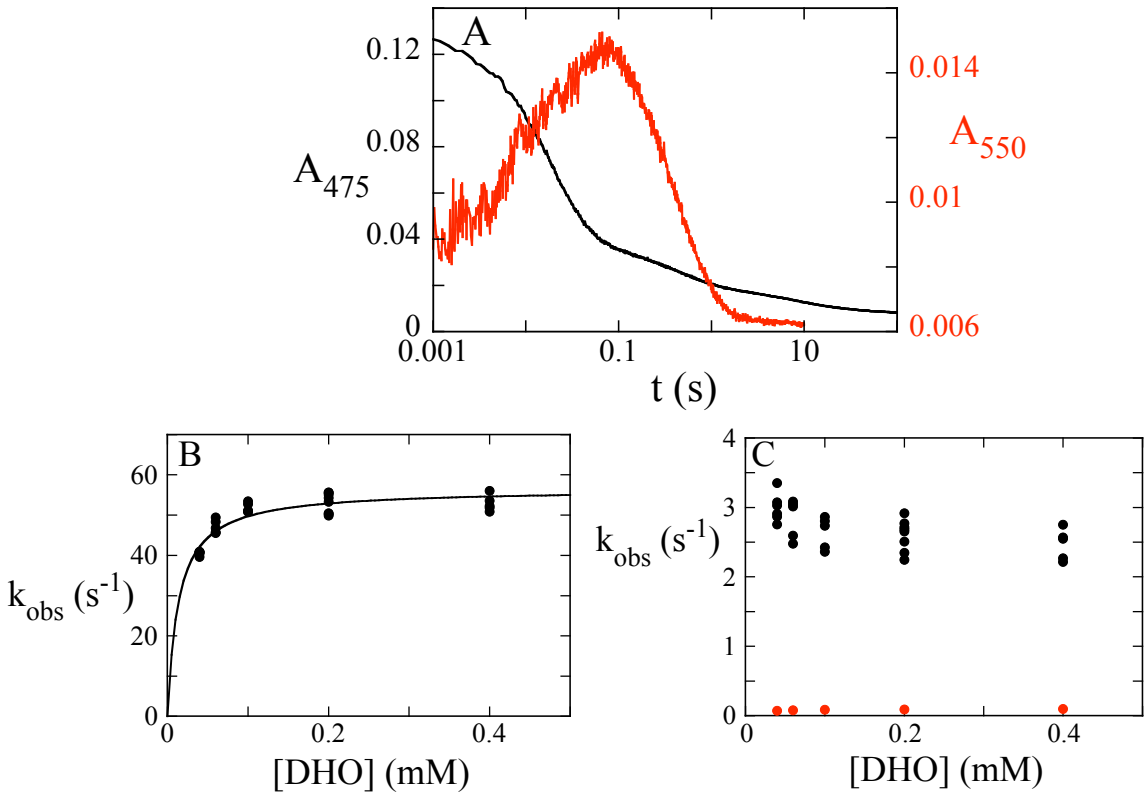

Figure 5-4: Reductive Half-Reaction of the Phe115Leu Mutant DHOD at pH 10

(A) At 475 nm (black), the reaction occurs in three phases. The first (large) phase represents the chemical step. The second phase represents product release. At 550 nm (red), flavin reduction is seen as an increase in absorbance and product dissociation is seen as a decrease in absorbance. (B) The observed rate constant of the first phase (flavin reduction) saturates with increasing DHO concentration, giving a reduction rate constant (k_{red}) of 56.5 ± 0.9 s^{-1} and a $K_{d,DHO}$ of 14 ± 2 µM at pH 10. (C) The observed rate constant of the second phase (black), OA release, decreases with increasing DHO concentration, giving a limiting value of 2.5 s^{-1}. The observed rate constant of the final phase (red) is ~0.08 s^{-1} and is independent of DHO concentration.

As mentioned earlier, flavin reduction is pH-dependent. The Class 2 DHOD from *E. coli* exhibits a pK_a of ~9.5 for the rate constant for flavin reduction (11). The pH dependence of the reduction rate constant was determined for the mutant enzymes[1] (Figure 5-5). In most cases, the reduction rate constant increased until reaching a break point, indicating a pK_a. The most conservative mutation studied (Thr178Ser) resulted in a pH dependence nearly identical to that of wild-type. The limiting k_{red} was ~500 s^{-1} (1.4-fold faster than wild-type). The observed pK_a was shifted by ~0.3 pH units to ~9.8 (Table 5-3). More dramatic effects were observed when Thr178 was mutated to alanine and valine. The limiting reduction rate constant (as fast as the enzyme could go) was ~2-fold slower than that of wild-type. In addition, the observed pK_a values were shifted ~1 pH unit to 10.4 (Thr178Ala) and 10.7 (Thr178Val). The Phe115Ala mutant enzyme had a limiting rate constant near that of wild-type. However, the observed pK_a was shifted to ~10.4. The most dramatic change in the pK_a was observed in the Phe115Leu mutant enzyme. The limiting rate constant of this mutant is estimated to be 830 s^{-1} (~2-fold faster than wild-type). The observed pK_a is shifted nearly two pH units to 11.2.

[1] The Phe155Trp mutant enzyme was only studied at two pH values and therefore a pK_a value could not be obtained.

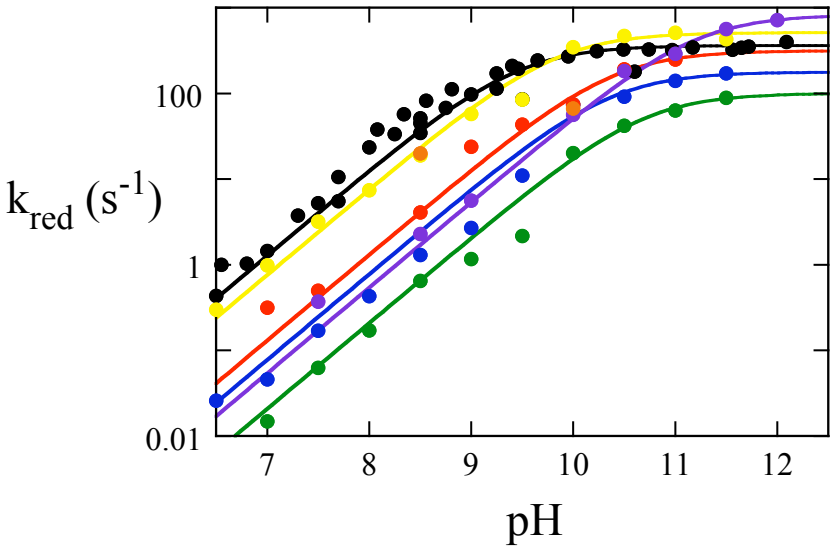

Figure 5-5: pH Dependence of Reduction Rate Constant

Wild-type, black; Thr178Ser, yellow; Thr178Ala, blue; Thr178Val, green; Phe115Ala, red; Phe115Leu, purple; Phe115Trp, orange. The limiting reduction rate constants and observed pK_a values can be found in Table 5-3.

Table 5-3: pH Dependence on Flavin Reduction

Enzyme	lim k_{red} (s^{-1})	pK_a
Wild-Type[a]	360 ± 20	9.5 ± 0.1
Thr178Ser	500 ± 30	9.8 ± 0.1
Thr178Ala	180 ± 10	10.4 ± 0.1
Thr178Val	100 ± 4	10.7 ± 0.1
Phe115Ala	315 ± 20	10.4 ± 0.1
Phe115Leu	830 ± 35	11.2 ± 0.1

[a]Data taken from (11).

The apparent K_d of DHO is also pH dependent. In wild-type, the K_d is low (~20 μM) until a pH of ~10. Then, the K_d increases giving a pK_a of ~10.3 (11). Almost all the mutant enzymes studied were very similar, with tight binding observed until a pH of ~10

(Figure 5-6). However, the Phe115Ala and the Phe115Trp mutant enzymes were quite different. The K_d of DHO for the Phe115Ala mutant enzyme, even at low pH, was in the hundreds of micromolar and was independent of pH. The Phe115Trp mutant enzyme was only studied at two pH values, but the apparent K_d was near 1 mM at both pH values.

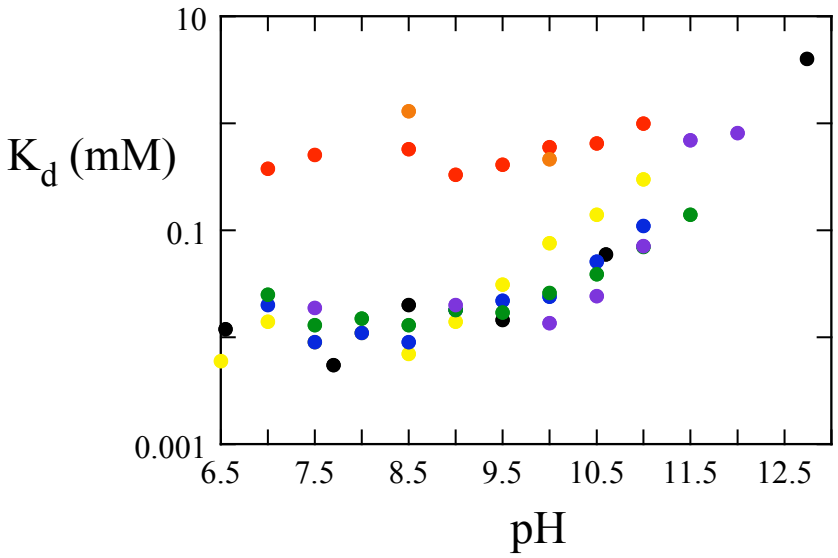

Figure 5-6: pH Dependence of the Apparent K_d of DHO

Wild-type, black; Thr178Ser, yellow; Thr178Ala, blue; Thr178Val, green; Phe115Ala, red; Phe115Leu, purple; Phe115Trp, orange.

In the wild-type enzyme, between pH 6 – 10, the average rate constant for product release is ~0.35 s^{-1} (11, 12). The same is observed in all the Thr178 mutant enzymes. In all instances where the rate constant for product release can be obtained, it ranges from

~0.2 – 0.6 s^{-1}, independent of pH. The Phe115 mutant enzymes behaved very differently. In the Phe115Ala mutant DHOD, product release was observed above pH 9. The rate constant (~8 s^{-1}) was independent of pH, but was about an order of magnitude larger than that of wild-type. In the Phe115Trp mutant enzyme, the rate constant of product release was also much faster (~3.5 s^{-1}) than wild-type at pH 10.5. The rate constant of product dissociation for the Phe115Leu mutant was pH-dependent. At lower pH (8-9.5), the rate constant was ~1 s^{-1}. However, as the pH increased, the rate constant decreased. At pH 12, the rate constant was only ~0.2 s^{-1}, near the values routinely obtained with the wild-type enzyme.

The pH dependence of the reductive half-reaction was also studied for the Ser175Ala mutant enzyme, whose active site base was removed. For this enzyme, flavin reduction was extremely slow at 4 ^{o}C and was therefore studied at 25 ^{o}C. At all pH values, a single reaction phase was observed representing flavin reduction. The reduction rate constant increased with increasing pH showing no observable pK_a (Figure 5-7).

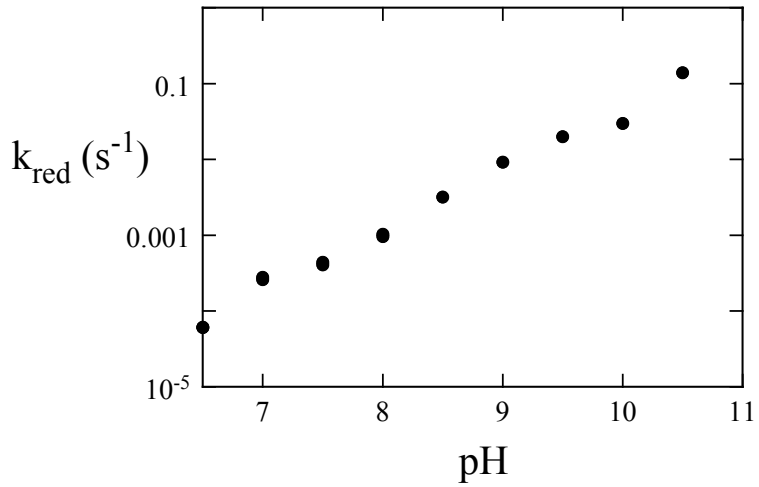

Figure 5-7: pH Dependence of Flavin Reduction in the Ser175Ala Mutant

The pH dependence was determined at 25 ^{o}C because the reaction was extremely slow at 4 ^{o}C.

Discussion

To oxidize DHO to OA, C5 must be deprotonated. Crystal structures show that a strictly conserved serine residue is properly positioned to act as an active site base (7-9). The pyrimidine-binding site of Class 2 DHODs is not exposed to solvent; therefore, the proton abstracted from C5 cannot go directly to the solvent. Instead, a hydrogen-bonding network connects the active site base to bulk solvent. The active site base hydrogen-bonds to a crystallographic water molecule sitting on a phenylalanine and hydrogen-bonded to a threonine – strictly conserved residues in Class 2 enzymes. In addition, molecular dynamics studies have shown that a water molecule occupies the tunnel almost

all of the time (13). Simulations were used to look for possible hydrogen-bond networks; the same network observed in crystal structures was also found in the simulations (13). This pathway seems the most reasonable for getting protons to bulk solvent. The proton would be passed from C5 of DHO to the active site base (Ser175 in *E. coli* DHOD), to the water molecule in the tunnel to a conserved threonine (Thr178 in *E. coli* DHOD) and finally to bulk solvent (Figure 5-8). In contrast, the active sites of Class 1 enzymes are much more solvent exposed (19, 22-25), negating the need for a hydrogen-bonding network. Site-directed mutilation was used to probe the role of the conserved proton relay network in the *E. coli* Class 2 DHOD.

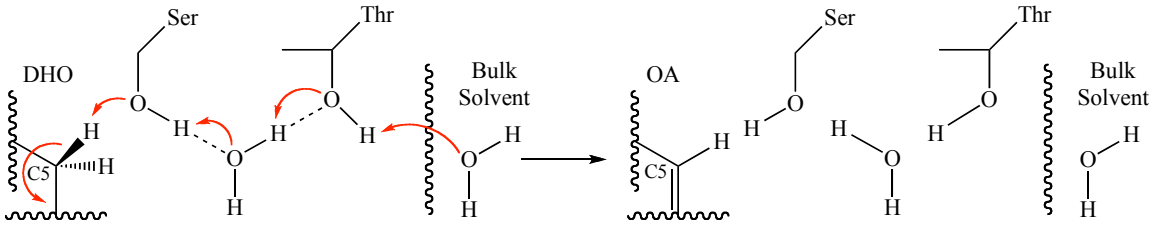

Figure 5-8: Proposed Proton Relay In Class 2 DHODs

The proton from C5 of DHO is shuttled to bulk solvent via a hydrogen-bonding network composed of both protein side-chains and water molecules.

The mutations seemed to have little effect on the pyrimidine-binding site and the flavin environment. The spectra of the oxidized enzymes were nearly identical to wild-type, with a maximum flavin peak at 456 nm. All the mutant enzymes exhibited the

usual spectral shift in the maximum flavin absorbance upon OA binding. The mutations also had little effect on the K_d of OA (Table 5-2), presumably because they are far away from the binding-site (9). The reduction potentials of most of the mutants were lowered (Table 5-1). Reduction potentials report on the differential affinities of the oxidized and reduced flavin for the apoenzyme. The oxidized mutant enzymes appear to bind flavin tightly; therefore, they are purified as holo enzymes. In addition, other probes of the behavior of the oxidized enzymes, such as OA binding, suggest that the oxidized enzymes are not greatly altered. Therefore, we suggest that the mutations have weakened the interactions between the protein and reduced FMN. The largest effects observed were changes of 40 mV (Thr178Ala and Ser175Ala) or 1.8 kcal mol^{-1}, about the strength of a typical hydrogen-bond. It is unclear why this occurs; the residues replaced are far away from the flavin itself (9).

Changes to the reductive half-reaction in the mutant enzymes were quantitative rather than qualitative. In all mutant enzymes, the reduction rate constant was pH-dependent, as it is in wild-type (11). In most of the enzymes, the reduction rate constant increased with increasing pH until a plateau was reached, indicating a pK_a. In wild-type, the observed pK_a is ~9.5 (11). Kinetic isotope effect studies have shown that DHO oxidation in the *E. coli* DHOD is stepwise (12). No isotope effect is observed at a pH

value above the pK_a when using DHO deuterated at the C5 position (12), indicating the observed pK_a is a kinetic pK_a, caused by the rate of deprotonation becoming so high it is no longer partially rate-determining.

When residues in the proton-relay network were mutated, significant shifts were observed in the pK_a values (Table 5-3). Residues were changed to increase or decrease the size of the tunnel and change the hydrophobicity of the tunnel. The higher pK_a values observed in the mutant enzymes imply that deprotonation has become less efficient since it takes higher pH values to make deprotonation too fast to be partially rate-determining. When either Thr178 or Phe115 were mutated to alanine, the observed pK_a was nearly one pH unit higher than in wild-type. These mutations would increase the size of the tunnel, giving water more room to move, thus making the hydrogen-bonding network less ordered. Decreasing the size of the tunnel and increasing the hydrophobicity had even greater effects. In the Thr178Val mutant enzyme, the pK_a is shifted to ~10.7. Valine is isosteric with threonine, but more hydrophobic. Valine would block the tunnel and its side-chain would presumably need to move to accommodate water and allow proton transfer. An even larger effect is observed in the Phe115Leu mutant enzyme, in which the pK_a is shifted to ~11.2. Replacing phenylalanine (an aromatic side-chain) with leucine (an aliphatic side-chain) will increase the hydrophobicity of the local

environment markedly. As a model, it is worth noting that the solubility of water in benzene is ~20 mM, while the solubility of water in hexane is ~10-fold lower (26). These data suggest that the mutation makes this area less hospitable for water.

Hydrogen-bonding pathways are very important for catalysis in many enzymes. Simulations have shown that the rate of proton transfer through hydrophobic channels can be increased by ~20-fold just by making a single-file chain of water molecules (27). Alcohol dehydrogenase contains a proton-relay network responsible for deprotonating water or an alcohol ligated to the catalytic zinc. In this instance, the base, a histidine located at the surface of the enzyme, is connected to the active site zinc ligand via a hydrogen-bond network. When the histidine is replaced, the pK_a controlling alcohol oxidation is shifted ~3 pH units higher than that in wild-type (28). Proton-relay networks are also known to play a major role in cytochromes P450 catalysis (29, 30). The important hydrogen-bonding networks contain both water molecules and protein residues. In wild-type crystal structures, well-ordered water molecules can be observed in the hydrogen-bonding networks. This is also seen in Class 2 DHODs. However, in structures of mutant cyctochromes P450 in which the hydrogen-bonding networks are perturbed, the water molecules are either not visible or have decreased occupancies,

indicating that protein mutations can affect the number and timely availability of water molecules important for catalysis (30, 31).

The pH dependence on flavin reduction was also studied for the Ser175Ala mutant enzyme – removal of the active site base. In this enzyme, reduction was extremely slow and thus was studied at 25 ^{o}C to speed the reaction. The reduction rate constant was pH-dependent – as in all other mutants – but there was no observable pK_a. The active site base mutant of the Class 1A DHOD from *L. lactis* (Cys130Ala) has been previously studied at 25 ^{o}C (32), allowing the direct comparison with the data presented here. The reduction rate constant of the Ser175Ala mutant enzyme was at least an order of magnitude faster than that of the Cys130Ala mutant enzyme at all pH values investigated. In both these enzymes, water occupying the cavity opened by mutation likely acts as the base. The Class 2 enzyme is better able to catalyze the reaction without its active site base than the Class 1A enzyme is. This is probably due to the presence of the proton-relay network in Class 2 enzymes, which would be properly positioned to shuttle a proton from the active site, even if it is from a disordered water molecule acting as base.

The reductive half-reaction of DHOD demands a route to remove a proton. Class 1A enzymes, which have much more solvent exposed active sites, presumably do this by

direct reaction with solvent. However, a hydrogen-bonding network is needed to accomplish this in Class 2 DHODs. In these enzymes, the active site serine alone is not sufficient. The entire ordered proton-relay network is needed for the most effective deprotonation of DHO.

Reference

1. Björnberg, O., Rowland, P., Larsen, S. and Jensen, K. F. (1997) *Biochemistry*, **36,** 16197-16205.

2. Jones, M. E. (1980) *Annu. Rev. Biochem.*, **49,** 253-279.

3. Nagy, M., Lacroute, F. and Thomas, D. (1992) *Pro.c Natl. Acad. Sci. U. S. A.*, **89,** 8966-8970.

4. Nielsen, F. S., Andersen, P. S. and Jensen, K. F. (1996) *J. Biol. Chem.*, **271,** 29359-29365.

5. Baumgartner, R., Walloschek, M., Kralik, M., Gotschlich, A., Tasler, S., Mies, J. and Leban, J. (2006) *J. Med. Chem.*, **49,** 1239-1247.

6. Hansen, M., Le Nours, J., Johansson, E., Antal, T., Ullrich, A., Loffler, M. and Larsen, S. (2004) *Protein Sci.*, **13,** 1031-1042.

7. Hurt, D. E., Widom, J. and Clardy, J. (2006) *Acta Crystallogr. D Biol. Crystallogr.*, **62,** 312-323.

8. Liu, S., Neidhardt, E. A., Grossman, T. H., Ocain, T. and Clardy, J. (2000) *Structure*, **8,** 25-33.

9. Nørager, S., Jensen, K. F., Björnberg, O. and Larsen, S. (2002) *Structure*, **10,** 1211-1223.

10. Walse, B., Dufe, V. T., Svensson, B., Fritzson, I., Dahlberg, L., Khairoullina, A., Wellmar, U. and Al-Karadaghi, S. (2008) *Biochemistry*, **47,** 8929-8936.

11. Palfey, B. A., Björnberg, O. and Jensen, K. F. (2001) *Biochemistry*, **40,** 4381-4390.

12. Fagan, R. L., Nelson, M. N., Pagano, P. M. and Palfey, B. A. (2006) *Biochemistry*, **45,** 14926-14932.

13. Small, Y. A., Guallar, V., Soudackov, A. V. and Hammes-Schiffer, S. (2006) *J. Phys. Chem. B*, **110,** 19704-19710.

14. Björnberg, O., Gruner, A. C., Roepstorff, P. and Jensen, K. F. (1999) *Biochemistry*, **38,** 2899-2908.

15. Palfey, B. A. (2003) Time resolved spectral analysis in *Kinetic analysis of macromolecules* (Johnson, K. A.), Oxford Unversity Press, New York.

16. Williams, C. H., Jr., Arscott, L. D., Matthews, R. G., Thorpe, C. and Wilkinson, K. D. (1979) *Methods Enzymol.*, **62,** 185-198.

17. Massey, V. (1990) in *Flavins and flavoproteins* (Curti, B., Ronchi, S. and Zanetti, G.), Walter de Gruyter, Berlin, Germany.

18. Marcinkeviciene, J., Jiang, W., Locke, G., Kopcho, L. M., Rogers, M. J. and Copeland, R. A. (2000) *Arch. Biochem. Biophys.*, **377,** 178-186.

19. Nørager, S., Arent, S., Björnberg, O., Ottosen, M., Lo Leggio, L., Jensen, K. F. and Larsen, S. (2003) *J. Biol. Chem.*, **278,** 28812-28822.

20. Wolfe, A. E., Thymark, M., Gattis, S. G., Fagan, R. L., Hu, Y. C., Johansson, E., Arent, S., Larsen, S. and Palfey, B. A. (2007) *Biochemistry*, **46,** 5741-5753.

21. Zameitat, E., Pierik, A. J., Zocher, K. and Loffler, M. (2007) *FEMS Yeast Res.*, **7,** 897-904.

22. Arakaki, T. L., Buckner, F. S., Gillespie, J. R., Malmquist, N. A., Phillips, M. A., Kalyuzhniy, O., Luft, J. R., Detitta, G. T., Verlinde, C. L., Van Voorhis, W. C., Hol, W. G. and Merritt, E. A. (2008) *Mol. Microbiol.*, **68,** 37-50.

23. Inaoka, D. K., Sakamoto, K., Shimizu, H., Shiba, T., Kurisu, G., Nara, T., Aoki, T., Kita, K. and Harada, S. (2008) *Biochemistry*, **47,** 10881-10891.

24. Rowland, P., Björnberg, O., Nielsen, F. S., Jensen, K. F. and Larsen, S. (1998) *Protein Sci.*, **7,** 1269-1279.

25. Rowland, P., Nørager, S., Jensen, K. F. and Larsen, S. (2000) *Structure*, **8,** 1227-1238.

26. Wolfenden, R. and Radzicka, A. (1994) *Science*, **265,** 936-937.

27. Voth, G. A. (2006) *Acc. Chem Res.*, **39,** 143-150.

28. LeBrun, L. A., Park, D. H., Ramaswamy, S. and Plapp, B. V. (2004) *Biochemistry*, **43,** 3014-3026.

29. Schlichting, I., Berendzen, J., Chu, K., Stock, A. M., Maves, S. A., Benson, D. E., Sweet, R. M., Ringe, D., Petsko, G. A. and Sligar, S. G. (2000) *Science*, **287,** 1615-1622.

30. Vidakovic, M., Sligar, S. G., Li, H. and Poulos, T. L. (1998) *Biochemistry*, **37,** 9211-9219.

31. Makris, T. M., von Koenig, K., Schlichting, I. and Sligar, S. G. (2007) *Biochemistry*, **46,** 14129-14140.

32. Fagan, R. L., Jensen, K. F., Björnberg, O. and Palfey, B. A. (2007) *Biochemistry*, **46,** 4028-4036.

Chapter 6
Conclusions and Future Directions

Enzymes that catalyze the conversion of dihydroorotate (DHO) to orotate (OA) – dihydroorotate dehydrogenases (DHODs) – have been known for many years (1). Initially, the differences in the enzymes were not clearly understood. Some DHODs were membrane-bound enzymes (2), while others were much larger cytosolic enzymes that used pyridine nucleotides as substrates as well as DHO (1, 3, 4). Within the last ten years or so, the increase in sequence information has allowed for the enzymes to be divided into two broad classes (5), with many properties of the enzymes segregating nicely into these classes.

The work presented in this thesis focused on Class 1A and Class 2 DHODs. Each class of DHODs utilizes a different oxidizing substrate – ubiquinone for the membrane-bound Class 2 enzymes (6) and fumarate for the cytosolic Class 1A enzymes (7). However, in the reductive half-reaction both classes catalyze the oxidation of DHO. The pyrimidine binding site - the site of DHO oxidation - is nearly identical in all DHODs (8-21). All DHODs contain an enzyme-bound FMN prosthetic group, an active site base

(either cysteine in Class 1A enzymes or serine in Class 2 enzymes), and a ring of highly conserved hydrogen-bounding residues that interact with the pyrimidine. Thus, different phylogenetic classes of DHODs catalyze the same chemical reaction – the oxidation of DHO – using very similar catalytic machinery.

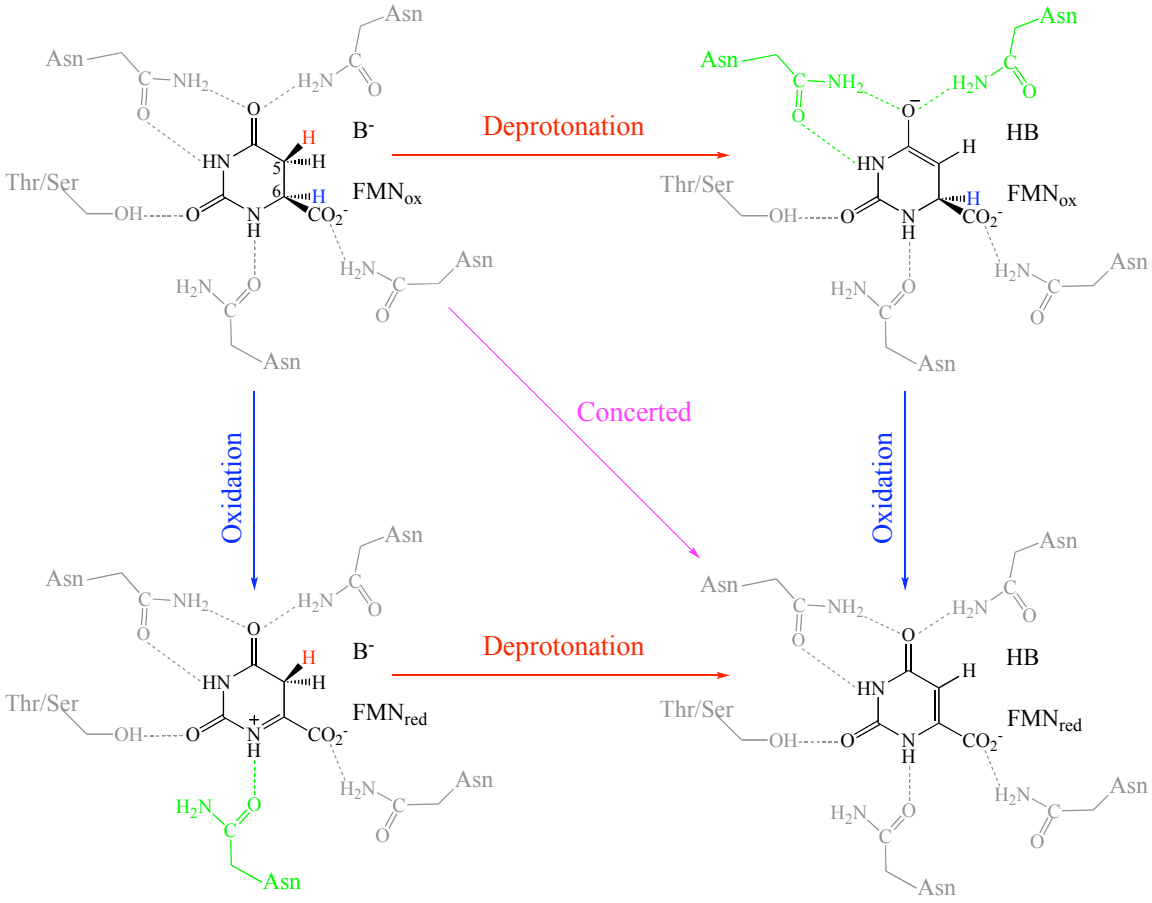

Figure 6-1: Possible Mechanisms of DHO Oxidation by DHODs

The two C-H bonds could break at the same time in a concerted mechanism or sequentially in one of two stepwise mechanisms. The ring of highly conserved hydrogen-bonding residues is shown around the pyrimidine. An interaction capable of stabilizing an intermediate is shown in green.

There are three possible mechanisms of DHO oxidation (Figure 6-1). Two C-H bonds are broken; the active site base deprotonates C5 of DHO and the hydrogen on C6 is transferred to N5 of the isoalloxazine ring of the flavin as a hydride. These two bonds could break sequentially, in a stepwise mechanism, or at the same time, in a concerted mechanism. Two stepwise mechanisms are possible, one in which deprotonation occurs first and an enolate intermediate is formed and the other in which hydride transfer occurs first and an iminium intermediate is formed.

The work presented in this thesis sought to address the question of whether these two phylogenetic classes of enzymes use the same mechanism for DHO oxidation. Surprisingly, despite the similarities between the enzymes, each class uses a different mechanism. Chapters 2 and 3 detail the use of kinetic isotope effects to probe the order of bond breaking. This work is the first published work addressing the order of bond breaking during DHO oxidation by DHODs by directly observing flavin reduction and showed that Class 2 DHODs use a stepwise mechanism, while Class 1A enzymes use a concerted mechanism. Chapter 4 focuses on the use of site-directed mutagenesis to probe the roles of conserved active site residues in DHO oxidation, demonstrating that some residues are important for binding, while others are vital for DHO oxidation. Intriguingly, analogous mutations in the two phylogenetic classes result in widely

different effects on binding and flavin reduction, further demonstrating the mechanistic differences between these enzymes. This is the first attempt to determine the roles most of these conserved active site residues play during DHO oxidation. Chapter 5 addresses the deprotonation of DHO by the active site base, serine, in Class 2 DHODs. Site-directed mutagenesis was used to probe the importance of a putative proton-relay network found only in Class 2 enzymes. Disrupting the proton-relay network has significant effects on the deprotonation of DHO, suggesting an important role in catalysis for this network. This work is currently the only experimental evidence of the importance of these residues in catalysis.

While the work presented here clearly shows that these two phylogenetic classes of DHODs use different mechanisms of DHO oxidation, there are still many unanswered questions. The isotope effect experiments presented in Chapters 2 and 3 do not address the order of bond breaking. Thus, it is still unclear whether DHO oxidation by Class 2 DHODs proceeds via enolate or iminium intermediate formation, i.e., which step occurs first. Determining heavy-atom isotope effects on DHO oxidation could give insight into which intermediate is forming. Equilibrium isotope effects at each position of DHO have been calculated theoretically for the formation of each intermediate, giving an idea of the maximum expected KIE at each position for the formation of either intermediate. If an

iminium intermediate is formed, an inverse ^{15}N isotope effect is expected at the N1 position of DHO. Heavy-atom isotope effect experiments have been conducted on orotidine 5'-monophosphate decarboxylase (22), the final enzyme in the pyrimidine biosynthetic pathway and the procedure used could be modified slightly to obtain ^{15}N isotope effects with DHODs. ^{13}C isotope effects could potentially be determined for all positions simultaneously via NMR (23), a procedure that has been used before for an enzyme-catalyzed reaction (24). Determining heavy-atom isotope effects on flavin reduction for Class 1A enzymes will give insight into the structure of the transition state that forms during the concerted oxidation of DHO. Transition state analogs are known to be excellent inhibitors (25, 26). Therefore, this information could greatly aid Class 1A-specific inhibitor design.

More work is needed to understand the importance of the proton-relay network studied in Chapter 5. The work completed thus far is on single mutants of the residues that form the relay. The importance of these residues could be further shown using double mutants for Thr178 and Phe115. In addition, my work has shown that when the base is replaced with alanine in both Class 1A and Class 2 DHODs, the reduction rate constant, while significantly slower than wild-type, is at least an order of magnitude faster for the mutant Class 2 enzyme than for the mutant Class 1A enzyme. We

hypothesize that this is due to the proton-relay network found in Class 2 DHODs. A triple mutant, in which the active base is replaced by alanine as well as replacing the threonine and phenylalanine in the proton-relay network, should decrease the observed reduction rate constant, making it closer to the value observed in the Class 1A active site base mutant.

In addition, several new questions have come to light. While this work shows that difference exists between the classes, it is still unclear what causes these differences. The crystal structures show that the active sites are very similar. Dynamics potentially plays some role in the mechanistic differences observed. Some of the site-directed mutagenesis in Chapter 4 points to active site loop dynamics being very importance for catalysis. Also, overall protein motion is likely important as well. Perhaps coupled motion exists between residues far outside of the active site pocket, and mutation of these residues could slow the reaction or change the mechanism employed. These important dynamic components could potentially be probed by NMR and kinetic investigations.

While the results presented here begin to detail the mechanistic differences in two phylogenetic classes of DHODs, further work could be done to better understand these differences. It is interesting that these enzymes use different mechanism to accomplish the same chemistry, even though they have very similar catalytic machinery. This shows

that mechanistic details cannot simply be inferred from structural similarities and leaves questions about the detailed mechanism of Class 1B DHODs, as well as other pyrimidine-metabolizing enzymes that share similar active sites with DHODs.

References

1. Lieberman, I. and Kornberg, A. (1953) *Biochim. Biophys. Acta.*, **12,** 223-234.

2. Taylor, W. H. and Taylor, M. L. (1964) *J. Bacteriol.*, **88,** 105-110.

3. Aleman, V., Handler, P., Palmer, G. and Beinert, H. (1968) *J. Biol. Chem.*, **243,** 2569-2578.

4. Graves, J. L. and Vennesland, B. (1957) *J. Biol. Chem.*, **226,** 307-316.

5. Björnberg, O., Rowland, P., Larsen, S. and Jensen, K. F. (1997) *Biochemistry*, **36,** 16197-16205.

6. Jones, M. E. (1980) *Annu. Rev. Biochem.*, **49,** 253-279.

7. Nagy, M., Lacroute, F. and Thomas, D. (1992) *Proc. Natl. Acad. Sci. U. S. A.*, **89,** 8966-8970.

8. Arakaki, T. L., Buckner, F. S., Gillespie, J. R., Malmquist, N. A., Phillips, M. A., Kalyuzhniy, O., Luft, J. R., Detitta, G. T., Verlinde, C. L., Van Voorhis, W. C., Hol, W. G. and Merritt, E. A. (2008) *Mol. Microbiol.*, **68,** 37-50.

9. Baumgartner, R., Walloschek, M., Kralik, M., Gotschlich, A., Tasler, S., Mies, J. and Leban, J. (2006) *J. Med. Chem.*, **49,** 1239-1247.

10. Hansen, M., Le Nours, J., Johansson, E., Antal, T., Ullrich, A., Loffler, M. and Larsen, S. (2004) *Protein Sci.*, **13,** 1031-1042.

11. Hurt, D. E., Widom, J. and Clardy, J. (2006) *Acta Crystallogr. D Biol. Crystallogr.*, **62,** 312-323.

12. Inaoka, D. K., Sakamoto, K., Shimizu, H., Shiba, T., Kurisu, G., Nara, T., Aoki, T., Kita, K. and Harada, S. (2008) *Biochemistry*, **47,** 10881-10891.

13. Liu, S., Neidhardt, E. A., Grossman, T. H., Ocain, T. and Clardy, J. (2000) *Structure*, **8,** 25-33.

14. Nørager, S., Arent, S., Björnberg, O., Ottosen, M., Lo Leggio, L., Jensen, K. F. and Larsen, S. (2003) *J. Biol. Chem.*, **278,** 28812-28822.

15. Nørager, S., Jensen, K. F., Björnberg, O. and Larsen, S. (2002) *Structure*, **10,** 1211-1223.

16. Pinheiro, M. P., Iulek, J. and Cristina Nonato, M. (2008) *Biochem. Biophys. Res. Commun.*, **369**, 812-817.

17. Rowland, P., Björnberg, O., Nielsen, F. S., Jensen, K. F. and Larsen, S. (1998) *Protein Sci.*, **7,** 1269-1279.

18. Rowland, P., Nielsen, F. S., Jensen, K. F. and Larsen, S. (1997) *Structure*, **5,** 239-252.

19. Rowland, P., Nørager, S., Jensen, K. F. and Larsen, S. (2000) *Structure*, **8,** 1227-1238.

20. Walse, B., Dufe, V. T., Svensson, B., Fritzson, I., Dahlberg, L., Khairoullina, A., Wellmar, U. and Al-Karadaghi, S. (2008) *Biochemistry*, **47,** 8929-8936.

21. Wolfe, A. E., Thymark, M., Gattis, S. G., Fagan, R. L., Hu, Y. C., Johansson, E., Arent, S., Larsen, S. and Palfey, B. A. (2007) *Biochemistry*, **46,** 5741-5753.

22. Rishavy, M. A. and Cleland, W. W. (2000) *Biochemistry*, **39,** 4569-4574.

23. Singleton, D. A. and Thomas, A. A. (1995) *J. Am. Chem. Soc.*, **117,** 9357-9358.

24. Lee, J. K., Bain, A. D. and Berti, P. J. (2004) *J. Am. Chem. Soc.*, **126,** 3769-3776.

25. Amyes, T. L. and Richard, J. P. (2007) *ACS Chem. Biol.*, **2,** 711-714.

26. Schramm, V. L. (2007) *J. Biol. Chem.*, **282,** 28297-28300.

Appendix A
Representative NMR spectra of deuterated dihydroorotate

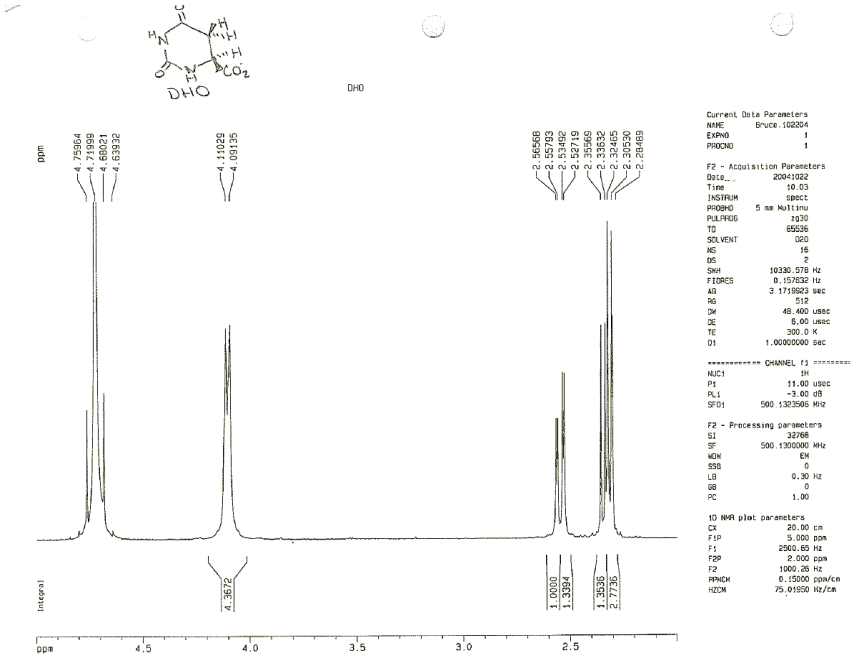

Figure A-1: NMR spectrum of protio-DHO

DHO resonances are: 2.3 ppm, C5 *pro S*, 2.5 ppm, C5 *pro R*; 4.0 ppm, C6. The HOD peak (4.7 ppm) was used as the chemical shift reference.

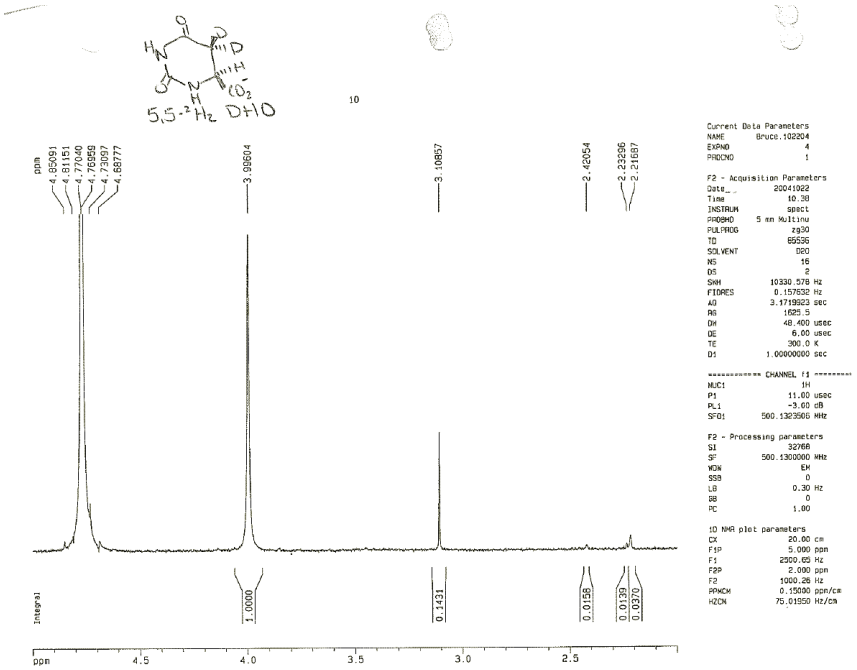

Figure A-2: NMR spectrum of 5,5-$^2H_2$ DHO

Methanol was used as an integration standard (3.1 ppm).

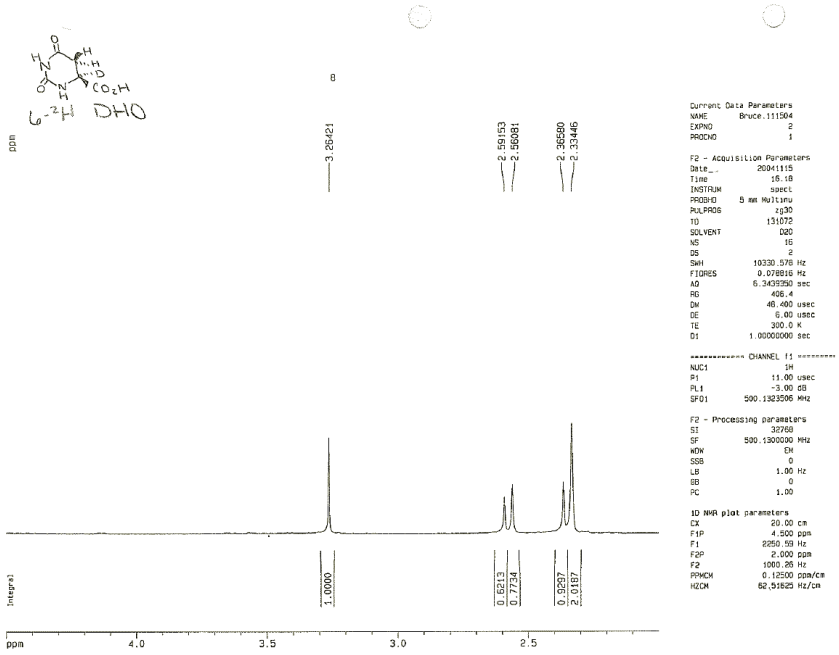

Figure A-3: NMR spectrum of 6-^{2}H DHO

Methanol was used as an integration standard (3.1 ppm).

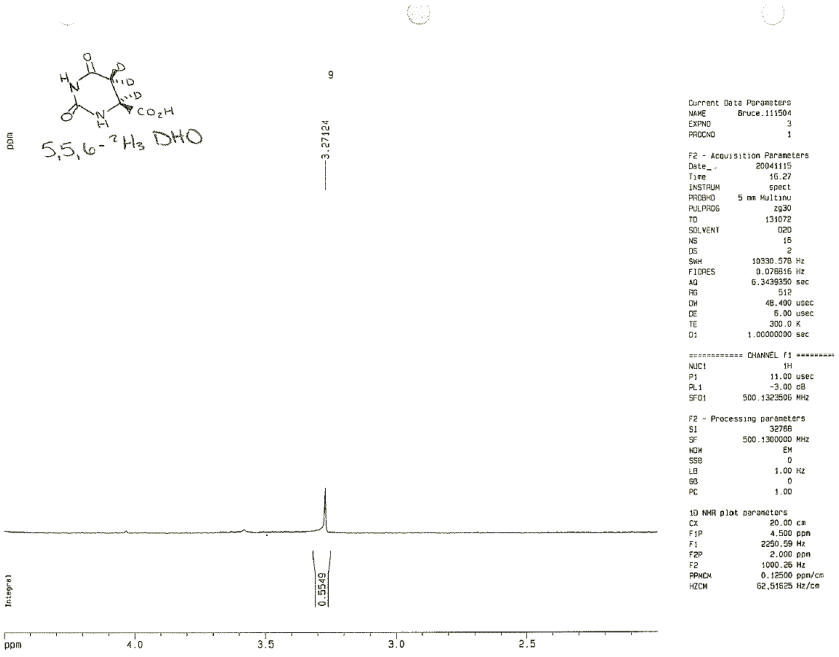

Figure A-4: NMR spectrum of 5,5,6-^{2}H$_3$ DHO

Methanol was used as an integration standard (3.1 ppm).

Appendix B
A two-step reaction showing only one phase

If the oxidation of DHO by Class 2 DHODs is actually stepwise, two reaction phases for flavin reduction in the stopped-flow experiments might be expected. However, only one phase of reduction is observed, *i.e.*, no spectral intermediates or lags are detected during the reaction. This is not inconsistent with behavior possible for a two-step reversible reaction sequence (Figure B-1). The exact solution of the system of differential equations describing a two-step reaction gives two eigenvalues for the two reaction phases. An extreme value of one eigenvalue can make a phase unobservable; many combinations of rate constants exist where only one of the two reaction phases that

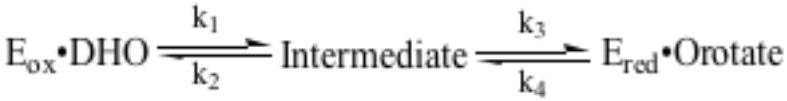

Figure B-1

are theoretically possible could be observed in practice. Sometimes this will occur when the intermediate forms in the rate-determining step, preventing its accumulation to detectable concentrations, although other conditions may also cause only one phase to be observed. The observed rate constant for the slower phase of a two-step reversible reaction is given by Equation 1, where the rate constants refer to the above scheme.

$$k_{obs} = \frac{k_1 + k_2 + k_3 + k_4 - \sqrt{\left(k_1 + k_2 + k_3 + k_4\right)^2 - 4\left(k_1k_3 + k_2k_4 + k_1k_4\right)}}{2} \qquad (1)$$

The chemistry associated with the rate constants in equation 1 cannot be uniquely specified from our data, but the data can be modeled with plausible assumptions. If the first step (k_1 and k_2) is assumed to be the redox reaction leading to an iminium intermediate, and the second step (k_3 and k_4) is arbitrarily assumed to be the acid/base reaction, then a set of rate constants and isotope effects consistent with the observed rate constants shown in Table 2-1 are, at pH 8.5, $k_1 = 94.6\ s^{-1}$, $k_2 = 9200\ s^{-1}$, $k_3 = 5620\ s^{-1}$, and $k_4 = 7.31\ s^{-1}$, with intrinsic isotope effects of 7.9 on the hydride transfer (k_1 and k_2) and 4.12 on the proton transfer (k_3 and k_4). Inspection of these values indicates that very little intermediate will ever accumulate. This was verified by numerical simulations using these rate constants and isotope effects along with plausible extinction coefficients. It must be emphasized that while the numbers presented here successfully model the data, other sets of numbers are also possible; the complexity of Equation 1 allows for many solutions. However the qualitative conclusion is clear – the reduction of the enzyme in a single-exponential phase is compatible with a two-step reaction mechanism.